AD-A081 714 EMMANUEL COLL BOSTON MASS F/G 22/2
ENERGETIC PARTICLE STUDIES: INSTRUMENTATION AND ANALYSIS.(U)
SEP 79 W BELLEW, A DAVIS, M P HAGAN F19628-76-C-0039
UNCLASSIFIED AFGL -TR-79-0223 NL

1 OF 2
AD
A081714

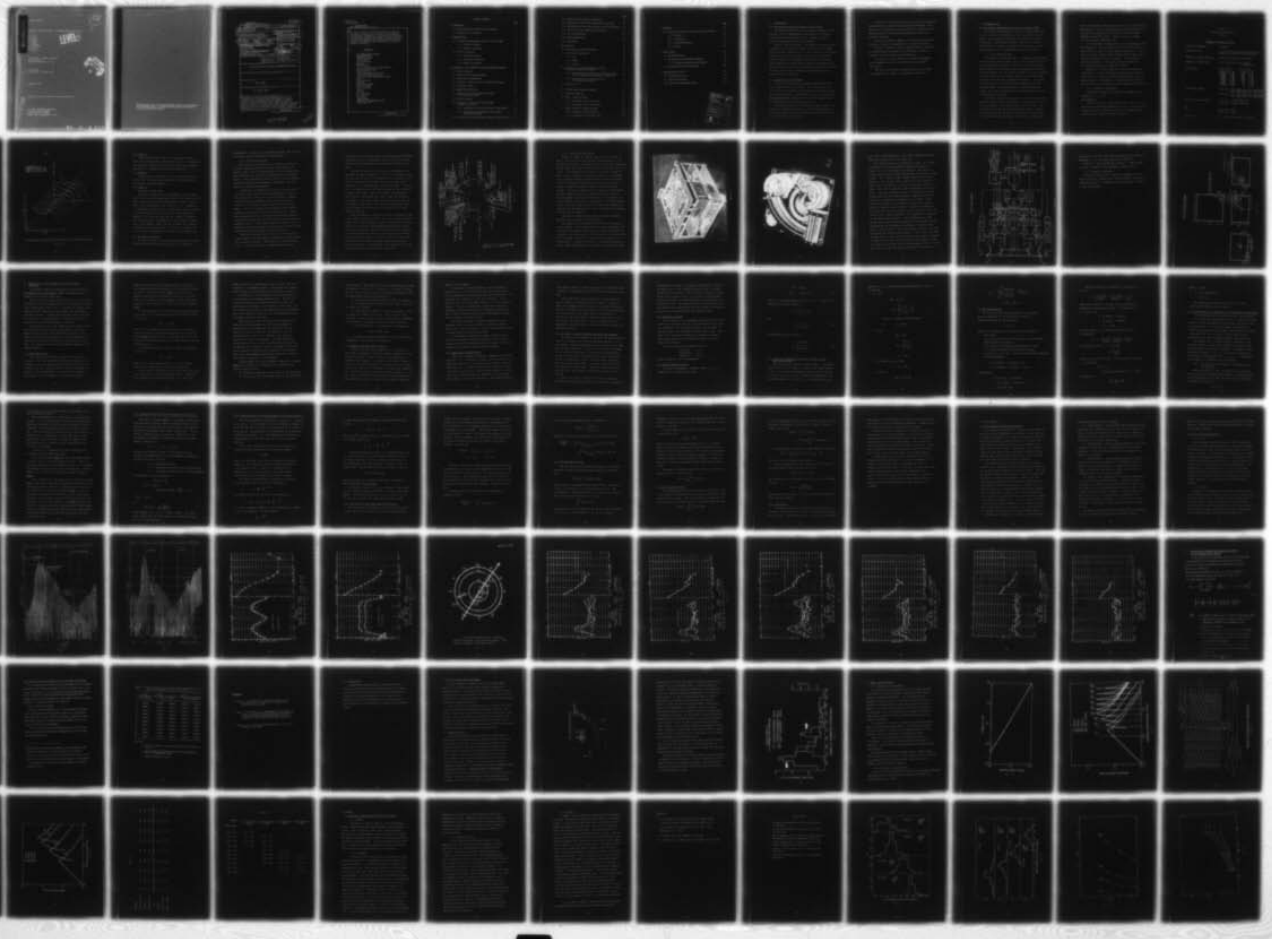

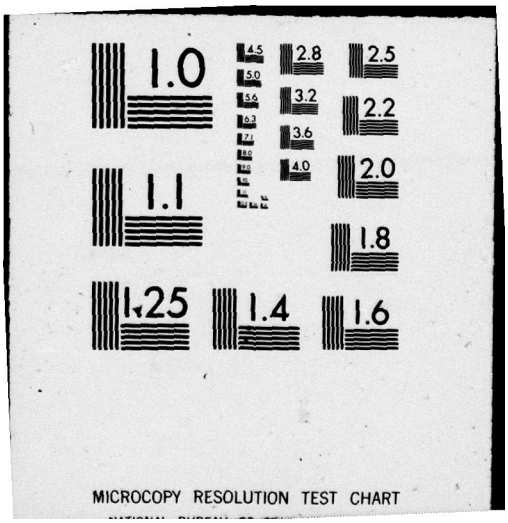
1.0
1.1
1.25
1.4
1.6
1.8
2.0
2.2
2.5
2.8
3.2
3.6
4.0
4.5
5.0
5.6
6.3
7.1
8.0
9.0
MICROCOPY RESOLUTION TEST CHART

AFGL-TR-79-0223

ENERGETIC PARTICLE STUDIES: INSTRUMENTATION AND ANALYSIS

W. Bellew
A. Davis
M.P. Hagan
E. Holeman
A. Huber
J. Pantazis
D. Parsignault
Y.V. Rao
R. Vesprini

The Trustees of Emmanuel College
400 The Fenway
Boston, Massachusetts 02115

Final Report
1 April 1976 - 31 March 1979

September 1979

Approved for public release; distribution unlimited

AIR FORCE GEOPHYSICS LABORATORY
AIR FORCE SYSTEMS COMMAND
UNITED STATES AIR FORCE
HANSCOM AFB, MASSACHUSETTS 01731

MIL-STD-847A
31 January 1973

UNCLASSIFIED

SECURITY CLASSIFICATION OF THIS PAGE (When Data Entered)

REPORT DOCUMENTATION PAGE

READ INSTRUCTIONS BEFORE COMPLETING FORM

1. REPORT NUMBER: AFGL-TR-79-0223	2. GOVT ACCESSION NO.
3. RECIPIENT'S CATALOG NUMBER	
4. TITLE (and Subtitle): ENERGETIC PARTICLE STUDIES: INSTRUMENTATION AND ANALYSIS	5. TYPE OF REPORT & PERIOD COVERED: FINAL Rept. 1 APR 76 — 31 MAR 79
6. PERFORMING ORG. REPORT NUMBER	
7. AUTHOR(s): W. BELLEW, E. HOLEMAN, D. PARSIGNAULT, A. DAVIS, A. HUBER, Y.V. RAO, M.P. HAGAN, J. PANTAZIS, R. VESPRINI	8. CONTRACT OR GRANT NUMBER(s): F19628-76-C-0039
9. PERFORMING ORGANIZATION NAME AND ADDRESS: THE TRUSTEES OF EMMANUEL COLLEGE, 400 THE FENWAY, BOSTON MA 02115	10. PROGRAM ELEMENT, PROJECT, TASK AREA & WORK UNIT NUMBERS: 61102F, 2311G1AC, G1
11. CONTROLLING OFFICE NAME AND ADDRESS: AIR FORCE GEOPHYSICS LABORATORY, HANSCOM AFB MA 01731, CONTRACT MONITOR: ROBERT C. FILZ/PHG	12. REPORT DATE: SEPTEMBER 1979
	13. NUMBER OF PAGES: 160
14. MONITORING AGENCY NAME & ADDRESS (if different from Controlling Office): 164	15. SECURITY CLASS. (of this report): UNCLASSIFIED
	15a. DECLASSIFICATION DOWNGRADING SCHEDULE

16. DISTRIBUTION STATEMENT (of this Report)

A - APPROVED FOR PUBLIC RELEASE; DISTRIBUTION UNLIMITED

17. DISTRIBUTION STATEMENT (of the abstract entered in Block 20, if different from Report)

18. SUPPLEMENTARY NOTES

TECH, OTHER

19. KEY WORDS (Continue on reverse side if necessary and identify by block number)

See Reverse Side

20. ABSTRACT (Continue on reverse side if necessary and identify by block number)

The general objectives of the program reported in this document were the implementation and support of research directed toward measurements of the energetic charged particle environment in near-earth space. Specific objectives were: the design, construction and calibration of instrument packages for the U.S. Air Force Satellites DMSP (Flights #2.

→ over

DD FORM 1 JAN 73 1473 EDITION OF 1 NOV 65 IS OBSOLETE

UNCLASSIFIED

SECURITY CLASSIFICATION OF THIS PAGE (When Data Entered)

128950

UNCLASSIFIED
SECURITY CLASSIFICATION OF THIS PAGE(When Data Entered)

20.
3, 4 and 5) and P78-1, and field support for the same missions; the study of the response, through computer and laboratory simulations, of existing proton-telescopes to the natural radiation environment; the data analysis of proton data obtained from previous satellite missions; finally the preliminary study and design of a charged particle telescope.

19. Key Words

AFGL Magnetometer Network
Background count
Computer programs
CR-39 plastic
CRL-251 payload
Detector
DMSP satellite
E^2-S^2 High Energy Proton Spectrometer
Effective path length
Energy spectra
Generalized geometrical factor
Long term duration mission
Low Energy Proton Spectrometer (LEPS)
MAGAF
Micropulsations
Modeling
Monte Carlo Method
Near-earth space
P78-1 satellite
Proton
Ray path
S3-2 satellite
S3-3 satellite
Shielding
SSJ/3 package
Sudden Storm Commencement (SSC)
Weighting factor

TABLE OF CONTENTS

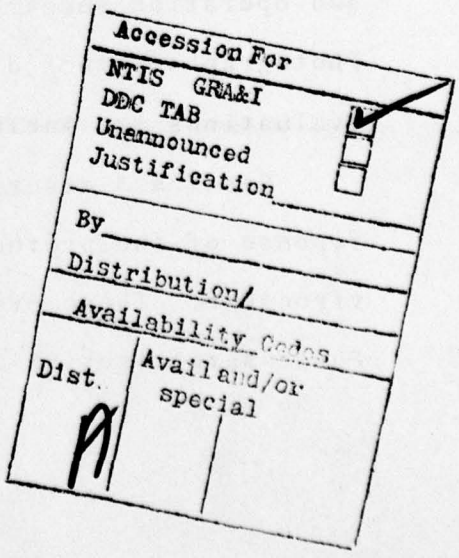

1. INTRODUCTION

1.1 General Objectives and Scope of the Program

The general objectives of the program reported in this document were the implementation and support of research directed toward measurements of the energetic charged particle environment in near-earth space.

Specific objectives were: the design, construction and calibration of instrument packages for the U.S. Air Force Satellites DMSP (Flights #2, 3, 4 and 5) and P78-1, and field support for the same missions; the study of the response, through computer and laboratory simulations, of existing proton-telescopes to the natural radiation environment; the data analysis of proton data obtained from previous satellite missions; finally, the preliminary study and design of a charged particle telescope.

1.2 Organization of the Report

Section 2 describes the instruments which were flown on the DMSP and P78-1 satellites. This section also contains a brief description of the objectives of each mission, and operation summary. Some sample data are also presented. Photographs, block diagrams and first launch engineering evaluations are included where applicable.

Section 3 describes the simulations made to model the reponse of the proton telescopes, LEPS, to the proton environment. These proton telescopes were flown on U.S. Air Force satellites S3-2 and S3-3.

In Section 4, the data analysis activities are presented. These include the data handling software development, some results of the analysis of data from the S3-2 satellite, and the evaluation of the generalized geometric factor of a particle telescope.

Section 5 contains a summary of the efforts toward the design of a proton spectrometer with a high sensitivity.

Section 6 contains a report (specifically) of research in the detection of protons in CR-39 plastic, aimed at interest in the Long Term Duration Mission.

In Section 7 various facets of software development for the MAGAF system are discussed and some programs are listed.

The use of data from the MAGAF network in the light of micropulsation studies is discussed in Section 8.

2. INSTRUMENTATION

2.1 The Defense Meteorological Satellite Program (DMSP)

The Defense Meteorological Satellite Program (DMSP) consists of a series of satellites in 450 nautical mile, polar orbits, each carrying a payload of meteorological sensors. In addition to the primary payloads, there are on each of the satellites, several instruments one of which is a small, light weight (3 lb.) electrostatic analyzer, the SSJ/3.

2.1.1 The SSJ/3 Payloads

The purpose of these payloads is to measure precipitating electron fluxes over the polar caps, in the auroral zones and at the plasma pause regions. These data, in particular the data acquired in the auroral zones during magnetic storm and substorm periods, will be analyzed together with data obtained by other sensors such as optical sensors on board the DMSP satellites, and the AFGL magnetometer networks. The outcome of such an analysis will be an improvement upon existing substorm models, the understanding of the mechanisms and sources of particle acceleration, and the possibility of predicting magnetic activity.

Each SSJ/3 payload consists of a set of two electrostatic analyzers which perform a differential energy analysis of low energy electrons in the energy range 50 eV to 20 keV. The analyzers are of the curved plate type and utilize channel electron multipliers to detect electrons of selected energy. A 16-point spectrum is produced each second. A sun sensor

turns the instrument off when the sun is in the field of view, prolonging the life of the channeltron electron multipliers. A detailed description of the SSJ/3 has been published elsewhere (AFGL-TR-77-0120). Table 2.1 lists a summary of the instrument characteristics.

Two independent calibrations have been performed on the SSJ/3 packages. First, before the first unit had flown, a calibration was done at the Aerospace Corporation. A comparison was made between this calibration and a Monte Carlo computer simulation of the instrument. The two were in excellent agreement. The results of this calibration have also been published (AFGL-TR-77-0102).

Because of the wide interest in the data from these instruments, a second calibration was performed recently on units 4 and 5 using a more sophisticated beam facility at Rice University. The results, to be published, confirmed the previous results and also provided data on UV sensitivity.

2.1.2 Summary of Operations

Four SSJ/3 packages were provided for DMSP block 5D flights #2, 3, 4 and 5.

a) Flight #2

This satellite was launched June 1977, and our instrument has been operating properly ever since. Data from this package has been reliable and useful to the DMSP effort. Typical data is shown in Figure 2.1 and 2.2.

Table 2.1

Electrostatic Analyzer

SSJ/3

Summary of Characteristics

Particles Detected	Electrons
Detectors Used	2 Channeltron Electron Multipliers for each of the two sets of ESA plates
Method of Energy Analysis	Voltage Stepping on ESA plates
Number of Energy Bins	8 for each set of ESA plates; Total of 16

Energy Bins

Large Plates		Small Plates	
20,000 eV	± 3%	1,045 eV	± 3%
13,700	± 3%	661	± 3%
8,990	± 3%	434	± 3%
5,500	± 3%	264	± 3%
3,790	± 3%	183	± 3%
2,290	± 3%	110	± 3%
1,590	± 5%	77	± 5%
1,060	± 6%	51	± 6%

Acceptance Angles	Large ESA: 1.6° FWHM across the apertures 8.0° FWHM along the apertures Small ESA: 3.7° FWHM across the apertures 4.8° FWHM along the apertures
Normalization Constants	Large ESA: 1.3×10^{-4} cm^2-ster. Small ESA: 4.3×10^{-5} cm^2-ster.
$\frac{\Delta E}{E}$	Large ESA: 4.0% Small ESA: 7.2%
Data Rate	One complete Spectrum per second

Table 2.1 (cont.)

Dwell Time at Each Energy Level	98 ms.
Digital Data Format	(9 bits per channel) x (16 channels) = 144 Bits

Note: Each 9 bits in every channel are in logarithmic form, the five least significant bits being the mantissa and the remaining four the exponent. This number is converted to decimal form according to the following relationship:

$$N = 2^{y}(x+32) - 33$$

Where; 0 0 0 0 0 0 0 0 0 ← LSB
(y = 0 0 0 0, x = 0 0 0 0 0)

Data Readout — The first bit to be read out is the least significant bit (LSB) of the highest channel followed by the next to the highest one etc., i.e.:

y x ..... y x y x — 1st bit out
0000000000 0000000000000000000
51 eV — 13,700 eV — 20,000 eV

[.....144 bits.....]

read out in one group
at the end of each second

Analog Monitors	Plate voltages: 5.0 volts to .25v Power supply : 2.5v Temperature : 2.5v at room temp.
Size	5.50in X 3.29in X 5.10in
Weight	3.046 lbs
Power Dissipation	.125 Watts

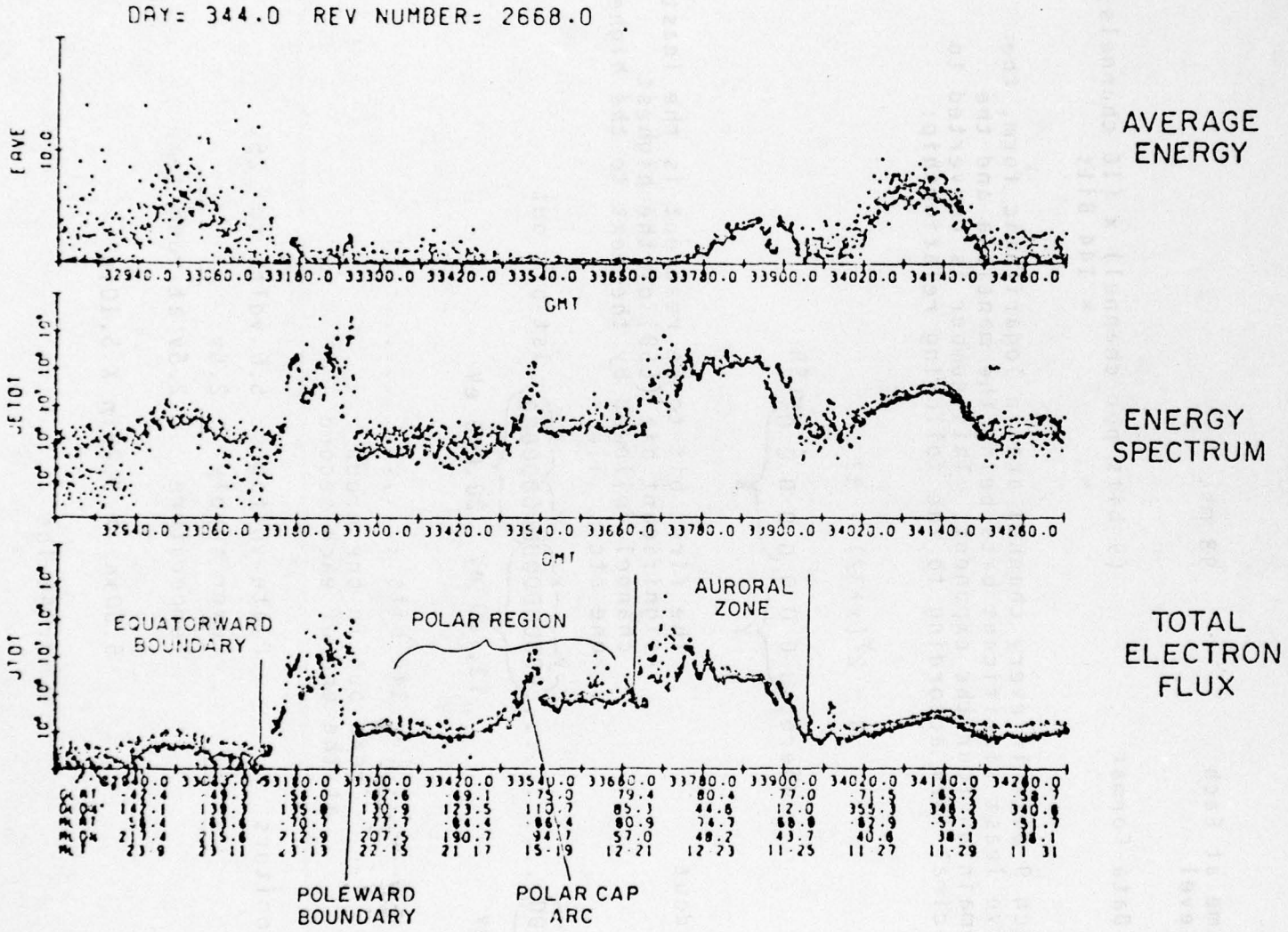
DAY= 344.0 REV NUMBER= 2668.0
EAVE
10.0
32940.0 33060.0 33180.0 33300.0 33420.0 33540.0 33660.0 33780.0 33900.0 34020.0 34140.0 34260.0
GMT
JE101
JT01
EQUATORWARD BOUNDARY
POLAR REGION
AURORAL ZONE
POLEWARD BOUNDARY
POLAR CAP ARC
AVERAGE ENERGY
ENERGY SPECTRUM
TOTAL ELECTRON FLUX

Fig. 2.1

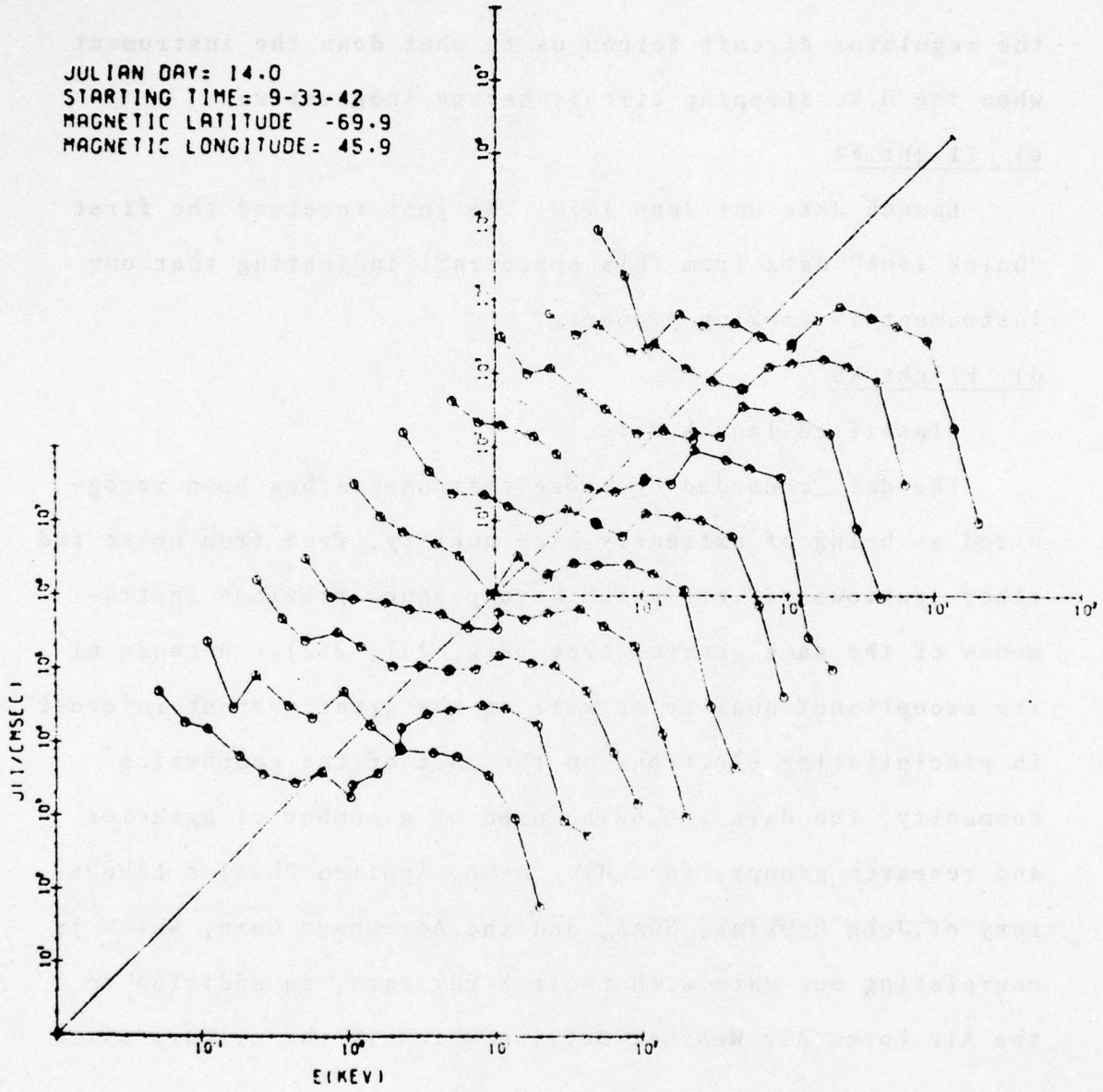

16-POINT ENERGY SPECTRUM OVER THE POLAR REGION FOR 10 CONSECUTIVE SECONDS

Fig. 2.2

b) Flight #3

Launch date was June 1978. Our instrument on this satellite functioned for a few months, but an I.C. failure in the regulator circuit forced us to shut down the instrument when the H.V. stepping circuit became inoperative.

c) Flight #4

Launch date was June 1979. We just received the first "quick look" data from this spacecraft indicating that our instrument is working properly.

d) Flight #5

Classified launch date.

The data recorded by these instruments has been recognized as being of extremely high quality, free from noise and other spurious effects which have plagued previous instruments of the same general type (Fig. 2.1, 2.2). Because of its exceptional quality as well as the great current interest in precipitating electrons on the part of the geophysics community, the data are being used by a number of agencies and research groups, including AFGL, Applied Physics Laboratory of John Hopkins, NOAA, and the Aerospace Corp. which is correlating our data with their X-ray data, in addition to the Air Force Air Weather Service which is the primary user.

2.2 The P78-1 Satellite

The main payload on the P78-1 satellite consists of the Advanced Research Projects Agency (ARPA), 301 Gamma Ray

Spectrometer. There are six secondary payloads, one of which is CRL-251, High Altitude Particle Spectrometer.

2.2.1 The CRL-251 Payload

The mission of this payload is to measure the flux of particles precipitating over the polar cap regions, the auroral zones, and in the plasma pause, and to provide boundary conditions for the particle population of the magnetosphere. These measurements provide data on the link between observed trapped and interplanetary populations, and the particles entering the atmosphere.

In addition, the payload will acquire electron data in the auroral zones, particularly during magnetic storm and substorm periods. The results of these studies, together with existing substorm models and with data from other sources, will be used to improve upon existing substorm models. This will include field-aligned currents and the mechanisms and sources of particle acceleration. Furthermore, these data will be correlated with the AFGL magnetic network data to help AFGL in their efforts toward predicting magnetic activity. The results should be useful to the experiments investigating high energy particles and the auroral regions including the primary mission objectives.

The CRL-251 payload consists of a set of four electrostatic analyzers which perform a differential energy analysis of low energy electrons, simultaneously in two look directions. A 16-point spectrum is produced for each look

direction every 256 msec by the low and high energy analyzers. The analyzers are a conventional curved (cylindrical) plate design with balanced positive and negative deflection voltages.

The CRL-251 sensor box is located in Compartment 9 of the wheel assembly (Figure 2.3). The box is oriented so that the look axis for one set of analyzers is 2.5 deg from the +X axis of the wheel and the look axis for the other set of analyzers is 2.5 deg from the -Y axis of the wheel. The spin axis is perpendicular to the orbital plane so that the wheel rotates in the plane. Thus, the sensors look toward and away from the earth during each spin. Since the particle pitch angle is the angle between the particle direction and the magnetic field vector, the sensors go through 360 deg. of pitch angles for the particles collected, with a good angular resolution.

This instrument was designed to collect electrons in the energy range of 50 eV to 20 keV. Two sets of curved parallel plates have a time-sequenced variable electrostatic field to deflect the electrons toward channeltron multipliers which are used as detectors. One set of plates collects electrons in the energy range of 50 eV to 1 keV, while the second one collects electrons from 1 to 20 keV. These are swept simultaneously to provide four complete spectra every second. Each set of plates is divided into eight energy bins, so that each set of spectra consists of 16 energy bins.

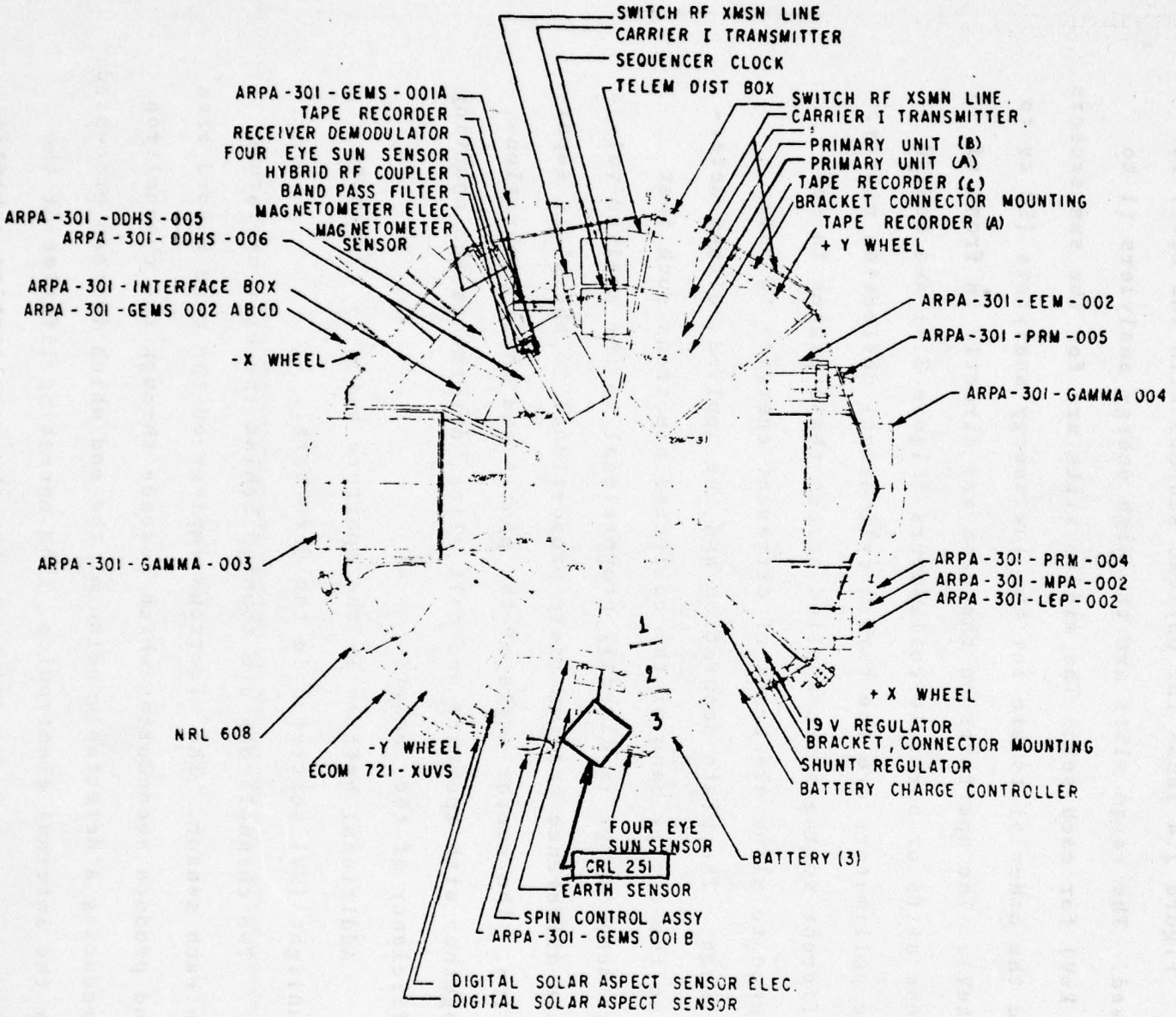

Fig. 2.3

2.2.2 Operational Description

Figure 2.4 shows the payload sensors with the cover removed. The large slits are the high energy analyzers (1 to 20 keV) for each set. The middle slits are for the sun sensors and the other slits are for the low energy analyzers (50 ev to 1 keV). The apertures on the case are directly in front of these slits or particle collimators (Figure 2.5) and behind the collimators are the curved cylindrical deflection plates. Different voltages are applied across these plates in sequence to allow electrons of different energies to pass through. The plate separation and the applied voltage determine the energy band of the collected electrons such that the mean energy is directly proportional to the applied voltage difference and inversely proportional to the plate separation. The sector angle of the plates and their separations, together with aperture and exit slits, determines the counting efficiency of the sensors.

Additional baffles in the aperture assembly eliminate sunlight (UV) scattered in the detectors.

Two channeltrons are mounted behind the exit aperature in each sensor. The electrons impinge on the cone-shaped area and produce secondaries which cascade through the channeltron producing a detectable pulse at the end which is then processed by the internal electronics. The operating lifetime of the channeltrons is extended by having the accelerating potential (3 kV) turned OFF whenever the instrument is looking into the

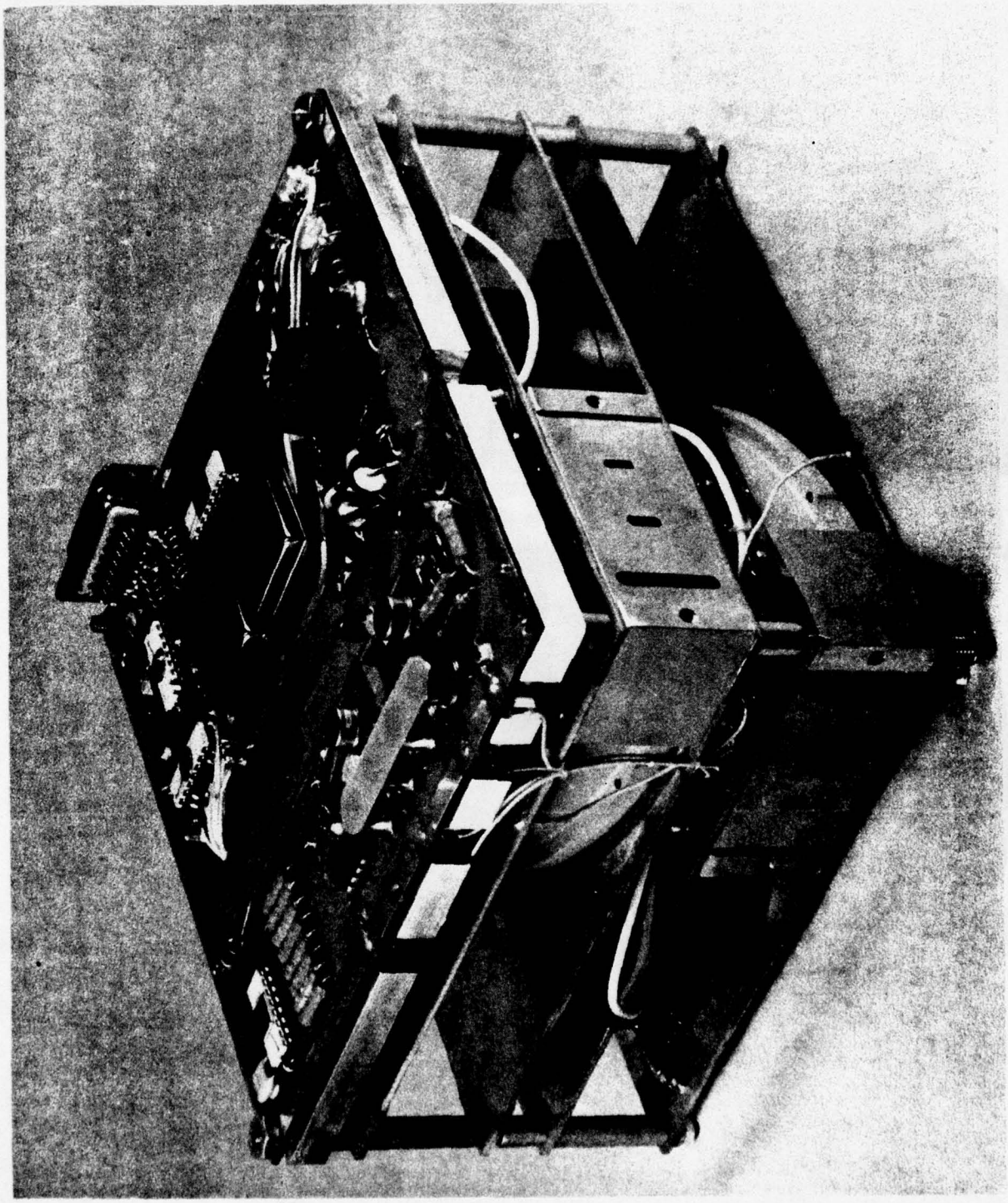

Fig. 2.4

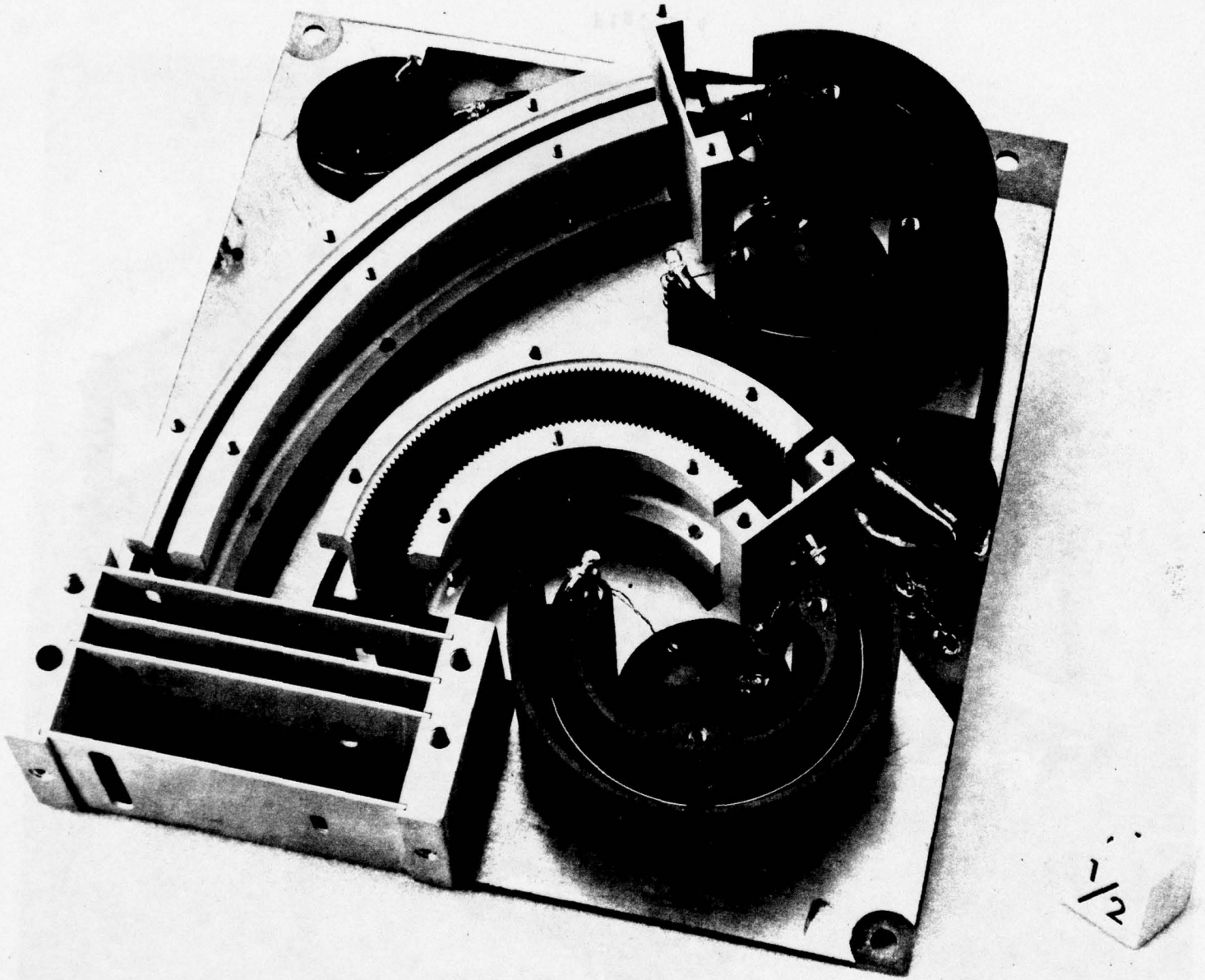

Fig. 2.5

sun. This is determined by a small photo-transistor mounted behind the middle slits of the detectors.

This payload has only one operational mode. All changes are internal and only ON and OFF commands are required. Figure 2.6 is the electrical block diagram. The dc-dc converter supplies power through the doublers to the plate voltage stepper. This supplies eight voltage steps each of 32-msec duration. Each voltage step is monitored to the telemetry. These steps are supplied to each set of analyzer plates as shown. The +3 kV is applied to the channeltrons of each analyzer. Collected electrons produce a cascade effect in the channeltrons and the resulting pulse is amplified and then passed to a logarithmic accumulator to be counted. Each accumulator produces a 5-bit mantissa and a 3-bit exponent and has a capacity of 8032 counts. Counts are accumulated for the 32 msec of each voltage step, at the end of which the contents of all four accumulators are transferred in parallel to the output shift register. The accumulators are then zeroed, the deflection step voltages are incremented, and the accumulators are reenabled for counting at the next energy levels. The contents of the shift register (32 bits) are read out during the following data interval. Since there are eight voltage steps in each sensor for each voltage sweep, a sequence of eight 32-msec data intervals produces two complete 16-channel spectra of electrons in the energy ranges of 50 eV to 1 keV and 1 keV to 20 keV (one spectra for each of the two look

CRL-251 BLOCK DIAGRAM

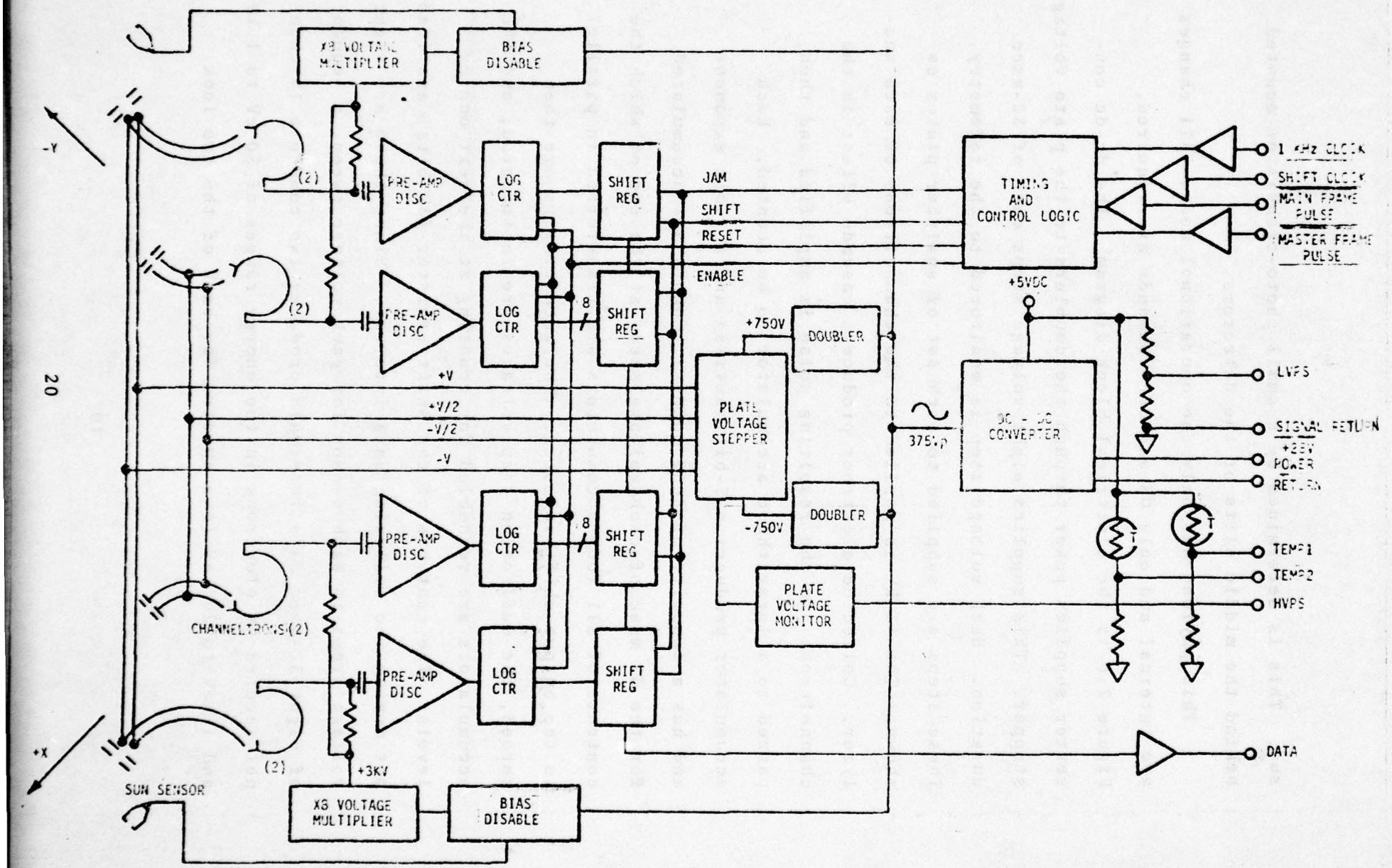

Fig. 2.6

directions). The data words from each analyzer are output to Mainframe 91, the low energy analyzer of Detector 1.

Figure 2.7 shows the CRL-251 enclosure. Finally Table 2.2 gives a summary of the instrument characteristics.

2.2.3 Summary of Operation

The P78-1 satellite was launched on February 24, 1979. "Quick look" data indicate that the electrostatic analyzer is operating nominally. Production data should start arriving at AFGL during FY80.

CRL-251 MECHANICAL DRAWING

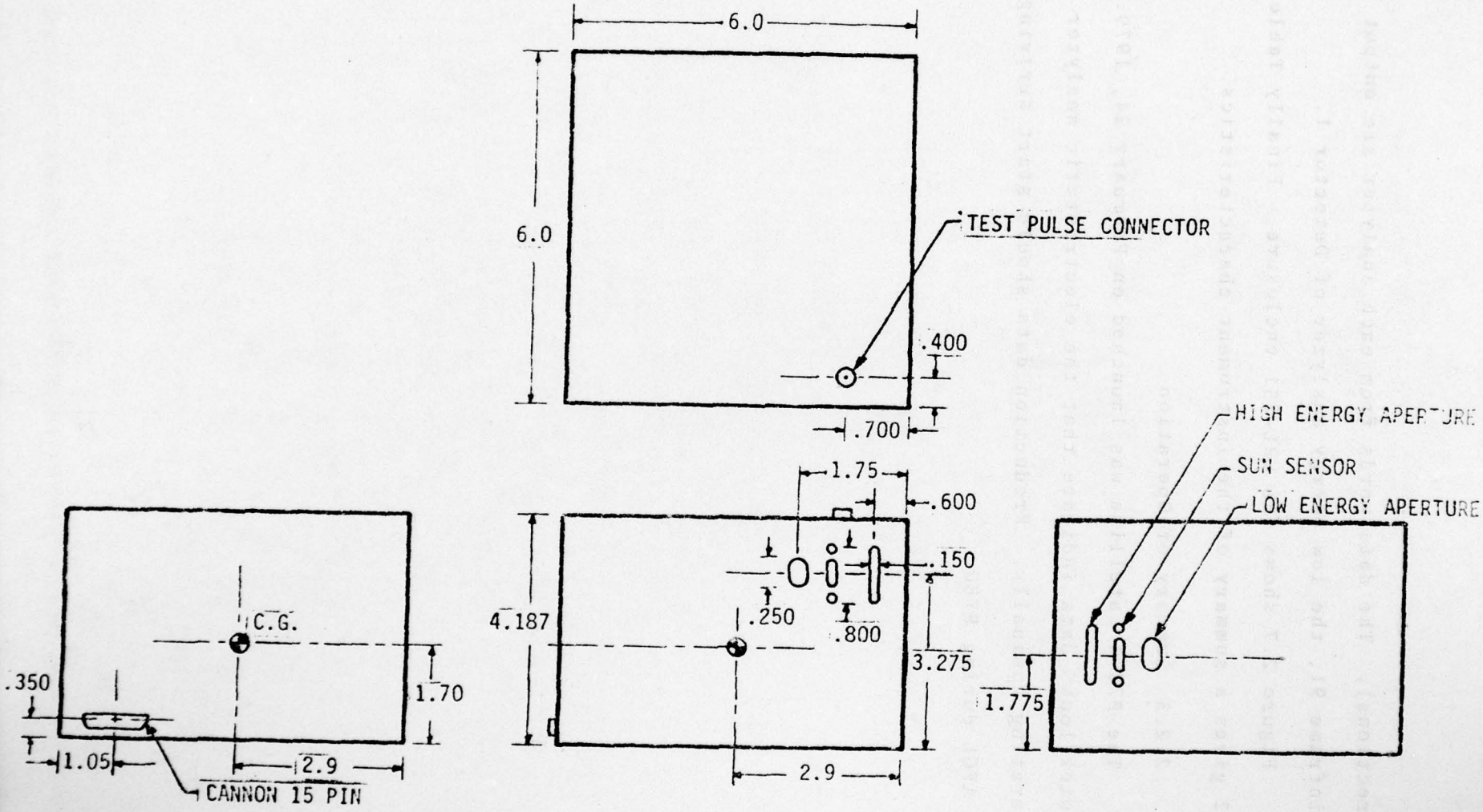

Fig. 2.7

Table 2.2

ELECTROSTATIC ANALYZER (ESA)

CRL-251

Summary of Characteristics

Particles Detected	Electrons
Number of ESAs	Four (two for each of two orthogonal look directions)
Detectors Used	2 Channeltron Electron Multipliers for each of the four sets of ESA plates
Method of Energy Analysis	Voltage Stepping on ESA plates
Number of Energy Bins	8 for each set of ESA plates

Energy Bins for each direction

Large ESA	Small ESA
20.000kev	1.000 kev
13.037	.652
8.498	.425
5.539	.277
3.611	.181
2.354	.118
1.534	.077
1.000	.050

Geometric Factor	Large ESAs : 4.85×10^{-5} cm^2-ster Small ESAs : 1.30×10^{-4} cm -ster
$\Delta E/E$	Large ESAs : 4.2% Small ESAs : 6.7%

Table 2.2 (cont.)

Data Rate	One complete spectrum per 1/4 sec for each look direction
Dwell Time at Each Energy Level	32 msec
Digital Data Format	(8 bits per channel)X(8 energies perESA)X(2 ESAs per direction)X(2 directions)==256 per 1/4 sec

Note: Each 8 bits in every channel are in logarithmic form, the five least significant bits being the mantissa and the remaining three the exponent. This number is converted to decimal form according to the following relationship:

$$N = 2^{y} (x+32) - 33$$

Where: 000 00000 ← LSB
y x

Weight	4.34 lbs
Size	6 in X 6 in X 4.187 in
Power Dissipation	.25 Watts
Analog Monitors	+ 28 Volts + 5 Volts ESA plate voltages Temperature 1 Temperature 2

3. SIMULATION OF LEPS RESPONSE IN ANY GIVEN PROTON BACKGROUND

Considerable amount of proton data were obtained by the Low Energy Proton Spectrometer (LEPS) instruments flown on board the S3-2 and S3-3 satellites.

However not all of the data were useful due to saturation and energy distortion problems which were encountered in areas where large proton fluxes exist. An attempt was made at simulating the LEPS response to a high proton flux environment, with mixed success: although the technique used was accurate to a high level of approximation, it could not be made to account for all observed artifacts in the data.

The technique used in the simulation of the LEPS assumed that the proton energy spectra as observed by the narrow angle instrument on S3-3 was sufficiently accurate to do a Monte Carlo type partial generation, and then determine the observed spectrum and count rates in the wide angle instrument. The simulation was written in FORTRAN language on the CDC6600 computer.

3.1 Model Description

This modeling of the LEPS instrument is divided into two parts. The first part characterizes the response of the instrument in a given angular (solid angle) distribution of a proton flux for a given orientation of the instrument with respect to this distribution. The second part calculates the response of the instrument to the above-mentioned

angular distribution for any given energy distributions. Two programs have been developed, which correspond to these two parts. The first program, MODEL, is run for every angular distribution and orientation which is to be simulated. For each run of program MODEL, various energy distributions can be then run by means of the second program, ENERGY.

As the programs are now structured, the angular distribution used is a so-called pitch-angle distribution which is of the form

$$f(\Omega) = A_{\Omega} \sin^{n}\psi$$

where A is the normalization constant and ψ is the angle between the particle path and the magnetic field vector B. Program ANGLE asks the user to specify both the 'n' in the pitch angle distribution and ψ_0, the angle between B and the instrument axis $\hat{z}$.

The energy distribution used is a power law spectrum of the form

$$f(E) = A_{E} E^{-N}$$

where A is a normalization constant, E is the incident energy, and N characterizes the power-law spectrum.

Other analytic functions could be substituted for these functions with just a few programming changes. Empirical data (probably in the energy spectrum, e.g., the Vette

model) could also be substituted with a few more, but not substantial, programming changes. Furthermore, the changes could be made so that the empirical data could be read in.

The geometry of the instrument has been simplified so as to be more easily modeled mathematically. Because the only major geometrical difference between the wide- and narrow-angle instruments is the diameter of the throat, only this change need be made to the dimensions of the instrument used in the program in order to have the program model one instrument instead of the other.

Individual ray paths are selected by the Monte Carlo method and traced geometrically thru the instrument to determine the path length thru the shielding, the path length thru the first detector, and whether or not the second detector is hit (i.e., whether or not the anti-coincidence circuit is triggered). The path length thru various materials used in the shielding has been reduced to an effective path length in silicon. By means of the appropriate angular distribution and orientation of the instrument axis, program MODEL computes and stores this information, which is then put on a disk memory.

Program ENERGY takes the information supplied by program MODEL and calculates the response of the instrument for various energy spectra.

The assumptions inherent in this model are the following:

1) The protons move in straight lines as they pass thru

the shielding. (Note that any other sub-atomic particle could be modeled as long as (a) it travels in a straight line thru matter, and (b) it has a known range-energy distribution without appreciable statistical fluctuation.)

2) There are no saturation effects taken into account.

3) Any effects where the back detector only is hit are not taken into account.

4) Only particles from the 'forward hemisphere' of the instrument are taken into account. (Note that the 'back hemisphere' could be added, but this would imply a knowledge of the effective shielding of the rest of the satellite.)

5) The spectrum f(E,) is assumed to be separable as

$$f(E,\Omega) = f_1(E)\ f_2(\Omega)$$

i.e., the particular angular dependence (or non-isotropy) is independent of the energy of the particle.

3.2 Modelling the Instrument Geometry

To model the LEPS on the computer it is advisable to reduce the instrument's relatively complex geometry to a simplified form which is more tractable to being modeled in FORTRAN on the computer. A picture of the LEPS is shown in Figure 1. With the exception of the magnets placed on either side of the throat, the instrument is cylindrically symmetrical. A cross-section of the LEPS is shown in Figure 2.1. In this cross-sectional view the geometry of the instrument has been simplified, and it is quite close to what is actually

modeled on the computer.

To calculate the path length thru the shielding of a particular ray, it is necessary to know what surfaces the ray has penetrated and what material(s) were penetrated. All particles are assumed to hit the front detector. (If a particle does not hit the front detector, it is not counted anyway.) The rays are therefore grouped into categories depending on which surfaces it has penetrated, and the ray path is then calculated from the ray-path parameters based on the category into which it fits.

The first separation is based on whether the front detector is hit at a point inside or outside the throat. Within each of these categories the rays are separated based on which surfaces have been penetrated.

In the computer program the surfaces which are penetrated are determined from the parameters of the ray path. Thru each part of the shielding the path length is then calculated in cm based on these ray-path parameters.

3.3 Range-Energy Considerations

Since the instrument shielding is composed of different materials, it is convenient to reduce the path length thru a particular material to an equivalent path length in any one given material. Silicon has been chosen since this is what the detector consists of. Hence the path length in cm thru each piece of the shielding is converted to an equivalent path length in silicon for that piece. The path lengths are

then added to produce a total equivalent path length thru the shielding in equivalent cm of silicon for that particular ray path.

The reason that a path length thru a certain material can be reduced to an equivalent path length in silicon is based on the empirical fact that when the range, expressed in gm/cm^2, is plotted versus the energy of the incident particle, for protons in MeV, the curves for all the materials in question are the same within a relatively small error. The path length thru each material in cm is multiplied by an appropriate conversion factor, this factor being (almost) independent of energy.

3.4 Ray-Paths — Selection Process by Monte Carlo Method

All particles are assumed to pass thru the front detector since, if a particle does not hit the front detector, it is not counted. Particles entering the back surface of the front detector are discounted. In reality the effective shielding of the satellite would have to be taken into consideration, and this is not at any rate known to any degree of accuracy. Particles entering the "sides" of the detector, producing what are called 'side tracks', have been considered but are not dealt with in this report. Hence only particles which pass thru the front surface of the front detector are considered.

Hence, a ray path is chosen by selection, a point on the surface of the front detector and a direction in space by

the Monte Carlo method. The point on the surface is chosen at random based on the assumption that the flux is uniform across any given surface. The direction is chosen at random based on an isotropic flux, i.e., the flux is proportional to the solid angle as seen by the point on the detector surface which is hit. The effective cross-section of the detector surface and any deviations from an isotropic distribution are put in as weighting factors as explained below.

3.5 Coordinate Systems

Let the origin of any coordinate system be at the center of the first detector with the z-axis the plane of the detector. Because of the cylindrical symmetry of the model, we need not specify the orientation of the x and y axes. (However, if for instance the magnets are added to the model, these axes would have to be defined relative to the positions of the magnets.)

We can use coordinate systems which are:

Cartesian	x, y, z
Cylindrical	r, θ, z
Spherical	ρ, α, β

These conventions are used throughout.

3.6 Random Number Selection

To select a parameter x randomly, where $x_1 \leq x \leq x_2$, weighted by a function f(x) we have

$$dr' = f(x)dx$$

$$\int_0^r dr' = A \int_{x_1}^{x} f(x')dx' \tag{1}$$

where r is the random number selected, $0 < r < 1$, and A is a normalization factor defined by

$$1 = A \int_{x_1}^{x_2} f(x')dx'$$

and

$$A = \frac{1}{\int_{x_1}^{x_2} f(x')dx'} \tag{2}$$

Combining (1) and (2) we have,

$$r = \frac{\int_{x_1}^{x} f(x')dx'}{\int_{x_1}^{x_2} f(x')dx'} \tag{3}$$

3.7 Selection of Ray Path Parameters by Means of the Monte Carlo Method

The ray paths are chosen by random numbers. Two random numbers can be used to specify a point on the front detector (r_i, θ_i) in cylindrical coordinates, and two more to specify a direction in space (α_i, β_i) in spherical coordinates. Let the random numbers be ξ_{ij} where i is the number of the ray

path and j is 1-4, the particular random number of the set i. We then have

1) for r

$$d\Omega_{i1} = r_i \, dr_i$$

$$\Omega_{i1} = \frac{\int_0^{r_i} r_i \, dr}{\int_0^{r_0} r_i \, dr} = \frac{r_i}{r_D}^2$$

where r_D = radius of front detector

or $$r_i = r_d \sqrt{\Omega_{i1}}$$

2) for θ

$$d\Omega_{i2} = d\theta_i$$

$$\Omega_{i2} = \frac{\int_0^{\theta_i} d\theta_i}{\int_0^{2\pi} d\theta_i}$$

$$\theta_i = 2\pi\Omega_{i2}$$

3) likewise for α_i we have

$$\alpha_i = 2\pi\Omega_{i3}$$

4) for β_i

$$d\Omega_{i4} = \cos\beta \, d\beta_i$$

$$\Omega_{i4} = \frac{\int_{-\pi/2}^{\beta_i} \cos\beta_i \, d\beta_i}{\int_{-\pi/2}^{\pi/2} \cos\beta_i \, d\beta_i} = \frac{\sin\beta_i + 1}{2}$$

$$\sin\beta_i = 2\Omega_{i4} - 1$$

3.8 Ray-Path Equation

We now have a point on the surface of the detector which we denote by ρ_0 and a direction in space $\hat{d}$. Hence the equation of the ray path is

$$\rho = \rho_0 + s\hat{d}$$

where ρ is the position of a given point with respect to the origin

ρ_0 is the position of an initial point on the detector with respect to the origin

$\hat{d}$ is a unit vector defining the direction in space

s is the path length from the detector surface

in terms of r, θ, α, and we have (note that the subscript i has been dropped):

$$\rho_0 = \hat{x}\, r_0\cos\theta_0 + \hat{y}\, r_0\sin\theta_0 + \hat{z} z_0$$

$$d = \hat{x}\cos\alpha\cos\beta + \hat{y}\sin\alpha\cos\beta + \hat{z}\sin\beta$$

and therefore

$$\rho = \hat{x}(r_0\cos\theta_0 + s\cos\alpha\cos\beta) + \hat{y}(r_0\sin\theta_0 + s\sin\alpha\cos\beta) + \hat{z}(s\sin\beta + z_0)$$

the path length can be expressed in terms of x, y, or z as

$$s = \frac{x - r_0 \cos\theta_0}{\cos\alpha\cos\beta} = \frac{y - r_0 \sin\theta_0}{\sin\alpha\cos\beta} = \frac{z - z_0}{\sin\beta}$$

where the subscript '0' is used to note the value of a parameter on the detector surface. The equations for x, y, and z are:

$$x = r_0 \cos\theta_0 + s \cos\alpha\cos\beta$$

$$y = r_0 \sin\theta_o + s \sin\alpha\cos\beta$$

$$z = z_0 + s \sin\beta$$

the path length (s_2-s_1) between two points 1 and 2 is therefore:

$$s_2 - s_1 = \frac{x_2 - x_1}{\cos\alpha\cos\beta} = \frac{y_2 - y_1}{\sin\alpha\cos\beta} = \frac{z_2 - z_1}{\sin\beta}$$

for the plane surface $z = z_s$, we have

$$s = \frac{z_s - z_0}{\sin\beta}$$

and we can solve for x and y. In the case of a cylinder $r = r_s$, we have

$$r_s^2 = x^2 + y^2$$

$$= r_0^2 + 2r_0 s \cos\beta\cos(\theta_0-\alpha) + s^2 \cos^2\beta$$

solving for s,

$$\frac{-B \pm \sqrt{B^2 - 4AC}}{2A}$$

where $A = \cos^2\beta$

$$B = 2r_0 \cos\beta\cos(\theta_0-\alpha)$$

$$c = r_0^2 - r_s^2$$

The intersection (if there is one) of a ray with a cone can be found in similar fashion.

3.9 Calculation of the Effective Path Length Thru the Shielding

3.9.1 Intersection of the Ray Path with a Given Surface

To solve for the intersection of the ray path with a given surface, we take the equation of the surface and plug it into the equation for ρ. For this instrument the geometrical figures of interest are the cylinder, plane surface at a given z, and the cone. This is part of the rationale for the simplification of the instrument geometry explained above.

The equation for ρ is then solved to determine s, the distance from the surface of the detector at which the ray path intersects the surface of interest. An example is here given for a surface $z = z_s$, i.e., one which is parallel to the surface of the detector, and $r = r_s$, i.e., a cylindrical surface which is concentric with the detector.

3.9.2 Calculation of the Effective Path Length Thru the Shielding

Knowing the points 1 and 2 at which the ray intersects the two appropriate surfaces which delimit a particular piece of the shielding, one can then calculate the path length in cm through this piece by

$$\Delta s = s_2 - s_1$$

This is then converted to equivalent cm in silicon s' by multiplication by the appropriate factor f

$$\Delta s' = f\Delta s$$

The sum of the effective path lengths R_s is then

$$R_s = \Sigma \Delta s' = \sum_i f_i \quad s_i'$$

If the particle comes straight down the throat, no shielding is penetrated, $R_s = 0$, and the ray is termed a 'legitimate' ray. Conversely, for $R_s > 0$, the ray is termed an 'illegitimate' ray.

3.10 Calculation of the Path Length Thru the Front Detector

The path length thru the front detector R_D is then calculated by the formula

$$R_D = \frac{t_D}{\sin\beta}$$

where t_D is the thickness of the front detector. Note that this calculation assumes that the ray passes out at the front detector thru its back surface and not thru the side. This is a reasonable approximation to the actual case since not many rays will pass thru the side. This effect is, however, taken into account when the sides of the detector are considered and is not treated in this report.

3.11 Weighting Factor and R_s vs R_D Matrices

These two path lengths and whether the anticoincidence is triggered provide the necessary information to determine the response of the instrument to a particle with the given particle path with a given energy. However, program MODEL

takes these quantities and enters a number in one of two matrices, one for which the anticoincidence is triggered and one for which is not. The element of the appropriate matrix to which the number is added is determined by the path length thru the shielding R_s, which determines the row of the matrix, and the path length thru the first detector R_D, which determines the column of the matrix. The number which is actually entered in this matrix element is determined by the angular distribution itself and by the effective cross section of the front detector.

The upper and lower limits for R_s and R_D are predetermined, and the 'boxes' of the matrices are evenly spaced logarithmically. For example, if R_s and R_D are a pair of path lengths we have

$$\frac{\log R_s}{\log(R_s)_{max}-\log(r_s)_{min}}(I_{max}-1) \leq I < \frac{\log R_s}{\log(R_s)_{max}-\log(R_s)_{min}} I_{max}$$

$$\frac{\log R_D}{\log(R_D)_{max}-\log(R_D)_{min}}(J_{max}-1) \leq J < \frac{\log R_D}{\log(R_D)_{max}-\log(R_D)_{min}} J_{max}$$

where I and J denote the matrix element, and I_{max} and J_{max} are the number of rows and columns in the matrix.

The selected ray is chosen with no regard as to the effective cross section of the detector surface or the angular distribution in question. These effects are added by means of a weighting factor. The effective area of the detector is $\cos\beta$, and the angular distribution function $f(\Omega)$ provides its weighting factor. In the case where $f(\Omega) = \sin^2\psi$ we have for a weighting factor $\cos\beta\sin^2\psi$ where $\psi = \psi(\alpha,\beta)$ is known. This function ψ

will depend on ψ_o, the angle between the instrument axis $\hat{z}$ and the magnetic field B.

This weighting factor is then added to the appropriate element I, J, calculated above, of one of the two matrices, depending on whether or not the anti-coincidence circuit is triggered. The program then goes back to select the next ray. The two matrices are thus built up as the requisite number of rays is processed. (10,000 rays seems to give good results, and this takes 5 seconds of computer time. For better accuracy 100,000 rays are recommended, which would take 50 seconds.)

If the ray is a legitimate ray the weighting factor is added to the legitimate ray count.

Note that in Program MODEL the anti-coincidence matrix is used as long as the second detector is hit. There are instances whrere the anticoincidence circuit is not triggered even though the particle hits the second detector. However, effects such as these are taken into account in Program ENERGY.

This concludes the calculation done by the first Program MODEL. The matrices and other information are printed on the line printer and are stored on a permanent file of the disc to be processed by the second Program, ENERGY. Given the particular instrument to be modeled, wide or narrow-angle, and given the pitch-angle distribution and the angle of the instrument axis with the magnetic field, MODEL provides the number of legitimate particles and histograms of path length thru the shielding versus path length thru the detector for illegitimate particles for both the coincidence and anti-coincidence mode.

3.12 Construction of the Joint Distribution of R_s and R_D

The input to program ENERGY is the number of legitimate particles and two matrices which are number densities as a function of R_s and R_D for the anticoincidence (AC) mode and the non-anticoincidence (NAC) modes, respectively. If N_{1ij} and N_{2ij} represent these two matrices, respectively, and L represents the number of legitimate particles, the total number of particles is

$$N_p = L + \sum_{i,j} N_{1ij} + \sum_{i,j} N_{2ij}$$

Dividing the elements of each of these matrices by N_p, we have an approximation to a joint probability distribution. Defining the mode m such that

m = 0 Legitimate particle

m = 1 Illegitimate particle with anticoincidence

m = 2 Illegitimate particle with no anticoincidence

we can express this distribution as

$$p(0,0,0) = \frac{L}{N_p}$$

$$\int_{R_s(i)}^{R_s(i+1)} \int_{R_D(i)}^{R_D(i+1)} p(R_s,R_D,m)\, dR_s dR_D = \frac{N_{mij}}{N_p} \qquad m = 1,2$$

or

$$p(R_s,R_D,m) = \frac{N_{mij}}{\Delta R_s \, \Delta R_D \, N_p}$$

where $\Delta R_s \Delta R_D$ is the 'area' of a matrix element. Note that these 'areas' will vary from element to element since they are set up logarithmically.

3.13 Determination of the Energy Dropped in the First Detector

The joint probability distribution $p(R_s,R_D,m)$ is a function of R_s and R_D. It is necessary to find the energy E_D dropped in the first detector for a given incident energy E_0 as a function of R_s and R_D. Then given E_0 we can determine the conditional distribution $\rho(E_D/E_0)$, i.e., the probability of an energy E_D being deposited in the front detector, given an incident energy E_0.

This is done through application of the range-energy relation (derived empirically from Barkas and Berger)

$$R = BE_0^M$$

where R is the range in silicon for a proton of incident energy E_0, and B and M are constants derived from the fit to the empirical data. Since R_s is understood to be equivalent cm of silicon, and R_D is the range through a silicon detector, this formula is all that is needed.

By algebraic manipulation we find that the energy E_x of the particle after it leaves the shielding is

$$E_x = E_0^M - \frac{R_s}{A}^{1/M}$$

The energy the particle has lost in the shielding is

$$E' = E_0 - E_x = E_0 - E_0^M - \frac{R_s}{A}^{1/M}$$

It is next determined whether or not the particle is stopped in the first detector. If the relation

$$R_D \quad BE^{1M}$$

is true, the particle is stopped in the first detector and we have

$$E_D = E' = E_0 - E_x$$

For $R_D < BE^{1M}$, we must find E_D in a manner similar to the way E' is found, and we have

$$E_D = E_x - \left(E_x^M - \frac{R_s}{A} \right)^{1/M}$$

Since the calculation of E_D is not straightforward, and it is not desirable to use the analytic expression for E_D, it becomes necessary to choose a number of values for E_D which adequately cover the energies of interest at the incoming flux. Then for each value of E_D a table is made of

$$E_D = E_D(R_s, R_D)_{E=E_D}$$

where the values of R_s and R_D in the table correspond to those input from program ANGLE.

At present 15 values of E_0 are calculated. These values span the interval from 10 to 500 MeV in a quasi-logarithmic manner. The actual values are 10, 20, 30, 40, 50, 60, 70, 80, 90, 100, 125, 150, 175, 200, 300, 400, and 500 MeV.

3.14 Calculation of the Conditional Distribution

For each value of E_0 chosen, the table of E_D (R_s, R_D) is scanned, and for all entries of E_D, which fall within the

channel width of interest, the value of N_{1ij} or N_{2ij} is added to make up the conditional distribution as explained below. We here define 'n' as the channel number and ε_n as the threshold energy of the nth channel. (The cutoff energy of the top, or 12th channel is 6 MeV). We are then calculating a function $F_c(E_0,n)$, which corresponds to a theoretical conditional probability distribution of E_D given E_0, which we will write $\phi(E_0/E_0)$. We then have

$$F_c(E_0,n) = \sum_{i,j} N_{2,i,j} + \sum_{i,j} N_{1,i,j}$$

$$\varepsilon \quad E_D \quad \varepsilon_{n+1} \qquad\qquad E_D = E_{ex}$$

The first term in this equation counts rays for which the anticoincidence circuit was not triggered due to the fact that the ray misses the second detector: this dictates the use of the matrix N_{2ij}. The second term counts rays for which the anticoincidence circuit was not triggered due to the fact that the ray was stopped in the front detector - hence the use of N_{1ij}.

Relating $F_c(E_0,n)$ to the theoretical distribution $\phi(E_D/E_0)$ we have

$$\frac{F_c(E_0,n)}{N_P} = \int_{\varepsilon_n}^{\varepsilon_{n+1}} \phi(E_D/E_0)\, dE_0$$

We can calculate an approximation to $\phi(E_D/E_0)$ by

$$\phi(E_D/E_0) = \frac{F_c(E_0,n)}{N_p(\varepsilon_{n+1}-\varepsilon_n)}$$

Relating it to the joint probability distribution we have

$$\frac{F_c(E_0,n)}{N_p} = \int_{\varepsilon_n}^{\varepsilon_{n+1}} dE_0 \iint_{\varepsilon_n \leq E_0 \leq \varepsilon_{n+1}} p(R_s,R_D,2)\, dR_s\, dR_D$$

$$+ \int_{\varepsilon_n}^{\varepsilon_{n+1}} dE_0 \iint_{E_0=E_{ex}} p(R_s,R_D,1)\, dR_s\, dR_D$$

3.15 The Incident Spectrum

Now the conditional distribution $\phi(E_D/E_0)$ is related by definition to the joint distribution $f(E_D,E_0)$ by the equation

$$f(E_D,E_0) = \phi(E_D/E_0)\ f_0(E_0)$$

where $f_0(E_0)$ is the marginal distribution of E_0. Physically $f_0(E_0)$ is equivalent to the incident spectrum, i.e., the distribution of incident energies of the protons, as long as the following normalization is maintained.

$$\int_{E_1}^{E_2} f_0(E_0)\, dE_0 = 1$$

where E_1 and E_2 are the bounds of the energy range of interest. E_1 is set to ε_1, the threshold ε_1 of the first channel

(=100 keV), and E_2 is set to the maximum energy for which there are still appreciable counts in the incident spectrum. We have chosen E_2 = 500 MeV.

In the program as it now stands, a power law distribution is used of the form

$$f_0(E_0) = AE_0^{-N}$$

where N characterizes the distribution and A is a constant found by solving the normalization condition explained above. Power law distributions with N=1,2,4,8 are used in the program. By means of fairly simple programming changes, this function could be changed to another empirical function, or empirical data with a simple interpolation scheme could also be substituted.

The number of legitimate particles $C_i(n)$ in a particular channel can now be calculated by

$$C_i(n) = \frac{L}{N_p} \int_{\varepsilon_n}^{\varepsilon_{n+1}} f_0(E)\, dE$$

3.16 The Background Count

The background which will be counted by the LEPS is equal to the marginal distribution of the energy E_D deposited in the first detector, $f_D(E_D)$. This can be found by integrating the joint distribution of E_D and E_0 over the whole energy spectrum,

$$f_D(E_D) = \int_{E_{min}}^{E_{max}} f(E_D, E_0) dE_0$$

To get the background counts in a given channel $C_B(n)$, we must integrate with respect to E_D over that channel's range of energy, and we have

$$C_B(n) = \int_{\varepsilon_n}^{\varepsilon_{n+1}} f_0(E_0)dE_0$$

$$= \int_{\varepsilon_n}^{\varepsilon_{n+1}} dE_D \int_{E_{min}}^{E_{max}} f(E_D,E_0)dE_0$$

In the program we calculate an approximation to $C_B(n)$ by

$$C_B(n) = \frac{1}{N} \sum_{E_i} F_c(E_i,n)\ f_0(E_i)\ (E_{i+1} - E_i)$$

where E_i are the incident proton energies.

For each channel, the total count $C_i(n)$ is the sum of the background and the legitimate particles

$$C_T(n) = C_B(n) + C_L(n)$$

the fraction p(n) of legitimate particles in the total count is then

$$p(n) = \frac{C_L(n)}{C_B(n) + C_L(n)}$$

when looking at real data, it is this quantity to which the data would be compared.

3.17 Conclusions

The modeling which has been developed will be used to interpret data which have been taken by existing LEPS instruments in orbit. Spectra measured by the LEPS will be input to

the programs, and the programs will produce the output which the respective spectra should have generated. Comparison will reveal whether the data actually taken were good.

Another task that is proposed is to input data from an existing model of the magnetosphere, such as the Vette model. The programs will provide output telling what the instrument should measure in the given environment. This output will then be compared with actual data taken by the LEPS. In this way the modeling of LEPS in conjunction with the LEPS data can be used to test existing models of the magnetosphere.

Further modifications can also be made to take into account electronic characteristics of the instruments. For instance, the program could be programmed to take into account any dead-time effects. This type of extension to the modeling would possibly require some laboratory work to exactly define the response of the instrument to a particlar effect. Once this effect has been sufficiently defined, it would then be modeled mathematically and coded into the programs.

4. DATA ANALYSIS

4.1 Data Handling Software Development

An interest was expressed in scanning the data bases of the S3-2 and S3-3 satellites for evidence of solar activity. In order to accomplish this, some restructuring of the data files was necessary to allow for analysis of a full 360° pitch angle distribution and remove an artificially low upper-limit on the "L-shell" calculations. This restructuring was done and one tape containing 25 orbits of data from the S3-2 satellite was reprocessed to serve as input for development of the data analysis software.

One initial goal of the S3-2 and S3-3 data analysis projects was to generate a complete graphical documentation of the data bases through calcomp-type CRT plots. This goal was abandoned when it became obvious that the existing CRT facilities at AFGL were inadequate. However, the CRT/Microfiche equipment recently installed at AFGL does have the capability we need for the project. Most of the required software was developed before the original abandonment of the project. However, our plotting software had to be updated to provide options for the additional capabilities of the new CRT facility. Also the original decision to fold the pitch angle dependence of the data base into a 180° system proved to be a mistake since it did not allow for adequate visualization of the polar region activity.

Specifically, updates were required in the following

data reduction/data analysis programs.

a) S2BLAF/S3BLAC. These programs add the magnetic field and pitch angle coordinates to the data files. It was necessary to begin reprocessing the data bases at this stage because the previous cutoff at "L" = 10.00 proved to be too low for analysis of the polar region data.

b) S2SBFK/S3SACD. These programs separate the data into sequential groups relative to predetermined "L" and "H_{min}" boundaries. Alterations were necessary to incorporate the new 360° data formats.

c) S2PLAA/S3PLAA. These programs process the output from the above stage and generate an intermediate file for input to our plotting software. An update was necessary in order to incorporate the 360° data format and to maintain compatability with our plotting software.

d) DCRVBH. This program and its associated subroutines is our basic plot generating software. Several revisions were made to it relative to the new capabilities provided by the recently installed CRT/Microfiche facility at AFGL. Also a major revision was made to enhance its frame blocking capabilities so that it is now possible to combine up to 15 plots into one frame in either a 1 by <15, 2 by <5, or 3 by <5 format. The previous version had only the 1 by <15 capability.

The above revisions were complete for the S3-2 satellite and the test tape was run giving satisfactory results.

However, the decision was made to proceed directly to the S3-3 data set, incorporating the ideas developed for S3-2 into the S3-3 graphics package.

4.2 S3-2 Proton Data Analysis

4.2.1 Goal

The Low Energy Proton Spectrometer (LEPS) on board the S3-2 polar orbiting satellite provides statistically significant proton data in the 100-200 keV energy range over the polar cap regions. These data are available over a six month interval from December 1975 to May 1976. The angular resolution of the pitch angle distribution is fifteen degrees, and thus provides valuable details in these observations. The purpose of this investigation was to study the different proton pitch angle distributions and their relation to the solar activity, magnetic activity, and possibly to the geographic longitude in connection with the South Atlantic anomaly.

4.2.2 Method

Initially, a graphical display of the raw data for the 100 or 200 keV protons offered a "quick look" at the data for particular polar passes. Figures 4.1 and 4.2 show plots of the count rates vs. time (in seconds) for typical passes. Varying flux distribution patterns are seen as the satellite moves from the trapped regions where the flux is modulated by the sixteen second spin period of the satellite

(cf. Fig. 4.3), to a region of quasi-trapped particles which exhibit a flat distribution outside the loss cone (cf. Fig. 4.4). Over the polar regions ($\Lambda > 70°$), we observe a peak, at approximately $|120°|$ in the pitch angle distribution (cf. Fig. 4.6 to 4.9). Figure 4.5 shows a typical polar pass in invariant latitude, magnetic local time coordinates.

Plots exemplified by Figures 4.1 and 4.2 enable us to set the spatial limits over which data can be superimposed and averaged (quasi-trapped, polar magnetic night or day). These averagings, over a given ΔL, were made over time intervals of approximately one hundred seconds.

For the purpose of uncovering any correlation of proton flux with solar activity, the active period of March 26 to April 1, 1976 was selected.

4.2.3 Results

The results of this investigation were presented at the 1978 Fall AGU Meeting (cf. EOS, 59, 1172, 1978). During the above-mentioned period of high solar activity, over the polar region above $\Lambda = 76°$, a peak repeatedly appeared in the pitch angle distribution at approximately -120° (cf. Figs. 4.6 to 4.9). This peak was not present during times of quiet sun and quiet magnetic field on April 17, 1976, as shown in Figures 4.10 and 4 11. On this date the count rates were very low ($\sim$1 sec^{-1}) for all pitch angles. This fact lead us to believe that there was no solar UV contamination of the observations. Also, because of the efficiency of the

sweeping magnets in the LEPS, we felt confident that there was virtually no electron contamination in the proton data. Further analysis of the data for other times in the six month period is projected in order to ascertain the possible correlation which seems to exist between the peculiar pitch angle distributions, as observed from March 26 - April 1, 1976, and the solar and magnetic activities, and possibly with the geographic longitude.

Documentation, overhauling, debugging, and testing are proceeding on the LEPS Monte Carlo simulation program. Major changes are being made which will: 1) make the program easy to use for those not familiar with computers and 2) make the simulation applicable to instruments other than the LEPS.

Whereas before, the specific geometry of the LEPS was actually written into the Fortran code, the program will now be independent of the particular dimensions and geometry of the instrument, as long as the geometry of the instrument is 'similar' to that which the program can accept. The program can then be used on instruments of somewhat different geometry without changing any of the Fortran code.

Debugging and testing of the program are proceeding concurrently with the above work.

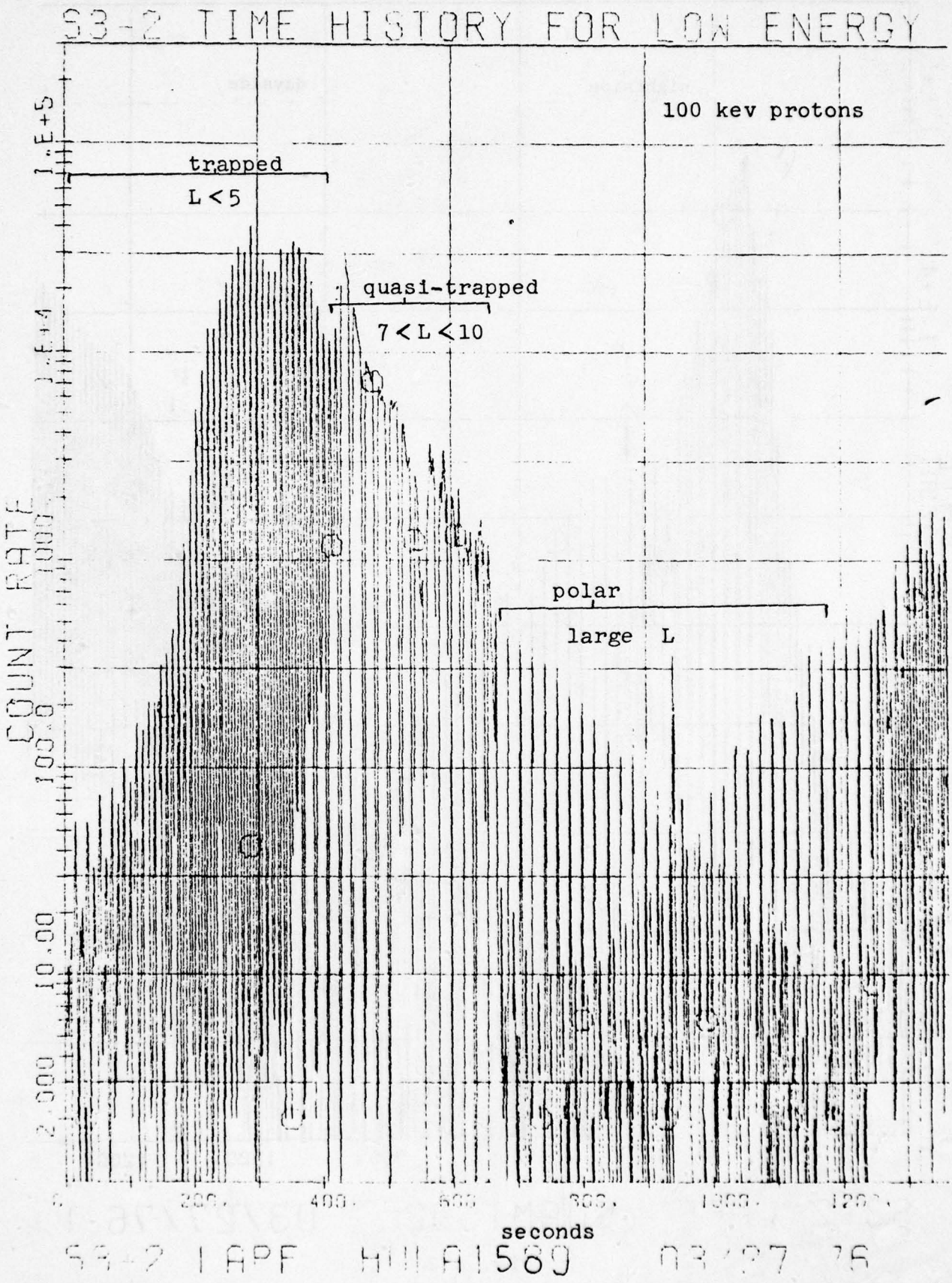
S3-2 TIME HISTORY FOR LOW ENERGY
100 kev protons
trapped
L<5
quasi-trapped
7<L<10
polar
large L
COUNT RATE
1.E+5
1.E+4
1000.
100.0
10.00
2.000
seconds
S3-2 IAPF HILA1580

Fig. 4.1

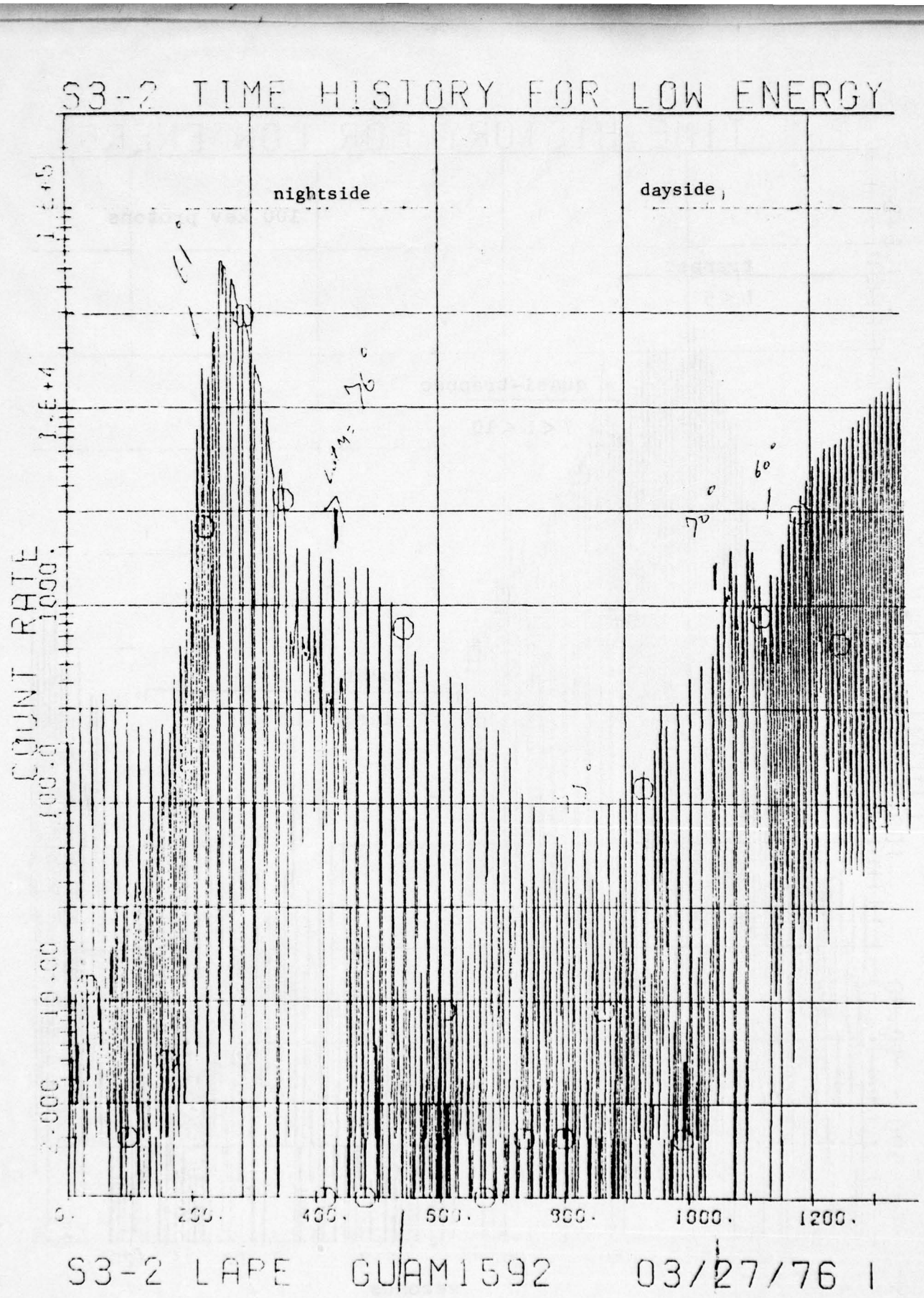
S3-2 TIME HISTORY FOR LOW ENERGY
nightside
dayside
COUNT RATE
1000.
100.0
10.00
2.000
0.
200.
400.
600.
800.
1000.
1200.
S3-2 LAPE GUAM1592 03/27/76

Fig. 4.2

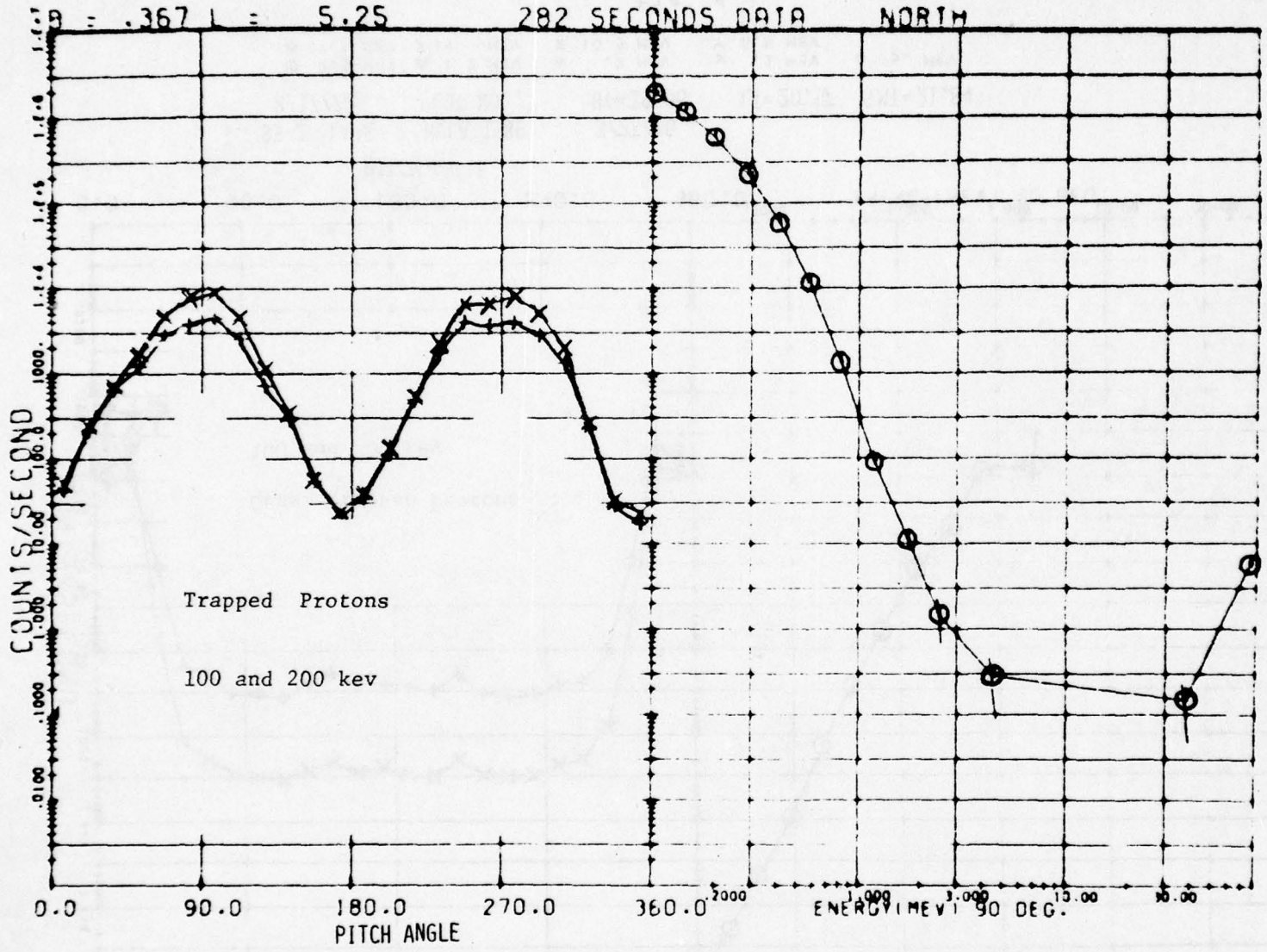
B = .367 L = 5.25 282 SECONDS DATA NORTH
COUNTS/SECOND
Trapped Protons
100 and 200 kev
0.0
90.0
180.0
270.0
360.0
PITCH ANGLE
ENERGY(MEV) 90 DEG.
S3-2 LAPE HULA 1589 03/27/76
08/17/78 PLOT NO.11 UT=19.61 LT=10.07 GMT= 9.96
4.5 MEV
1.2 MEV
.2 MEV
.1 MEV
75. MEV
37.5 MEV
19 MEV
10.5 MEV
6.8 MEV

Fig. 4.3

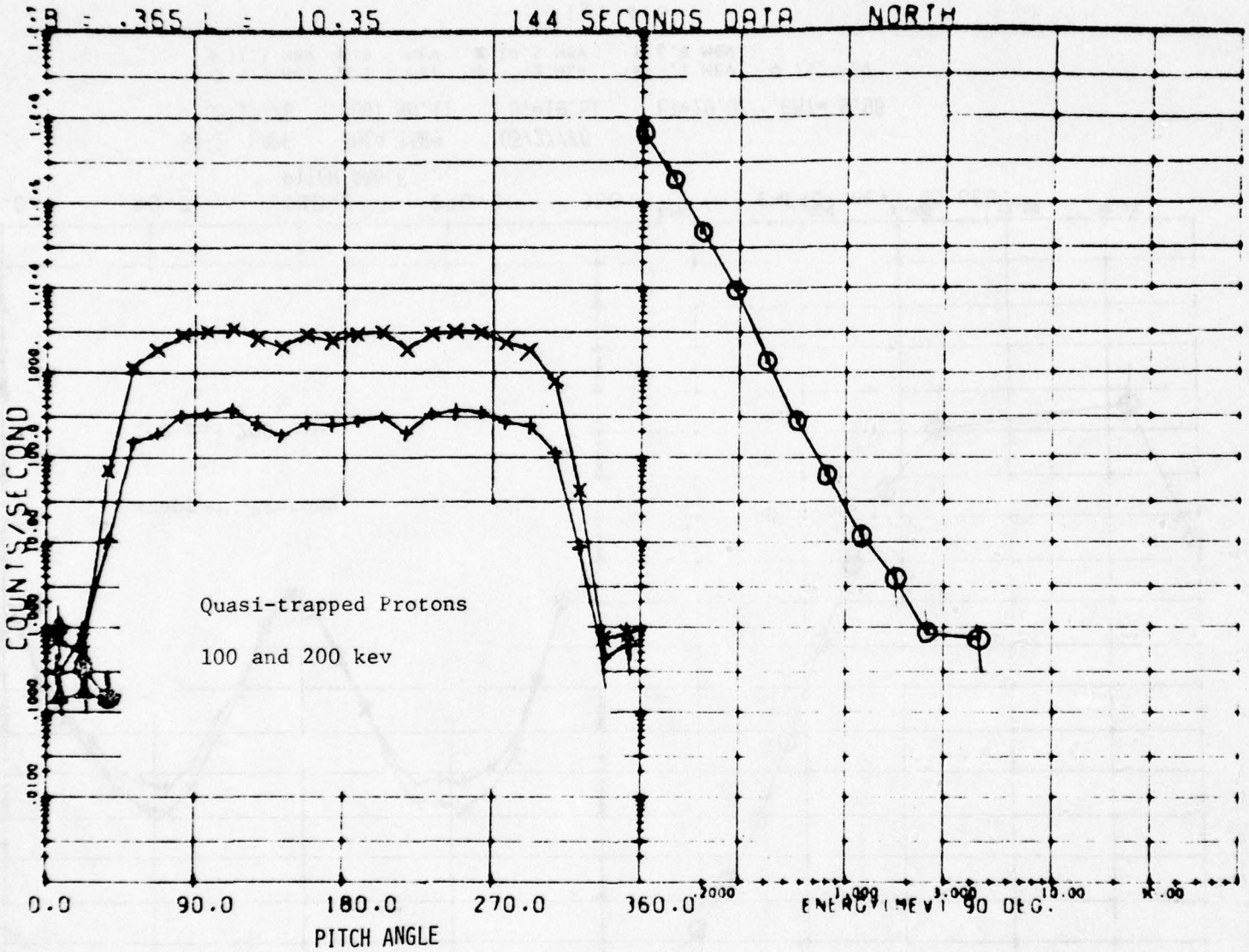
B = .365 L = 10.35
144 SECONDS DATA
NORTH
COUNTS/SECOND
Quasi-trapped Protons
100 and 200 kev
0.0
90.0
180.0
270.0
360.0
PITCH ANGLE
ENERGY (MEV) 90 DEG.
S3-2 LAPE
HULA 1589
3/27/76
8/17/78
PLOT NO. 2
UT=19.06
LT=20.57
GMT=21.84
4.5 MEV
1.2 MEV
.2 MEV
.1 MEV
75. MEV
37.5 MEV
19 MEV
10.5 MEV
6.8 MEV

Fig. 4.4

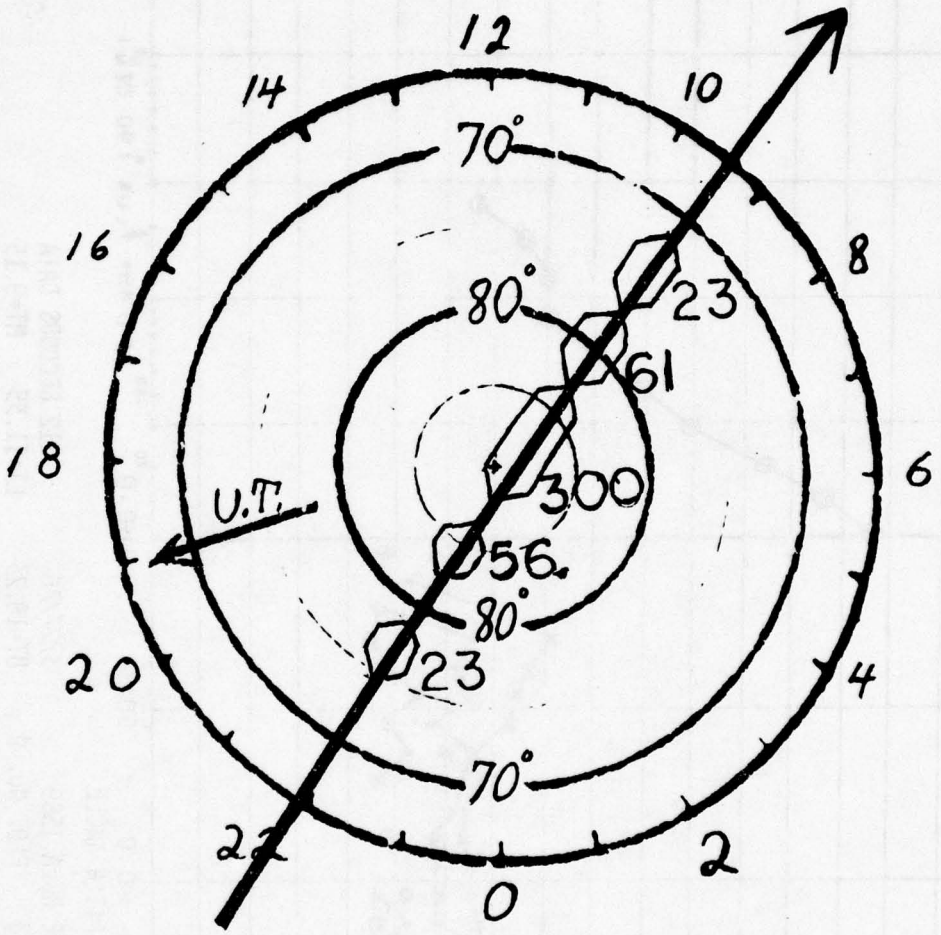

S3-2 polar orbital pass in invariant latitude, magnetic local time coordinates. Boxes enclose "snapshot" L averaged regions.

Fig. 4.5

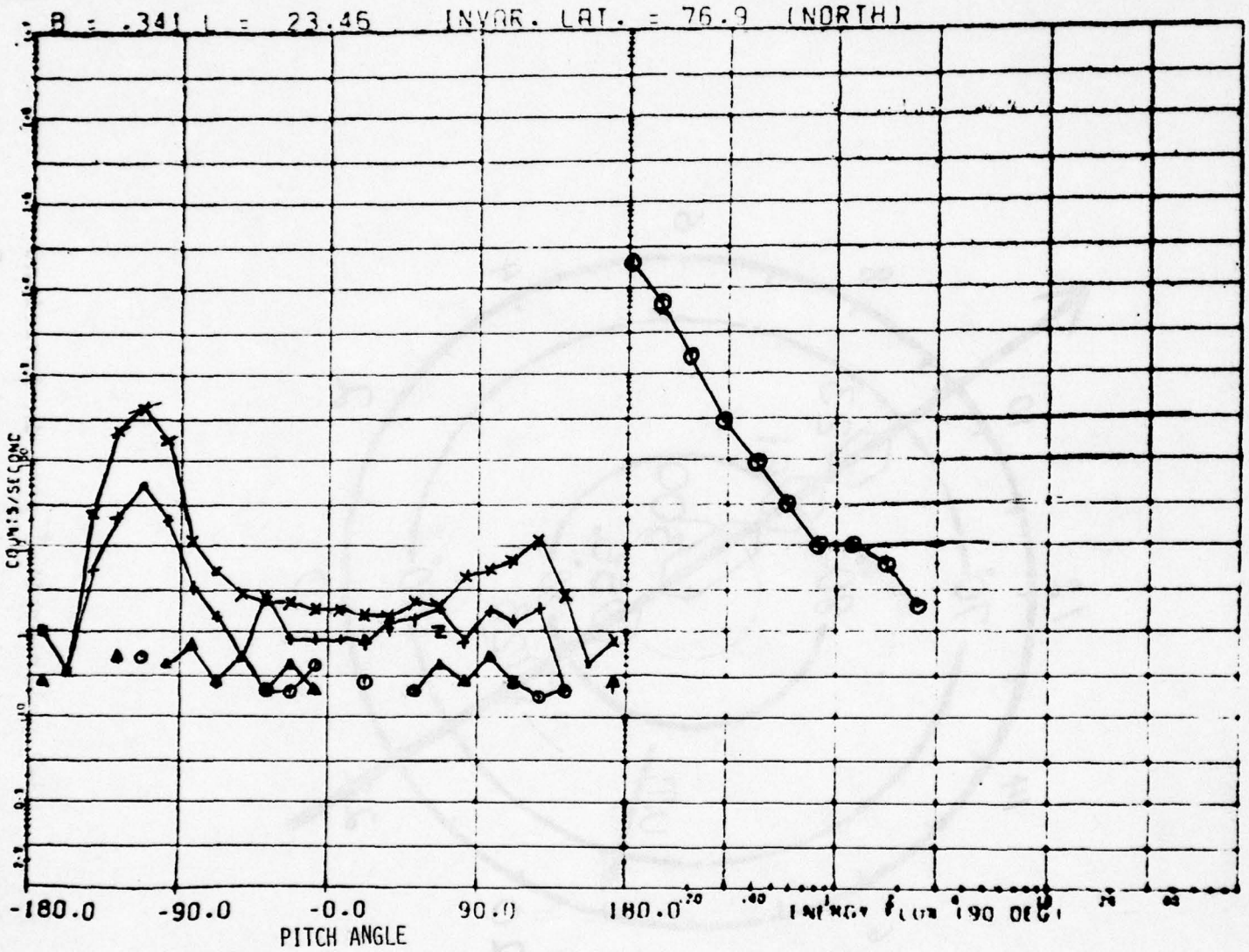

S3-2 LAPE HULA 1589 3/27/76 112 SECONDS DATA
11/17/78 PLOT NO. 9 UT=19.23 LT=11.35 MT=9.15

○ 4.5 MEV △ 1.2 MEV + .2 MEV × .1 MEV ◇ 75. MEV
◬ 37.5 MEV ⧗ 19 MEV Z 10.5 MEV Y 6.8 MEV

Fig. 4.6

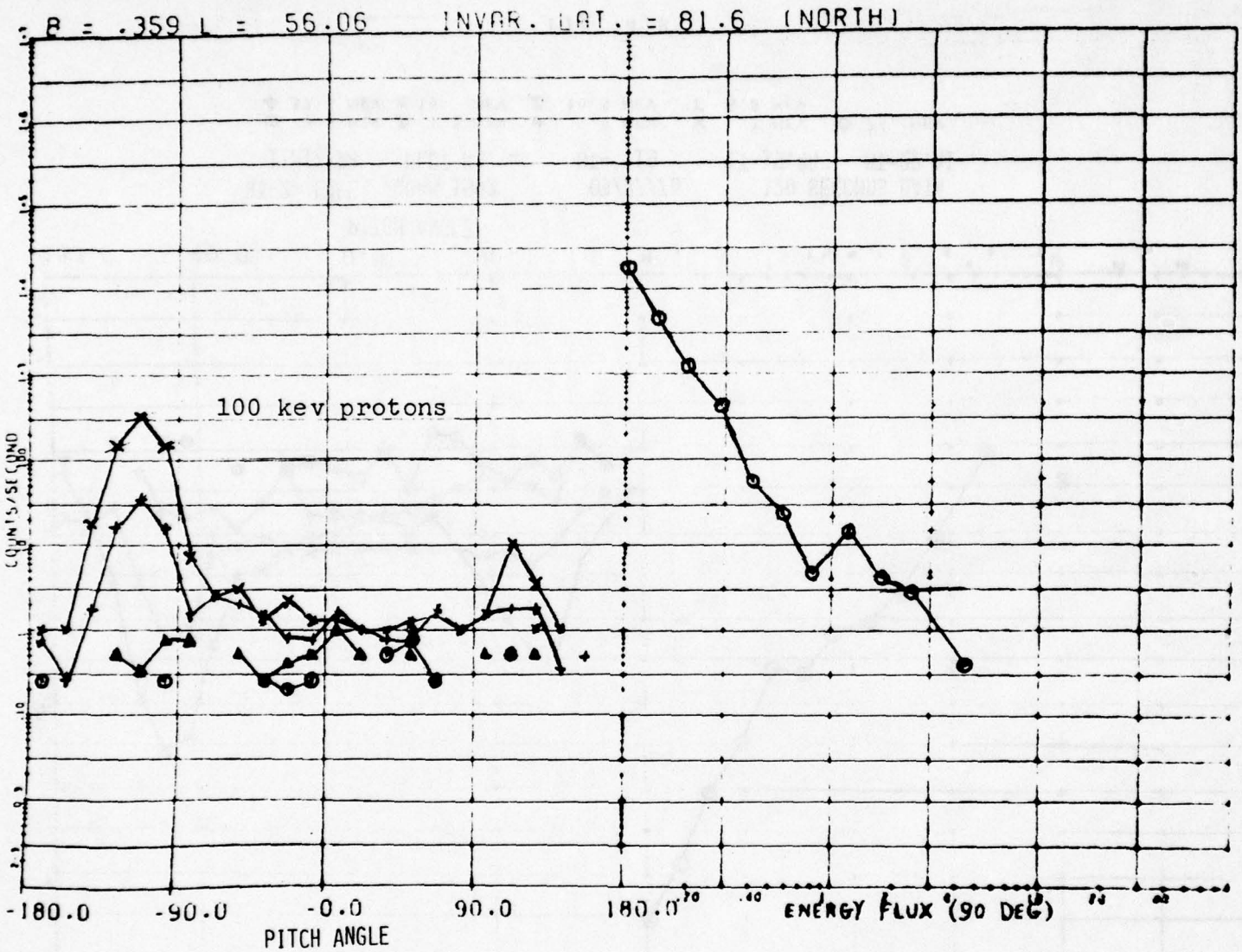

S3-2 LAPE HULA 1589 03/27/76 80 SECONDS DATA
11/17/78 PLOT NO. 4 UT=19.12 LT=17.78 MT=22.30

○ 4.5 MEV △ 1.2 MEV + .2 MEV × .1 MEV ◇ 75. MEV
✦ 37.5 MEV ✕ 19 MEV ⧗ 10.5 MEV Y 6.8 MEV

Fig. 4.7

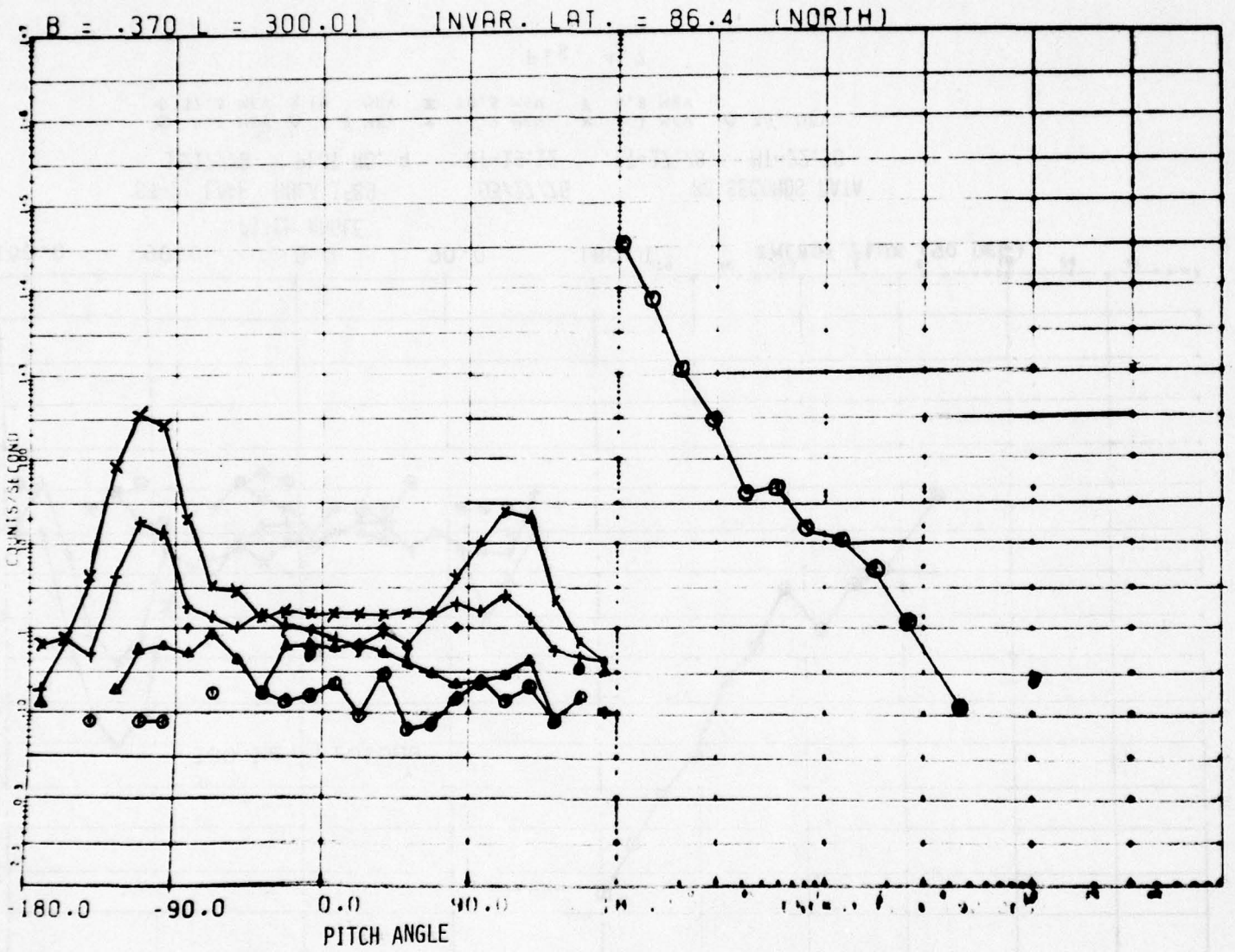
B = .370 L = 300.01 INVAR. LAT. = 86.4 (NORTH)
COUNTS/SECOND
-180.0
-90.0
0.0
90.0
PITCH ANGLE
S3-2 LAPE GUAM 1592 03/27/76 120 SECONDS DATA
11/17/78 PLOT NO. 4 UT= .19 LT=19.44 MT=22.41
4.5 MEV 1.2 MEV .2 MEV .1 MEV 75. MEV
37.5 MEV 19 MEV 10.5 MEV 6.8 MEV

Fig. 4.8

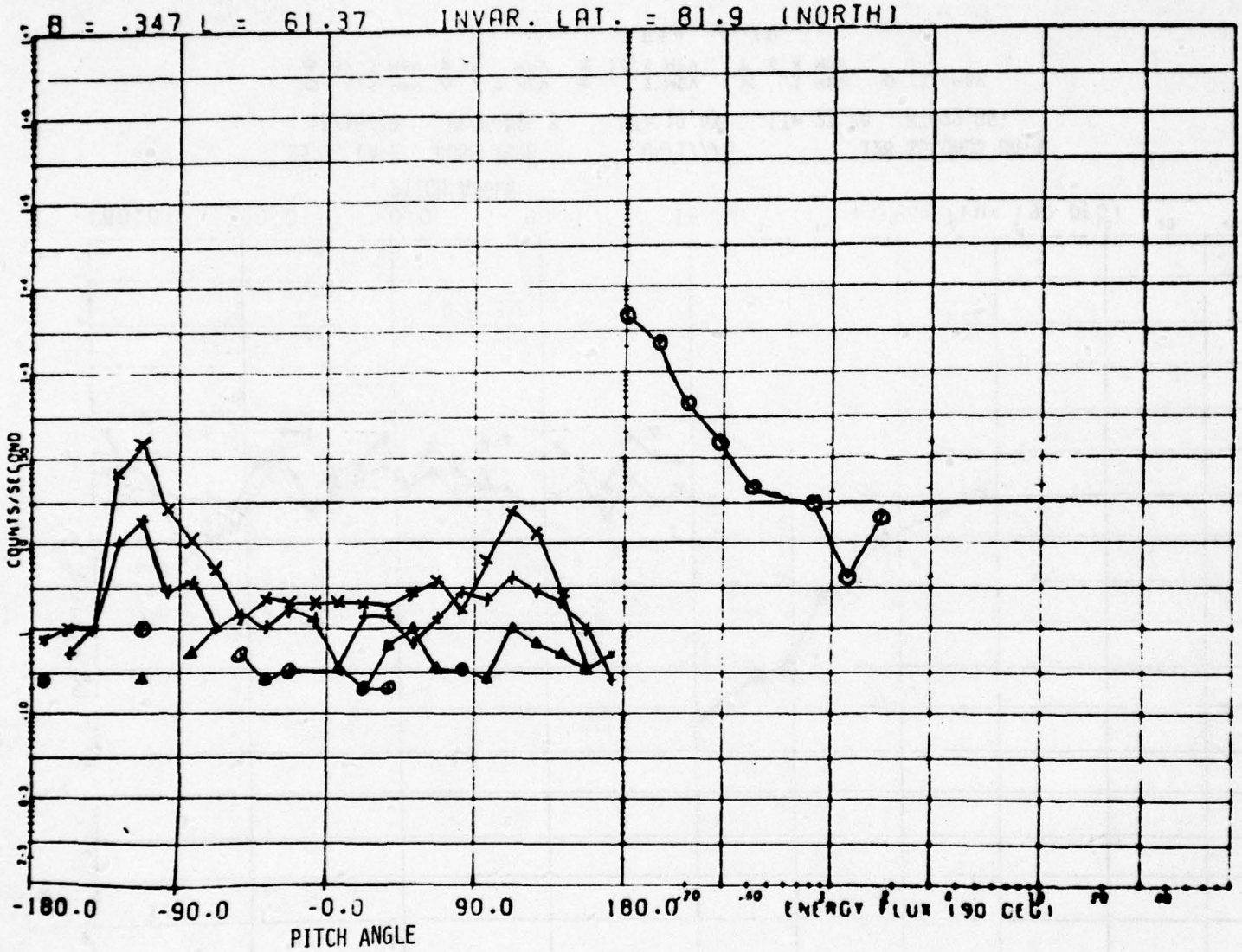

S3-2 LAPE HULA 1589 03/27/76 80 SECONDS DATA
11/17/78 PLOT NO. 8 UT= 19.20 LT= 11.78 MT=8.82

○ 4.5 MEV △ 1.2 MEV + .2 MEV × .1 MEV ◇ 75. MEV
▲ 37.5 MEV ⧗ 19 MEV Σ 10.5 MEV Y 6.8 MEV

Fig. 4.9

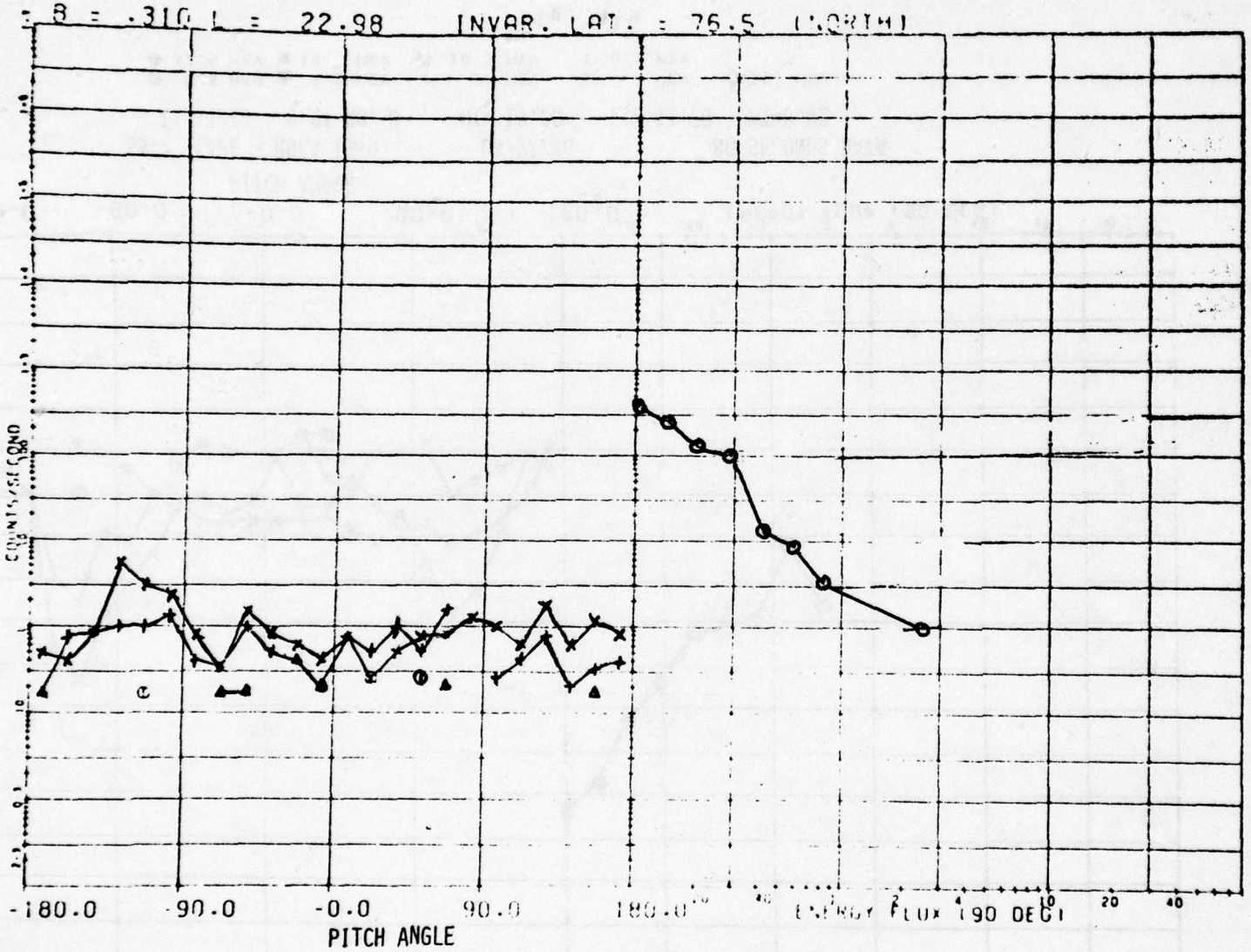

S3-2 LAPE BOSS 1888 04/17/76 128 SECONDS DATA
11/16/78 PLOT NO. 3 UT= 18.43 LT= 21.74 MT=22.86

⊙ 4.5 MEV △ 1.2 MEV + .2 MEV × .1 MEV ◇ 75. MEV
♠ 37.5 MEV ⧗ 19 MEV ⧖ 10.5 MEV Y 6.8 MEV

Fig. 4.10

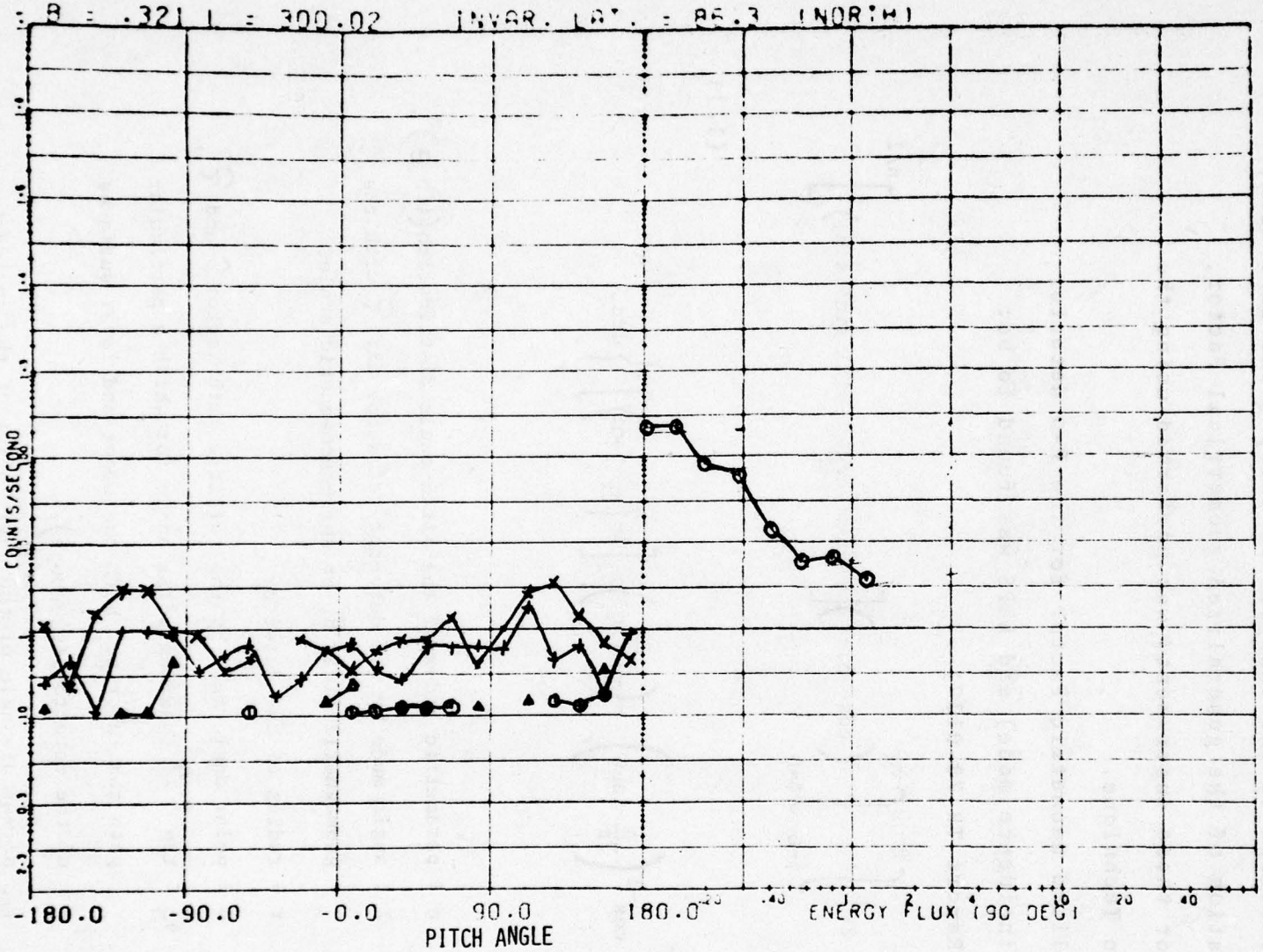

S3-2 LAPE BOSS 1888 04/17/76 190 SECONDS DATA
11/16/78 PLOT NO. 6 UT=18.51 LT=12.60 MT=6.72

○ 4.5 MEV △ 1.2 MEV + .2 MEV × .1 MEV ◇ 75. MEV
♠ 37.5 MEV ⧗ 19 MEV ⧖ 10.5 MEV Y 6.8 MEV

Fig. 4.11

4.3 Evaluation of Generalized Geometrical Factor by Use of Monte Carlo Method

In the course of the analysis of the p-α and LEPS data, a reformulation of the generalized geometrical Factor, ($G(\lambda,n)$) for these instruments was performed using the Monte Carlo Technique.

The Generalized Geometric Factor for the P-α detector (in the coincidence mode) and LEPS was found to be: (cf. AFGL Report TR-78-0137)

$$G(n,\lambda) = 2r^2 \int_{\phi=0}^{2\pi} \int_{\theta=0}^{\theta_M} \left(\cos\theta \sin\theta\right)\left[1-\left(\cos\lambda \cos\theta - \sin\lambda \sin\theta \sin\phi\right)^2\right]^{n/2}$$

$$\left\{ \cos^{-1}\left(\frac{D}{2r}\tan\theta\right) - \left(\frac{D}{2r}\tan\theta\right) \times \left[1-\left(\frac{D}{2r}\tan\theta\right)^2\right]^{\frac{1}{2}} \right\} d\theta d\phi \qquad (1.1)$$

where

- $n \equiv$ parametric index of the pitch-angle distribution $(\sin\theta')^n$,
- $\lambda \equiv$ angle made by the detector telescope axis $\hat{\tau}$ with the geomagnetic field $\vec{B}$, or spin-geomagnetic angle,
- $r \equiv$ radius of the detector,
- $\theta \equiv$ polar angle made by the particle path vector $\hat{p}$ and $\hat{\tau}$,
- $\theta_M \equiv \tan^{-1}\frac{2r}{D}$ (maximum polar angle for which a particular path can intersect both the upper and lower surfaces of the detector telescope),
- $\phi \equiv$ azimuthal angle of the entry point of the incident particle in the detector coordinate system as shown in Fig. 4.1,
- $D \equiv$ length of the telescope cylinder.

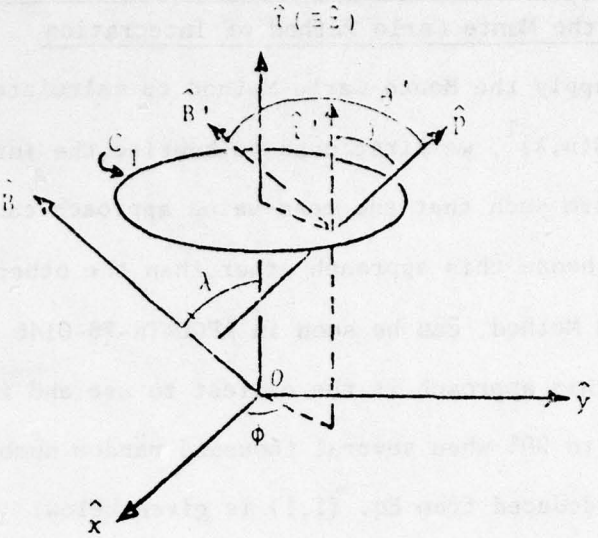

Fig. 4.12 Satellite Coordinate System

For the convenience of reference, the sketch of the coordinate system is reproduced in Fig. 1.1.

The values of $G(n,\lambda)$ as a function of n and λ have been evaluated by means of numerical integration, and these results were presented in aforementioned AFGL report in the form of tables and graphs.

For the purpose of testing the results, we have re-evaluated $G(n,\lambda)$ by use of the Monte Carlo Method[1]. The method is best illustrated by applying it to the *gambler-ruin problem*[2].

It has been known[3] that a number of approaches have been devised in order to increase the accuracy of the Monte-Carlo evaluation by reducing the variance, or the standard deviation, of the calculations. We have used a simple example, $\int_0^1 e^x ds$, to test six different approaches. The results clearly show that any approach can be chosen so long as a large enough sample is used. Since the first approach ("mean value" approach) is the easiest to use, we chose it to evaluate $G(n,\lambda)$ as given by (1.1). The results are presented in this report and compared with the results of AFGL Report TR-78-0137.

4.3.1 Calculation of the Generalized Geometrical Factor $G(n,\lambda)$ by Use of the Monte Carlo Method of Integration

In order to apply the Monte Carlo Method to calculate the generalized geometric factor $G(n,\lambda)$[1], we first need to rewrite the integral formula, Eq. (1.1), in a form such that the mean-value approach can be used[2]. The reason for us to choose this approach other than the other five approaches to the Monte Carlo Method, can be seen in AFGL-TR-78-0146 which shows that this approach is the easiest to use and its accuracy can be brought up to 99% when several thousand random numbers are used. The suitable form deduced from Eq. (1.1) is given below:

$$G(n,\lambda) = 2r^2 \frac{2\pi\theta_M}{N} \sum_{i=1}^{N} g(\theta_i,\phi_i) \qquad (2.1)$$

where

$$g(\theta_i,\phi_i) = \left(\cos\theta_i \sin\theta_i\right)\left[1 - (\cos\lambda\cos\theta_i - \sin\lambda\sin\theta_i\sin\phi_i)^2\right]^{n/2}$$

$$\left\{\cos^{-1}\left(\frac{D}{2r}\tan\theta_i\right) - \left(\frac{D}{2r}\tan\theta_i\right)\left[1 - \left(\frac{D}{2r}\tan\theta_i\right)^2\right]^{\frac{1}{2}}\right\} \qquad (2.2)$$

In evaluating $G(n,\lambda)$ through Eq. (2.1), we pick two random numbers, say μ_i, ν_i, at a time. Since the range of μ_i and ν_i is from 0 to 1, these numbers must be transformed to θ_i and ϕ_i as follows:

$$\begin{cases} \theta_i = \theta_M \mu_i & \left(\text{where } \theta_M = \tan^{-1}\frac{2r}{D}\right) \\ \phi_i = 2\pi\nu_i \end{cases} \qquad (2.3)$$

The computer program written to generate $G(n,\lambda)$ by the Monte Carlo Method follows. The results are given in Section 3.

4.3.2 Values of $G(n,\lambda)$ as Evaluated by Use of the Monte Carlo Method

For a comparison of the values of $G(n,\lambda)$ calculated by use of numerical integration and the Monte Carlo Method, we list the results for $n = 5$ for various λ's in Table 3.1.* It is clear that even with 3000 random numbers (i.e. $N = 3000$), both results agree within two significant figures. Excellent agreement is reached when the random numbers increase to 100,000. See Table 4.1 of Report TR-78-0137 for comparison.

Here we indicate two aspects:

(i) For a simple integration in one or two dimensions, the results can be obtained easily by either method. However, for a complicated multi-dimensional integral for which the numerical integration becomes increasingly cumbersome, the Monte Carlo Method might turn out to be the only workable means of evaluation.

(ii) For handling data of a statistical nature, the use of the Monte Carlo Method has an additional advantage because it also yields the standard deviations.

---

*The calculation was based on the geometry of the Narrow-angle LEPS which has a collimator of a radius of 0.347 cm and a length of 3.175 cm. Therefore the limits of θ are from 0 to $\tan^{-1}(2r/D) = 12.3°$. The limits for ϕ are from 0 to 2π, which, are based on the assumption of the axisymmetry of the particle flux with respect to the local geomagnetic field.

Table 4.1 $G(n,\lambda)$ Evaluated from Numerical Integration and from Monte Carlo Method for n=5, $\lambda=0°$ to $90°$

λ	$G(5,\lambda)$ (From numerical integration)	$G(5,\lambda)$ (From Monte Carlo Method with N = 3000)	σ	$G(5,\lambda)$ (From Monte Carlo Method with N = 100,000)	σ
0	.4648E-6	.4815E-6	.9212E-8	.4655E-6	.1580E-8
10	.8903E-5	.8931E-5	.2226E-6	.8906E-5	.3863E-7
20	.1014E-3	.9803E-4	.1831E-5	.1017E-3	.3238E-6
30	.5218E-3	.5165E-3	.7616E-5	.5218E-3	.1315E-5
40	.1655E-2	.1667E-2	.2043E-4	.1651E-2	.3535E-5
50	.3789E-2	.3779E-2	.4153E-4	.3784E-2	.7282E-5
60	.6818E-2	.6783E-2	.7010E-4	.6784E-2	.1219E-4
70	.1011E-1	.1006E-1	.1013E-3	.1011E-1	.1728E-4
80	.1269E-1	.1249E-1	.1221E-3	.1274E-1	.2108E-4
90	.1367E-1	.1364E-1	.1292E-3	.1364E-1	.2265E-4

Note that:

n ≡ Parametric index in the theoretical pitch-angle distribution $(\sin\theta')^n$,

λ ≡ Angle between the telescope spin axis and the geomagnetic field (Spin-geomagnetic Angle),

σ ≡ Standard deviation of $G(n,\lambda)$.

References

1. Feller, W., An Introduction to Probability Theory and Its Applications, Vol. 1, Ch. 14, pp. 313-318, 2nd ed., John Wiley and Sons, (1966).

2. Hammer, M. and Crannel, C.J., Determination of the Geometrical Factor and of the Spacial Distributions of Particles for a Cosmic Ray Telescope Using a Monte Carlo Approach, Goddard Space Flight Center Report X-661-73-218, (1973).

3. Shreider, Yu.A., The Monte Carlo Method, Chap. 2, pp. 91-115, Pergamon Press, (1966).

4.4 Satellite S72-1

A documentation package containing a tape copy of our S72-1 data base in the form of a latitude-longitude sort into a one degree grid preserving the pitch-angle and energy spectrum information was prepared for distribution. Specifically, it was made up at the request of Dr. Vette to be incorporated into his next version of proton model AP4, but it will be made on a request basis to qualified parties.

5. E^2-S^2 HIGH ENERGY PROTON SPECTROMETER

In order to expand our capability in the field of magnetospheric physics, it was decided to study, design and build a charged-particle (proton) telescope. A literature survey was begun to determine the latest techniques used in the construction of such a telescope. We also initiated a search into the scientific literature to determine the outstanding problems concerning the trapped proton fluxes.

It was found that a proton telescope capable of measuring small proton fluxes in a high radiation environment of high energy electrons, in the 1-100 MeV energy range, but more particularly in the 1-24 MeV range, should be built. Indeed, the completeness and reliability of the existing data covering this energy range for protons leave much to be desired. This instrument should have good background (high energy electrons, bremsstrahlung) rejection characteristics, together with a high sensitivity.

5.1 Background Rejection

The background problem was investigated using a program from the Radiation Shielding Information Center at Oak Ridge National Laboratories. This program, called "Tiger", is a comprehensive software system for solving one-dimensional multilayer electron/photon transport problems. From our computer simulations, we calculated that a grated shielding made of copper and lead, would be very adequate for the measurements to be performed in the heart of the radiation belts where substantial electron fluxes exist. Indeed, it was shown that when an electron spectrum, as shown in Fig. 5.1, interacts with a shield of adequate thickness to stop 100 MeV Protons, a substantial amount of bremsstrahlung is generated which of course will interact with the Si(Li) detectors of the telescope. Such simple shielding had been used in a previous proton telescope. Figure 5.2 shows the normalized transmitted bremsstrahlung

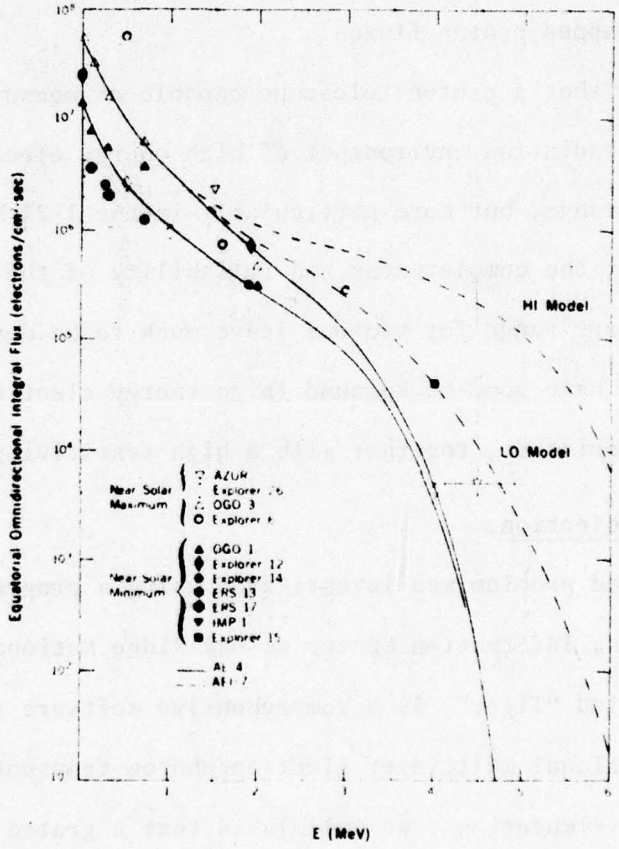
Equatorial Omnidirectional Integral Flux (electrons/cm²-sec)
E (MeV)
HI Model
LO Model
Near Solar Maximum
AZUR
Explorer 26
OGO 3
Explorer 6
Near Solar Minimum
OGO 1
Explorer 12
Explorer 14
ERS 13
ERS 17
IMP 1
Explorer 15
AE 4
AE 7

Fig. 5.1

spectrum resulting from the interaction of an electron input spectrum as shown in Fig. 5.1 (High mode), with a 1.32 cm copper shielding (Curve 1). The relative intensity is normalized to 1 electron/cm^2-sec. 5.3% of the electrons will produce bremsstrahlung with the indicated photon spectrum. The peak of the distribution occurs at ∿300 keV. The probability of interaction of these photons with the Si(Li) detector is rather high since the average thickness of each detector as far as the bremsstrahlung is concerned is several times greater than the actual thickness of the detector because of the average angle of incidence of the photons. The second curve (2) shows the transmitted bremsstrahlung spectrum through the same 1.32 cm of copper followed by 1.20 cm of lead. The lead is added to absorb preferably the photon peak at ∿300 keV. The total photon spectrum is thus reduced by a factor of ∿32. Furthermore the peak energy in the photon spectrum is displaced to ∿900 keV where the interaction cross section with silicon is reduced by ½ as compared to the 300 keV cross section.

At low altitudes (few thousand of km or lower), where the electron flux are smaller, but high energy (E > 100 keV) proton fluxes are troublesome, the inclusion of an active shield, together with the passive shielding, would probably be advisable.

Two different approaches, as far as the detector logic configuration is concerned, are being considered. The first one makes use of the well-defined energy-range relationships for protons. The second approach utilizes the relationship between incident energy and energy deposited in a given thickness of silicon.

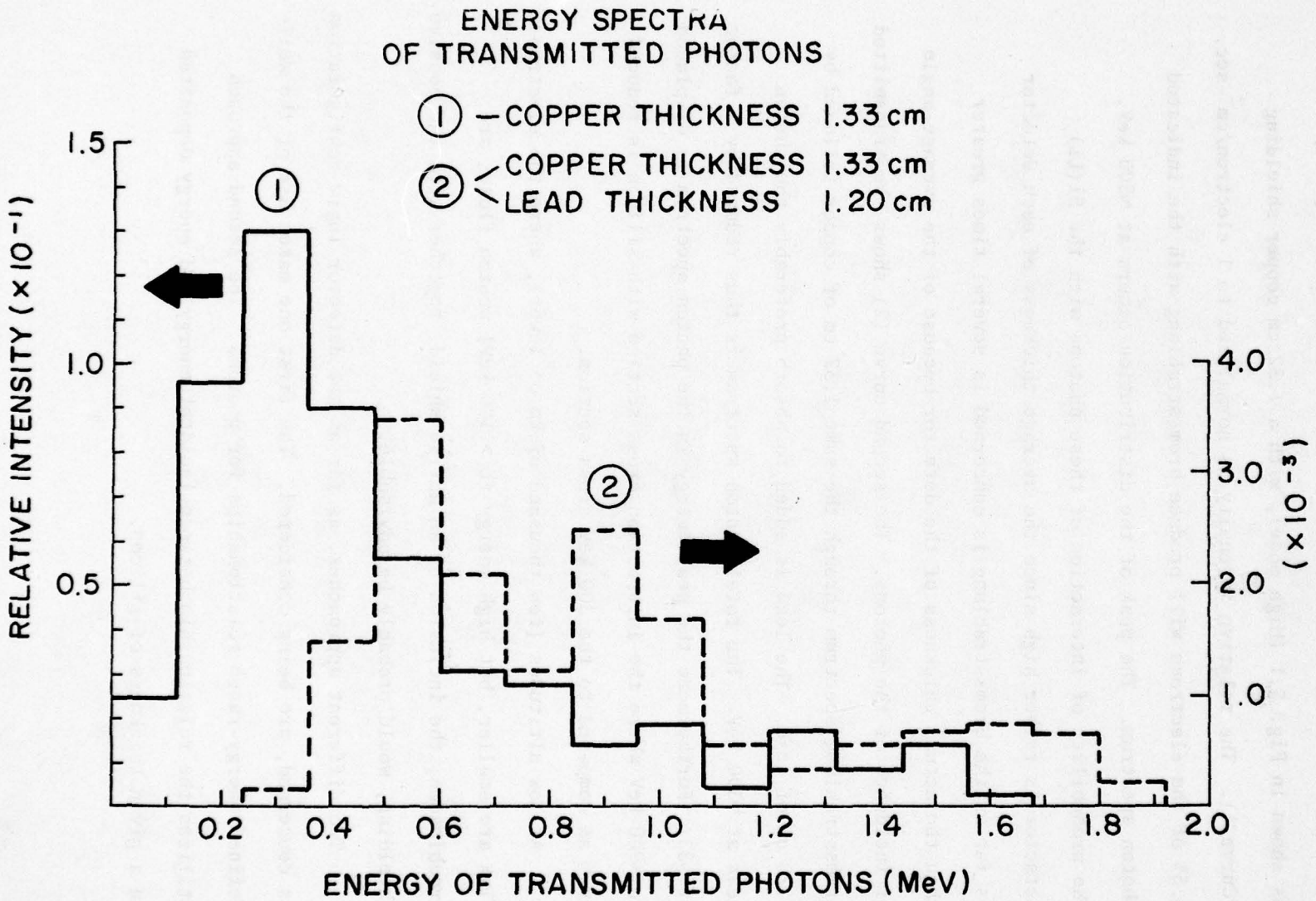
ENERGY SPECTRA
OF TRANSMITTED PHOTONS
① —COPPER THICKNESS 1.33 cm
② COPPER THICKNESS 1.33 cm
LEAD THICKNESS 1.20 cm
RELATIVE INTENSITY (×10⁻¹)
(×10⁻³)
1.5
1.0
0.5
4.0
3.0
2.0
1.0
0.2
0.4
0.6
0.8
1.0
1.2
1.4
1.6
1.8
2.0
ENERGY OF TRANSMITTED PHOTONS (MeV)

Fig. 5.2

5.2 Range - Energy Telescope

5.2.1 Description of the Instrument

In this approach, the telescope will consist of n totally depleted Si(Li) detectors of various thicknesses, separated from one another by absorbers of appropriate thicknesses. Each detector-absorber pair determines an energy channel. The energy of an incident proton will be determined by the last detector to record the passage of that particle. Figure 5.3 is a plot of the range-energy law for protons in aluminum. The same curves can be used for silicon since the ranges of protons of equal energies in the two materials, different by little more than 1% between 6 and 100 MeV.

As one example of this type of telescope, we use 9 detector-absorber pairs, thus determining 9 energy channels. A tenth detector provides the anti-coincidence to eliminate events occurring from the back of the detector, as well as an additional energy channel 100-300 MeV.

Table 5.1 shows the different energy channel characteristics of the telescope. The thickness of absorbers following the detectors is also given. Figure 5.4 shows the energy deposited vs the incoming proton energy relation.

The entrance aperture of the instrument contains a sweeping magnet which will deflect electrons with $E \lesssim 1$ MeV away from the silicon detectors. The telescope will utilize totally depleted, transmission type, ring mounted, silicon surface-barrier detectors.

5.2.2 Description of the Circuit Logic

Figure 5.5 is a block diagram of the circuitry for the proposed instrument. Each detector feeds a standard modular pre-amplifier, amplifier, and discriminator-shaper in cascade.

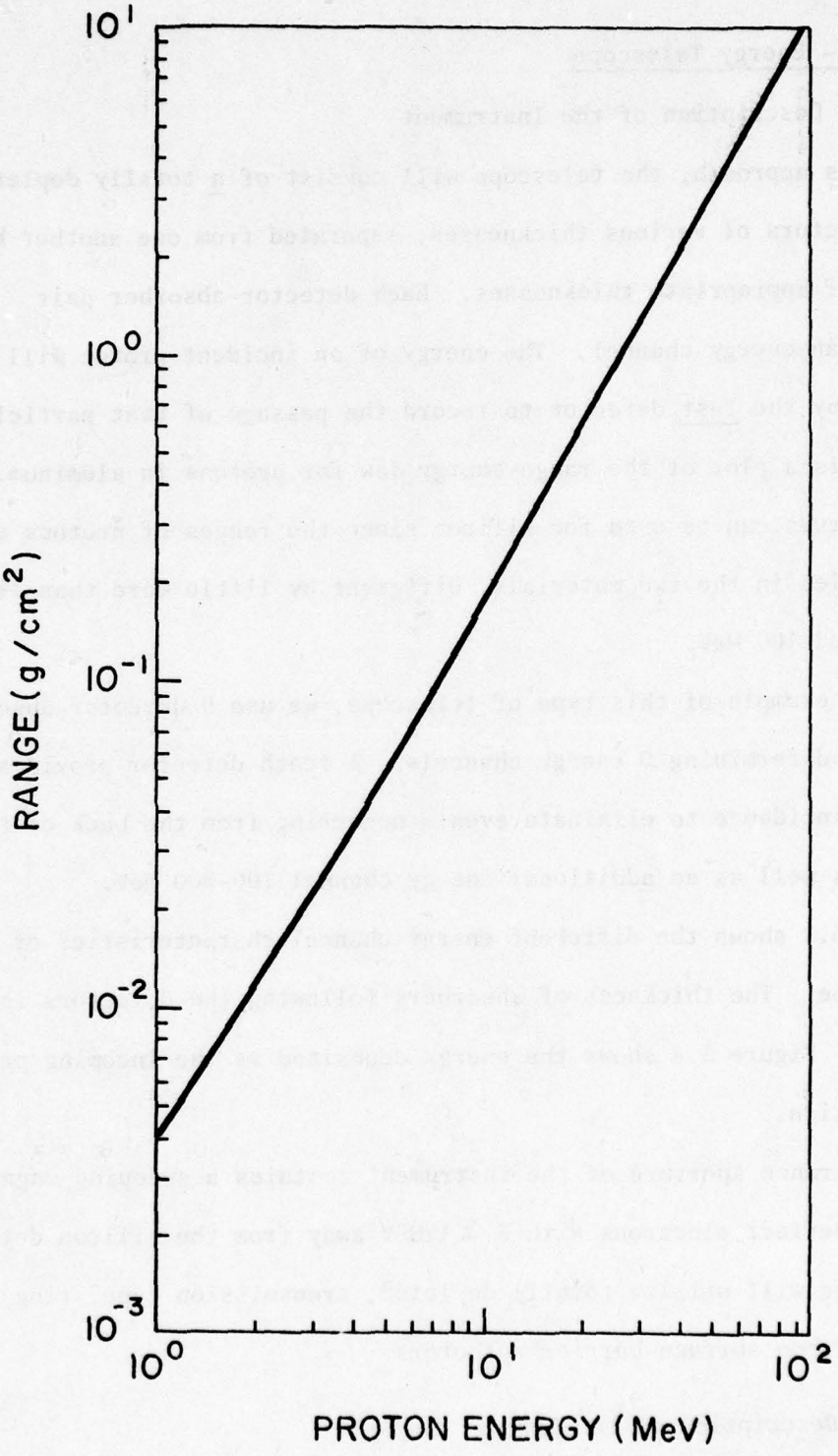

Fig. 5.3

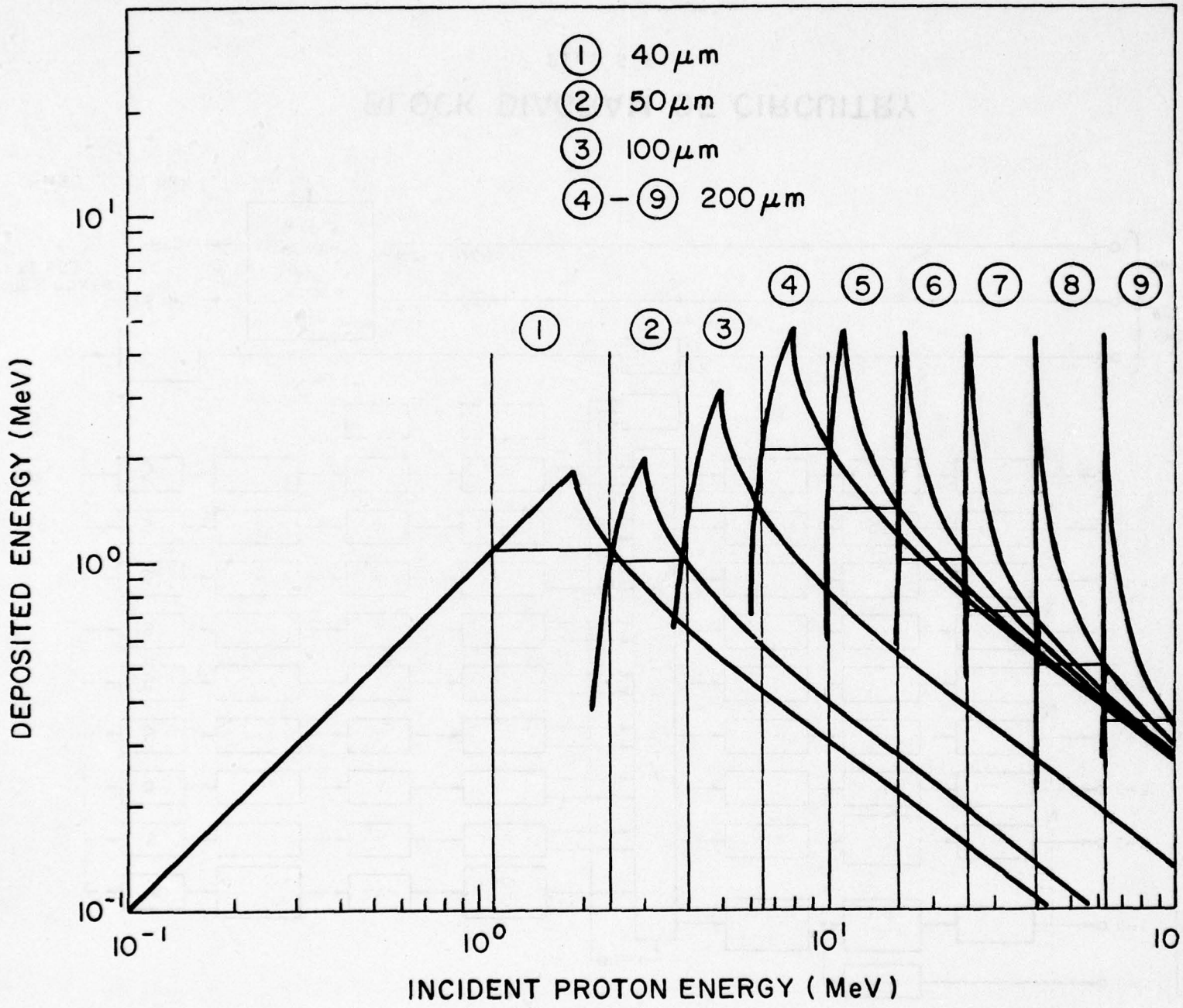
① 40μm
② 50μm
③ 100μm
④ – ⑨ 200μm
DEPOSITED ENERGY (MeV)
INCIDENT PROTON ENERGY (MeV)
10^1
10^0
10^-1
10^-1
10^0
10^1
10^2

Fig. 5.4

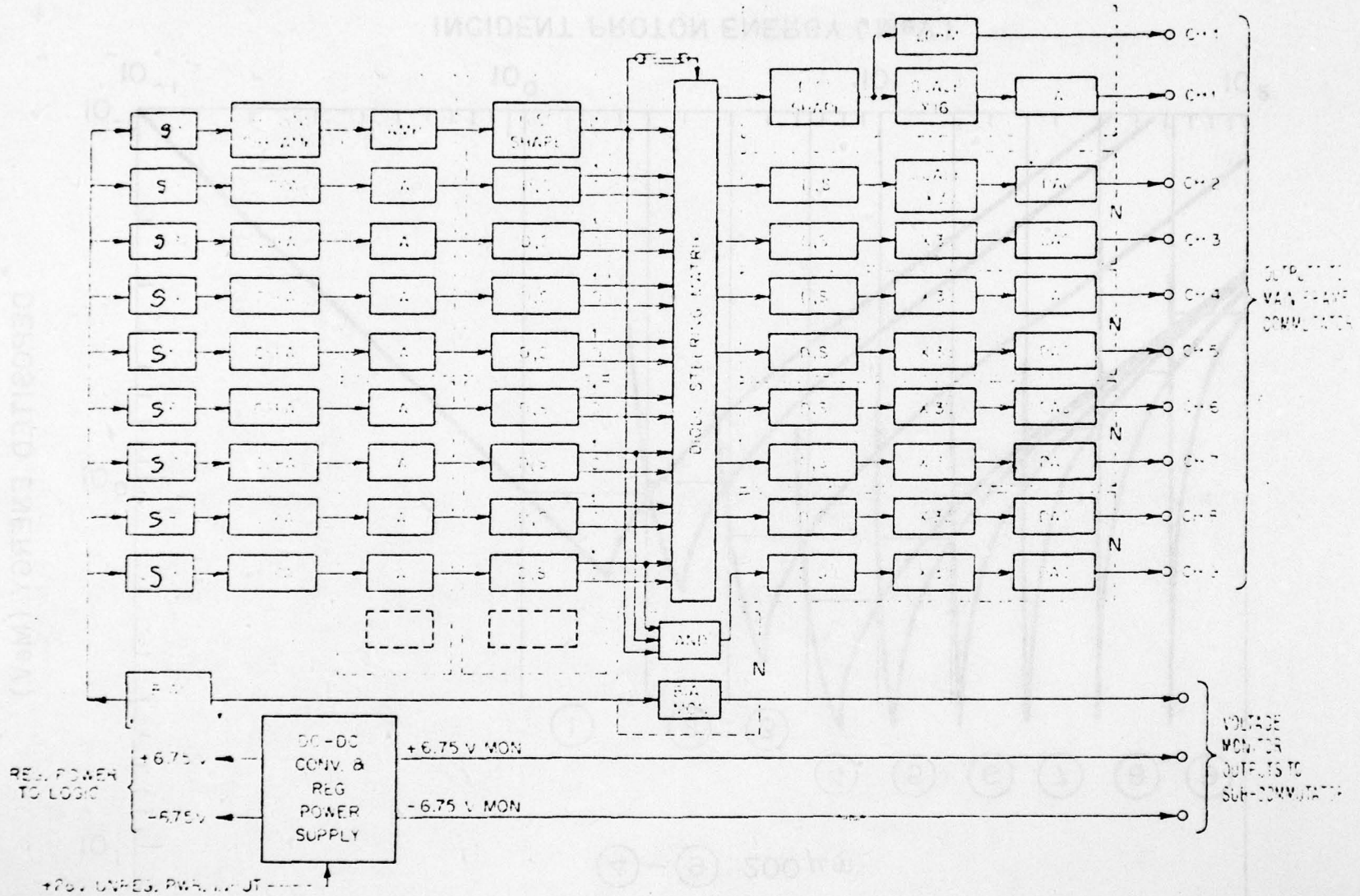

BLOCK DIAGRAM OF CIRCUITRY

Fig. 5.5

The discriminators in channel 4 through 9 are set to fire at 300 keV, the average energy deposited by a 100 MeV proton in 200 micron depleted detectors; the thresholds for channels 1 and 2 are set at 60 keV, and that of 3 is set at 100 keV. The instrument will not, therefore, be sensitive to protons above 300 MeV, nor to electrons, which on the average deposit about 14, 17, 35 and 70 keV in 40, 50, 100 and 200μm of silicon.

The shapers in channels 1 through 9 set up biases within the diode steering matrix in such a way that the delayed "write" pulse generated from the firing of the channel 1 shaper is steered only to the one output wire corresponding to the last solid state detector which has produced a pulse in sequence. Thus, the condition for a signal appearing on the channel n wire is an n-fold coincidence of pulses in all detectors 1 through n, and a (9-n) fold anti-coincidence of pulses in all detectors (n+1) through 9. This logic eliminates essentially all background arising from particles (or bremsstrahlung) which penetrate the shielding on the sides of the detectors.

Additional AND logic is provided for recording protons greater than 100 MeV in energy (those which penetrate all detectors). This is a 3-fold AND gate, requiring signals from the first (1), and the last (9), and the central (7) detector to reduce accidental coincidences.

The outputs of the steering matrix and the AND gate all feed counting logic. In channel 1, the counting logic is a standard logarithmic count-rate meter (LCRM) and a x 16 Scaler with digital-to-analog converter (DAC) fed by a single-shot circuit (SS)

The LCRM output in this channel will allow for extremely high counting rates which might otherwise lead to ambiguous interpretation of DAC outputs. In the remaining channels, 2 through 9, each counting logic consists simply of a X32 scaler with DAC, fed by a SS. The scaler-DAC's are mounted in pairs on circuit boards.

5.3 Energy Deposited - Energy Telescope

5.3.1 Description of the Instrument

In this approach, the telescope will make use of 4 totally depleted, transmission-type, ring mounted, silicon surface-barrier detectors. Again, a fifth detector with an absorber of appropriate thickness in front of it will be used for anti-coincidence purposes for protons with $E > 100$ MeV, and events occurring from the back of the telescope.

Figure 5.6 shows the energy - incident energy in such a telescope, consisting of 4 detectors of thickness 30, 200, 1000 and 2000 μm. Table 5.2 indicates the energy deposited in each detector for given incident energies. The energy range has been divided into 10 energy channels

5.3.2 Description of the Circuit Logic

This instrument makes use of similar modules described in the previous section. However, now the output voltages from each detector are A/D converted. These voltages are then compared to a matrix of digitized voltage interval values as shown in Table 5.2. When following an event, the proper relationship in one, two or three detectors is shown to exist, the proper energy channel is incremented.

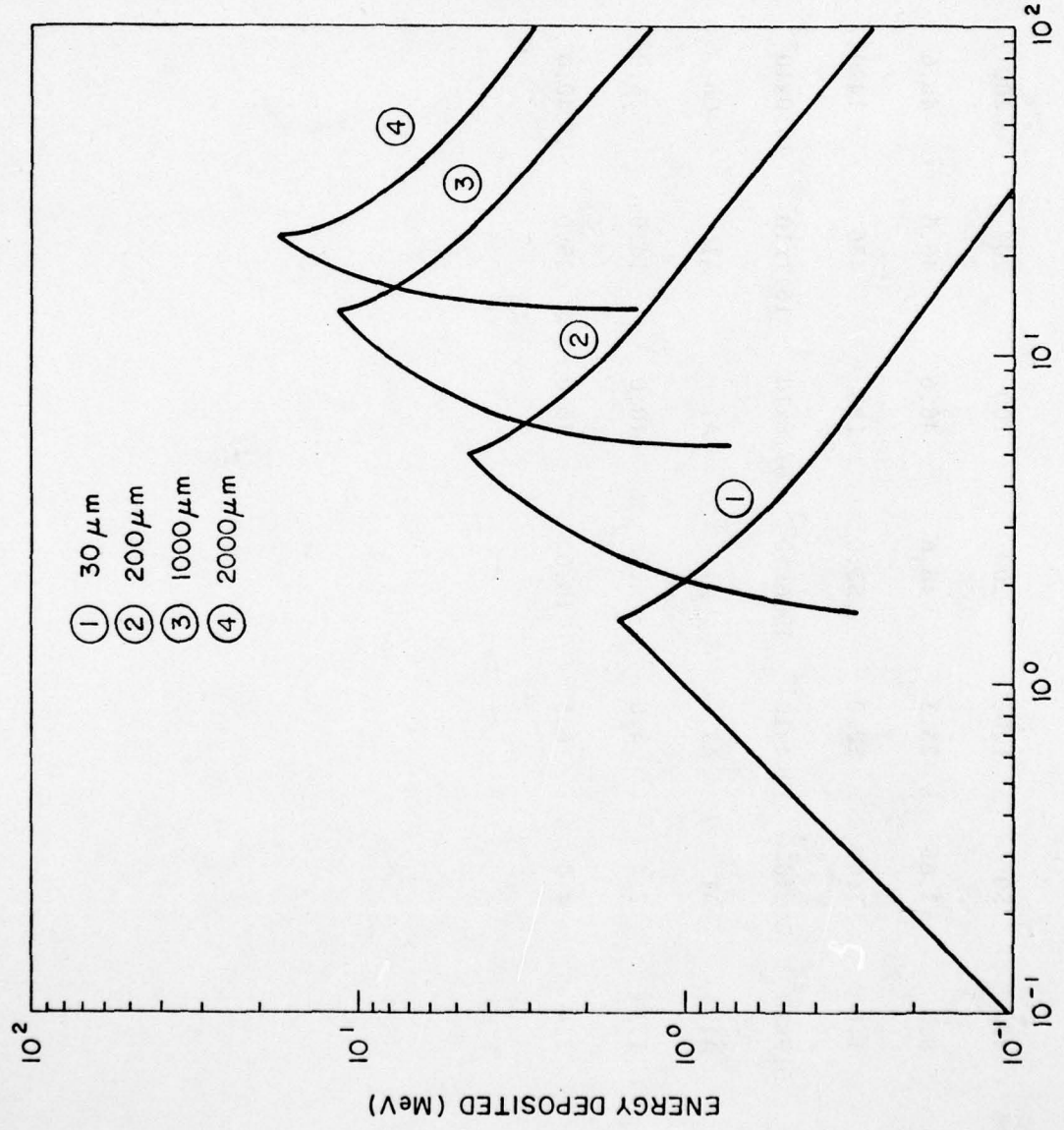
ENERGY DEPOSITED (MeV)
INCIDENT PROTON ENERGY (MeV)
10^2
10^1
10^0
10^-1
10^-1
10^0
10^1
10^2
① 30 μm
② 200μm
③ 1000μm
④ 2000μm
①
②
③
④

Fig. 5.6

Table 5.1

DETECTORS									
Detector Thickness	40	50	100	200	200	200	200	200	200
(mg/cm^2)	9.3	11.65	23.3	46.6	46.6	46.6	46.6	46.6	46.6
Absorber(gm/cm^2)	1.6	7.0	19.0	53.0	183	436	1429	3166	7270
(cm)	5.9×10^{-4}	26×10^{-4}	70.4×10^{-4}	19.6×10^{-3}	67.8×10^{-3}	16.1×10^{-2}	16.0×10^{-2}	35.5×10^{-2}	81.5×10^{-2}
Material	Al	Al	Al	Al	Al	Al	Cu	Cu	Cu
Lower Limit(MeV)	1.1	2.4	4.0	6.5	10.0	16.0	25.0	40.0	63.0
Upper Limit(MeV)	2.4	4.0	6.5	10.0	16.0	25.0	40.0	63.0	100.0

Table 5.2

Detector	1	2	3	4
Energy (MeV)	Energy Deposited (MeV)	Energy Deposited (MeV)	Energy Deposited (MeV)	Energy Deposited (MeV)
1.00 - 1.65	1.00 - 1.65			
1.65 - 2.50	1.40 - 0.70	0.30 - 1.65		
2.50 - 3.60	0.70 - 0.52	1.65 - 3.10		
3.60 - 5.40	0.52 - 0.38	3.10 - 4.60		
5.40 - 8.50		4.00 - 2.10	1.5 - 6.3	
8.50 - 14.0		2.10 - 1.30	6.3 - 11.5	
14.0 - 23.0		1.30 - 0.87	10.0 - 4.8	3.0 - 17.3
23.0 - 38.0		0.87 - 0.58	4.8 - 3.0	17.3 - 6.5
38.0 - 65.0			3.0 - 1.8	6.5 - 4.0
65.0 - 100.0			1.8 - 1.2	4.0 - 2.8

6. DETECTORS

6.1 Detection of Protons in CR-39 Plastic Track Detector

6.1.1 Abstract

CR-39 plastic is used as a detector to observe monoenergetic protons. Several samples of CR-39 were exposed to protons of energies 1.5 MeV, 2.2 MeV, 3.2 MeV and 4.3 MeV. After etching measurements were carried out on track diameters produced by protons in all samples, the diameter distributions clearly showed an excellent energy resolution of protons of different energies. From our preliminary analysis of the data, it appears that the response function for registering protons in CR-39 may be much less complicated than in cellulose nitrate.

6.1.2 Introduction

In recent years Solid State Nuclear Track Detectors have found widespread application [1]. The production of tracks by energetic ions in insulating materials is a widely-used technique for detection and identification of ions. Their utilization showed to be very successful in the study of very heavy primary cosmic rays and the recording of fission fragments, Also, there have been some investigations exploring the possibility of their application to detect protons. Cellulose Nitrate plastic has been employed as a detector to record protons, however, CN suffers from being inhomogeneous and anistropic with regard to its physical characteristics. These defects manifest themselves in non-geometrical track profiles, differences in sensitivity in a given sheet, and varying bulk etch rate. The use of plastic sheets cast from CR-39 monomer (allyl diglycol carbonate) with excellent etching properties, high sensitivity, and high uniformity as a nuclear track was reported recently [2]. This material was found to have a lower detection threshold ($Z/\beta = 9$) than cellulose nitrate ($Z/\beta = 30$) and a smaller variation of

response (∿1%) to particles of a given ionization rate than Lexan polycarbonate (∿3 to 8%). Commercially available CR-39 is capable of recording protons of 1 MeV and below as well as 6 MeV alpha particles. In this work an attempt is made to investigate further the properties of CR-39 as a nuclear track detector with particular reference to detection of protons.

6.1.3 Experimental Details

For this study Polytech CR-39 (1500 μm thick) was used. Samples of size (2.5x2.5 cm) were cut out and exposed to a beam of protons from the Van de Graaff generator at Brookhaven National Laboratory. The beam was tuned to four different energies, viz., 1.5 MeV, 2 2 MeV, 3.2 MeV and 4.3 MeV. The corresponding fluences were: 2.8×10^5 particles/cm^2, 0.44×10^6 particles/cm^2, 0.67×10^6 particles/cm^2 and 0.91×10^6 particles/cm^2. All irradiations were carried out in such a manner that particles are nearly normally-incident to the surface of the plastic sheet. After irradiation the samples were etched in a solution of 6.25N NaoH at 50°C for different durations. The samples were suspended by means of nichrome wires in polyethylene vessels containing etchant. Temperature control was achieved by placing the polyethylene containers into a regulated water bath. Samples were selected from all four irradiations and etched in four different batches for 7 hours, 17 hours, 30 hours, and 48 hours. In order to distinguish the background against tracks of protons, always a virgin sample of CR-39 was etched with each batch. All measurements were made on a Koristka R4 microscope using a 80 Zeiss objective and x10 wide field American Optical eyepiece. A total of 1000 tracks were measured to obtain data on track diameters.

6.1.4 Results

In Figures 1 and 2 are shown the distributions of track diameters for protons. The sheets were etched for 17 hours (figure 1) and 30 hours (figure 2). In the case of 17-hour etch, there is some spread in track diameter distribution for 4.3 MeV protons. This may be of statistical nature and/or spread in the beam energy. The superior properties of CR-39 as a track detector are clearly demonstrated in figure 2. Here the energy resolutions for protons is excellent. Once again the peak in track diameter distribution for 4.3 MeV protons is very broad. Figure 3 shows etch pit diameter as a function of proton energy. The samples etched for 48 hours show a maximum slope thereby indicating a better resolution. Figure 4 shows etch pit diameter as a function of amount of bulk material removed from one surface. From our preliminary data, it appears that the dependence of etch pit diameter on the amount of bulk material removed from one surface seems to be less complicated than in CN. Particle identification by measurements of etch pit diameter was first suggested by Somogyi [3]. Recently Somogyi and Szalay [4] discussed the kinetics of track diameter growth in considerable detail. In principle the method should work with particles incident at arbitrary angles on a solid surface, but in practice it is much simpler if the detector can be positioned such that particles are nearly normally incident. For tracks with large cone angles such as those of protons, the diameter is a more sensitive function of ionization rate than is track length. Finally figures 5 and 6 show tracks of 1.5 MeV and 2.2 MeV protons respectively.

It is a pleasure to thank Drs. Norman Rohrig and Steve Marino of Brookhaven National Laboratory for help with proton irradiations.

References:

1. R.L. Fleischer, P.B. Price and R.M. Walker, Nuclear Tracks in Solids (University of California Press, Berkeley, 1975).

2. B.G. Cartwright, E.K. Shirk and P.B. Price, Nucl. Instr. Methods, 153, 457, 1978.

3. G. Somogyi, Nucl. Instr. Methods, 42, 312, 1966.

4. G. Somogyi and S.A. Szalay, Nucl. Instr. Methods, 109, 211, 1973.

Figure Captions

1. The diameter distribution of the etch pits of protons (17 hour etch)
2. The diameter distribution of the etch pits of protons (30 hour etch)
3. Etch pit diameter (D) as a function of proton energy (E) The parameter on each curve represents etching time.
4. Etch pit diameter (D) as a function of amount of bulk material removed from one surface ($V_g t$)
5. Tracks of 1.5 MeV protons in CR-39. The etching time was 30 hours.
6. Tracks of 2.2 MeV protons in CR-39. The etching time was 30 hours.

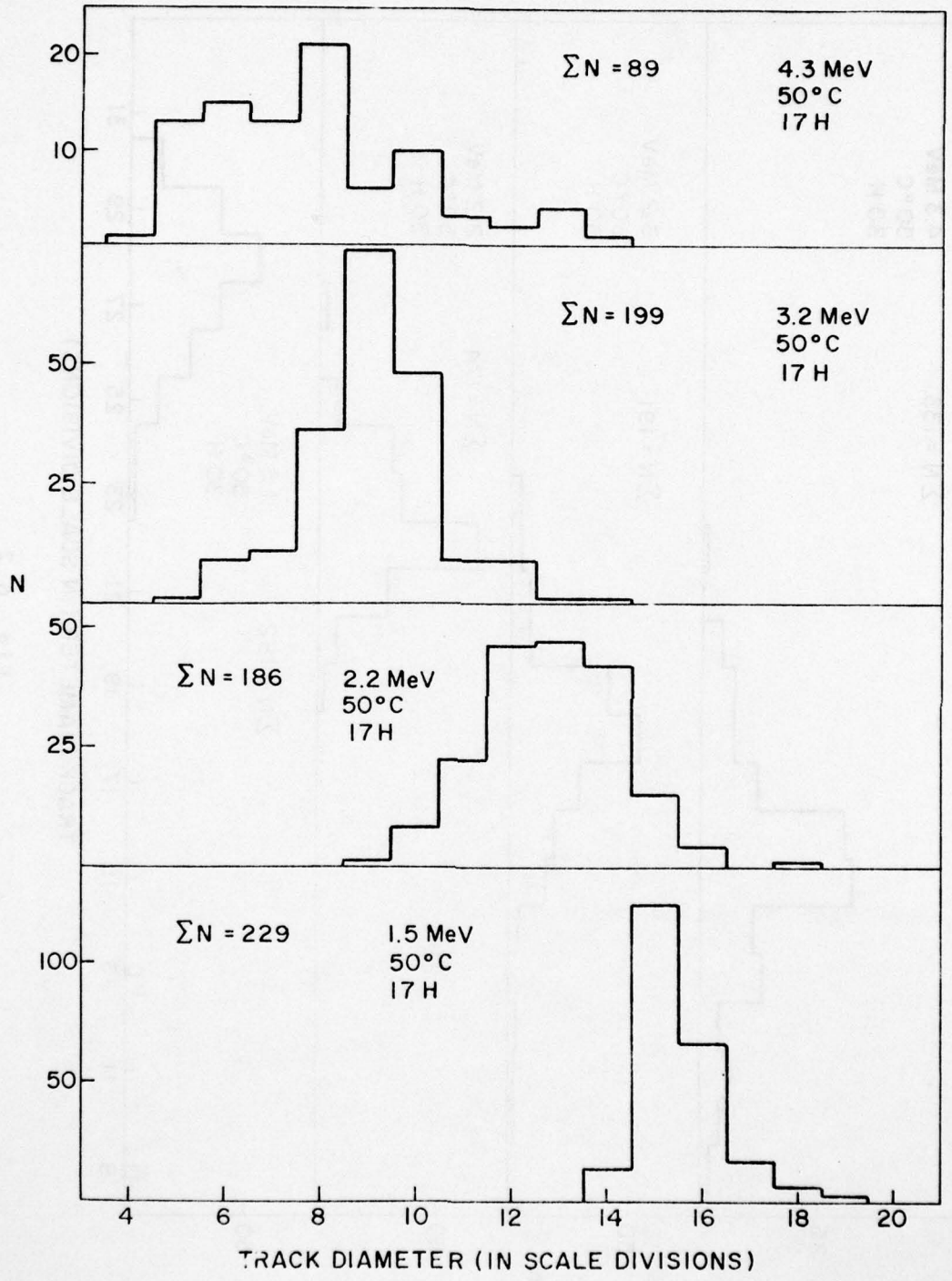
ΣN = 89
4.3 MeV
50°C
17 H
ΣN = 199
3.2 MeV
50°C
17 H
ΣN = 186
2.2 MeV
50°C
17 H
ΣN = 229
1.5 MeV
50°C
17 H
N
20
10
50
25
50
25
100
50
4
6
8
10
12
14
16
18
20
TRACK DIAMETER (IN SCALE DIVISIONS)

Fig. 6.1

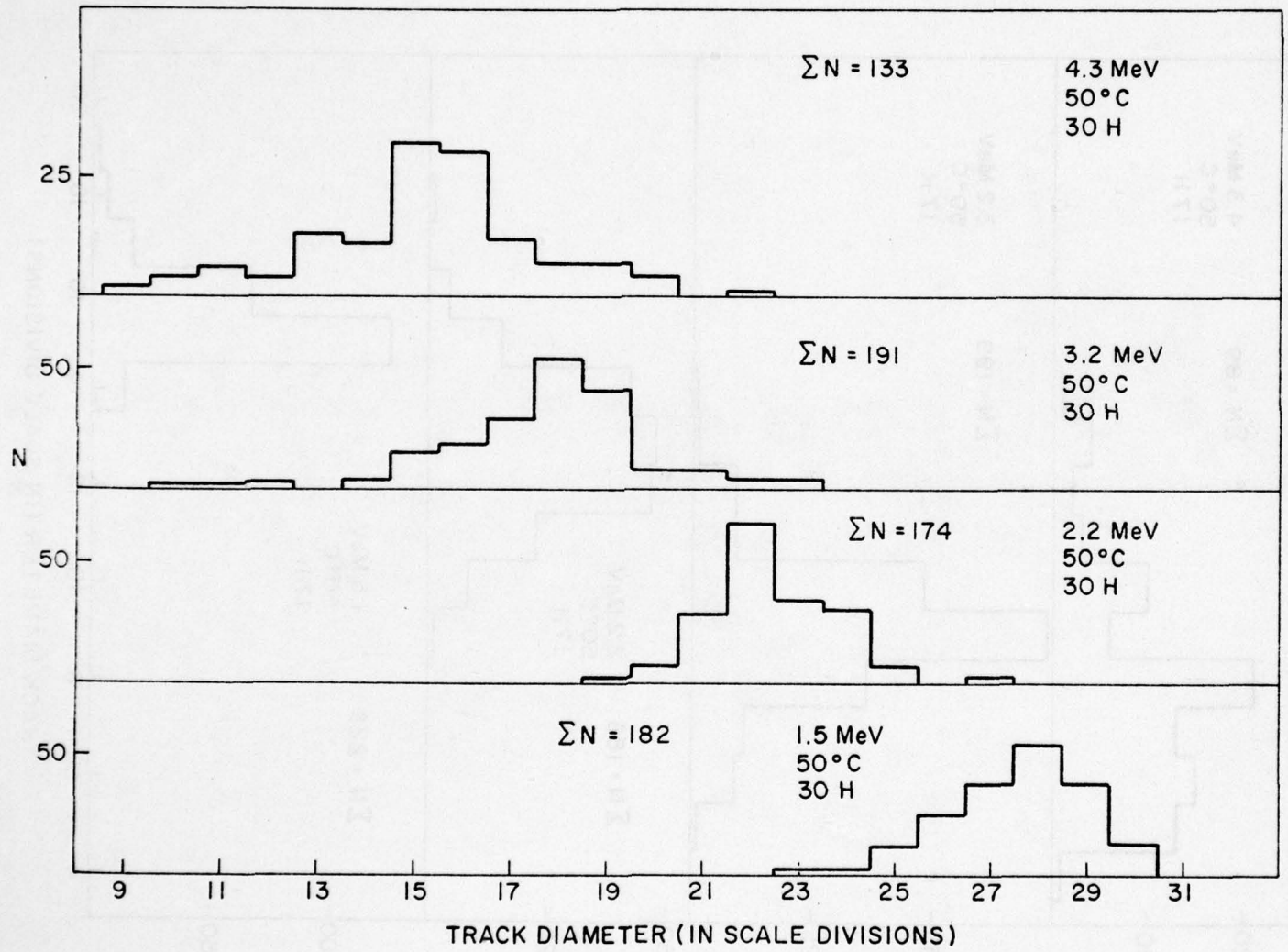
ΣN = 133
4.3 MeV
50°C
30 H
ΣN = 191
3.2 MeV
50°C
30 H
ΣN = 174
2.2 MeV
50°C
30 H
ΣN = 182
1.5 MeV
50°C
30 H
25
50
50
50
N
9
11
13
15
17
19
21
23
25
27
29
31
TRACK DIAMETER (IN SCALE DIVISIONS)

Fig. 6.2

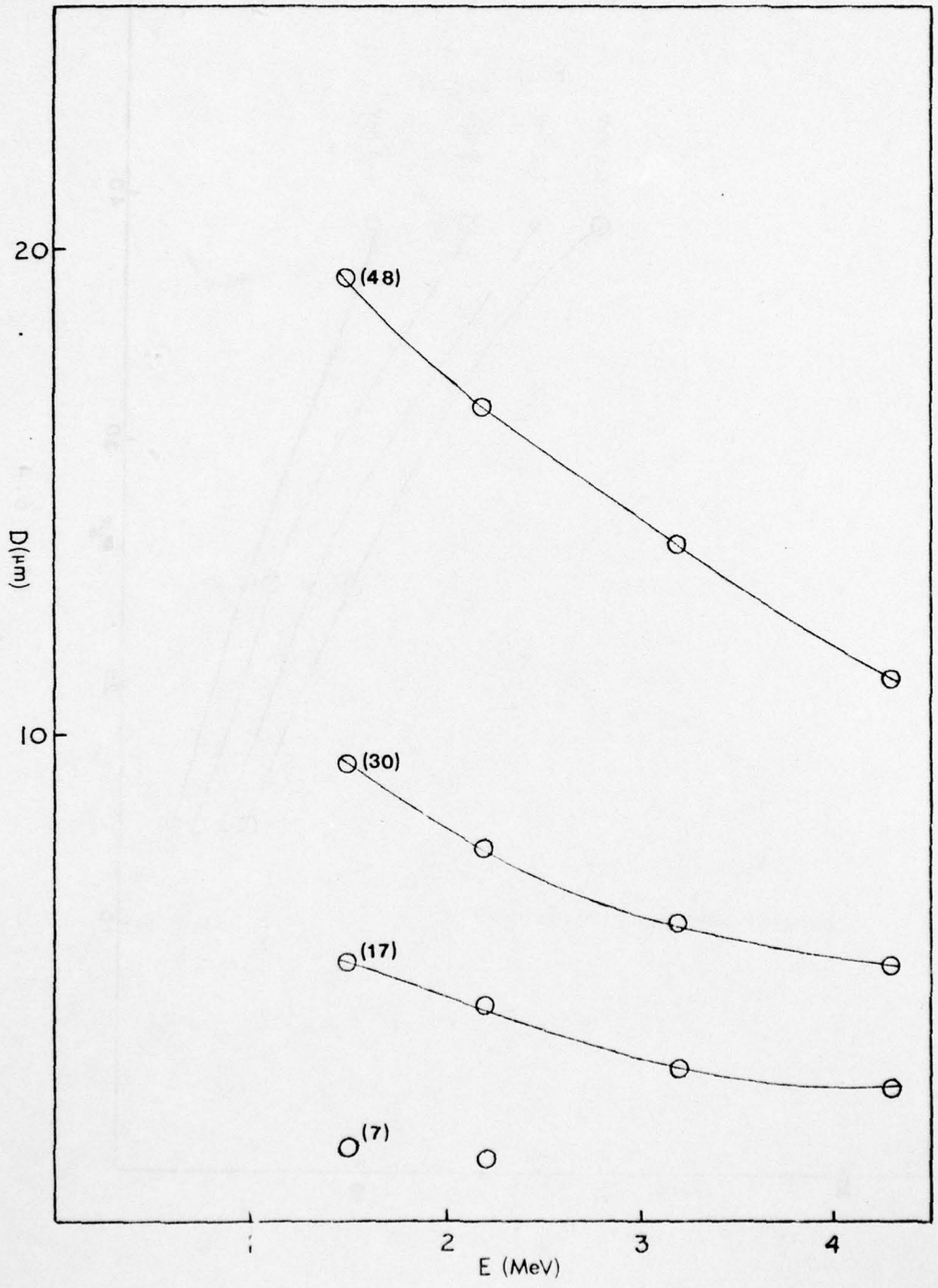

Fig. 6.3

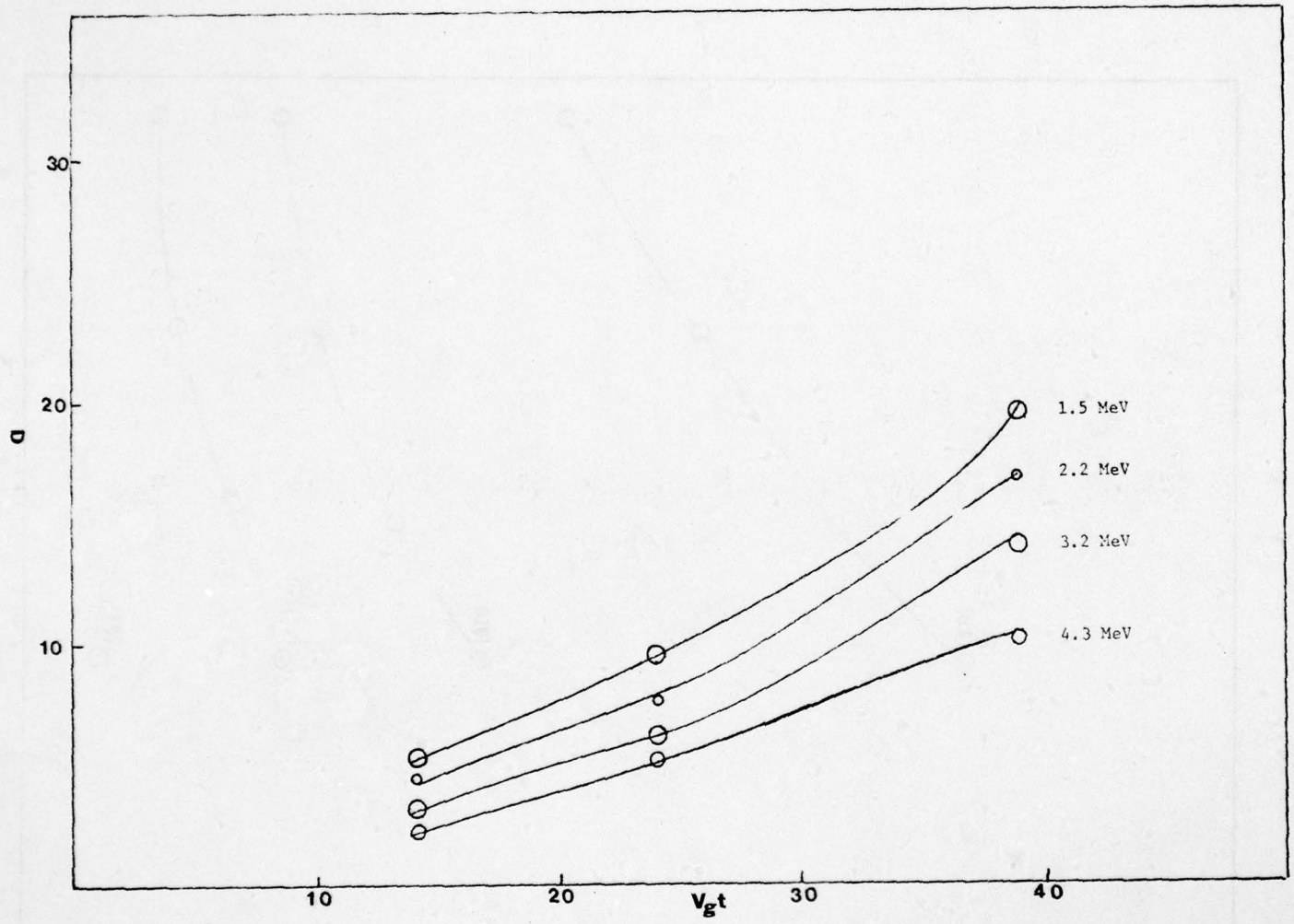

Fig. 6.4

AD-A081 714 EMMANUEL COLL BOSTON MASS F/G 22/2
ENERGETIC PARTICLE STUDIES: INSTRUMENTATION AND ANALYSIS.(U)
SEP 79 W BELLEW, A DAVIS, M P HAGAN F19628-76-C-0039
UNCLASSIFIED AFGL -TR-79-0223 NL

2 OF 2
AD A081714

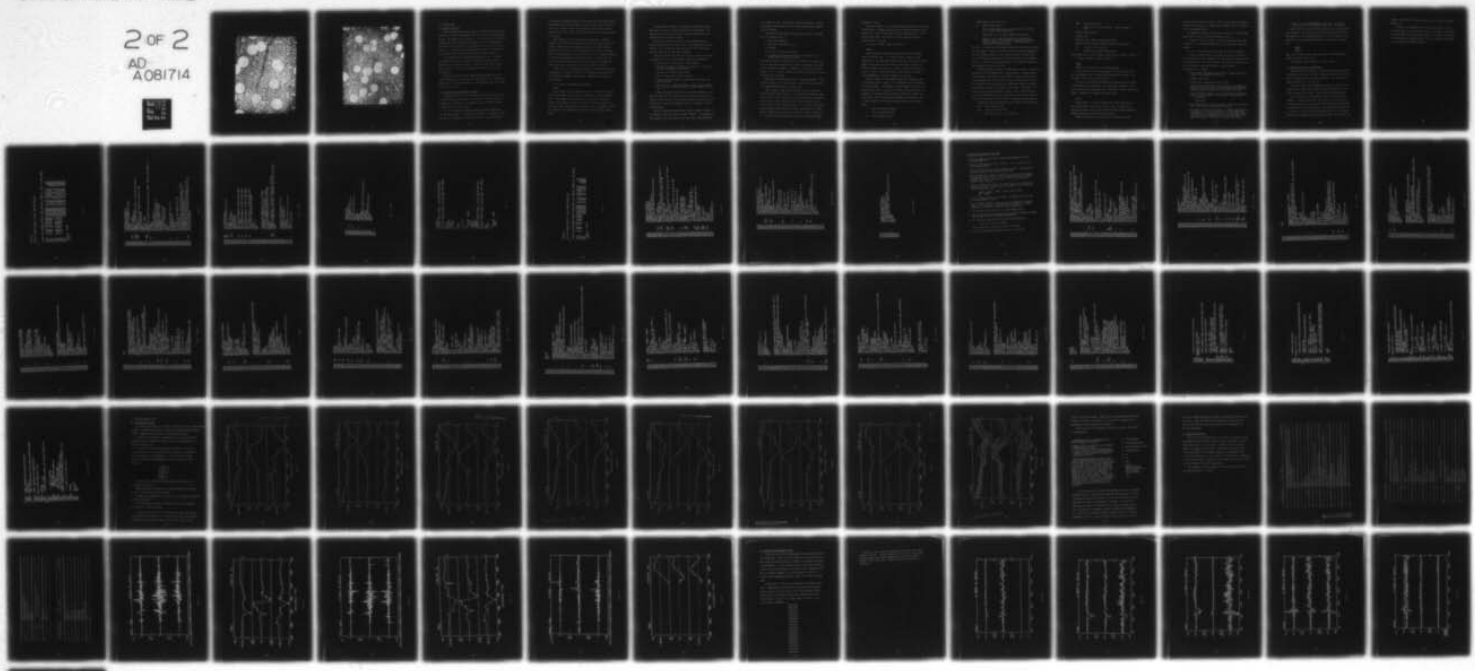

END
DATE FILMED
4-80
DTIC

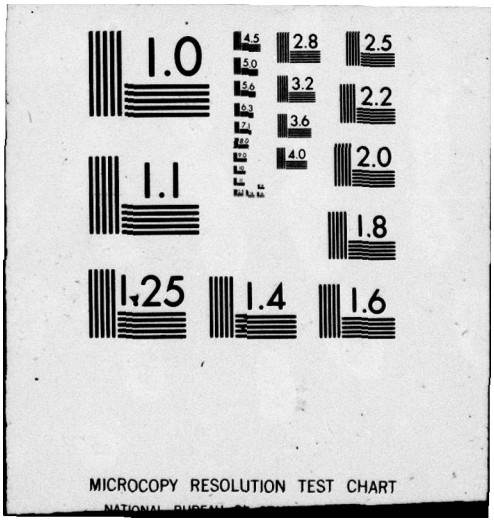
1.0
1.1
1.25
1.4
1.6
1.8
2.0
2.2
2.5
2.8
3.2
3.6
4.0
4.5
5.0
5.6
6.3
7.1
8.0
MICROCOPY RESOLUTION TEST CHART

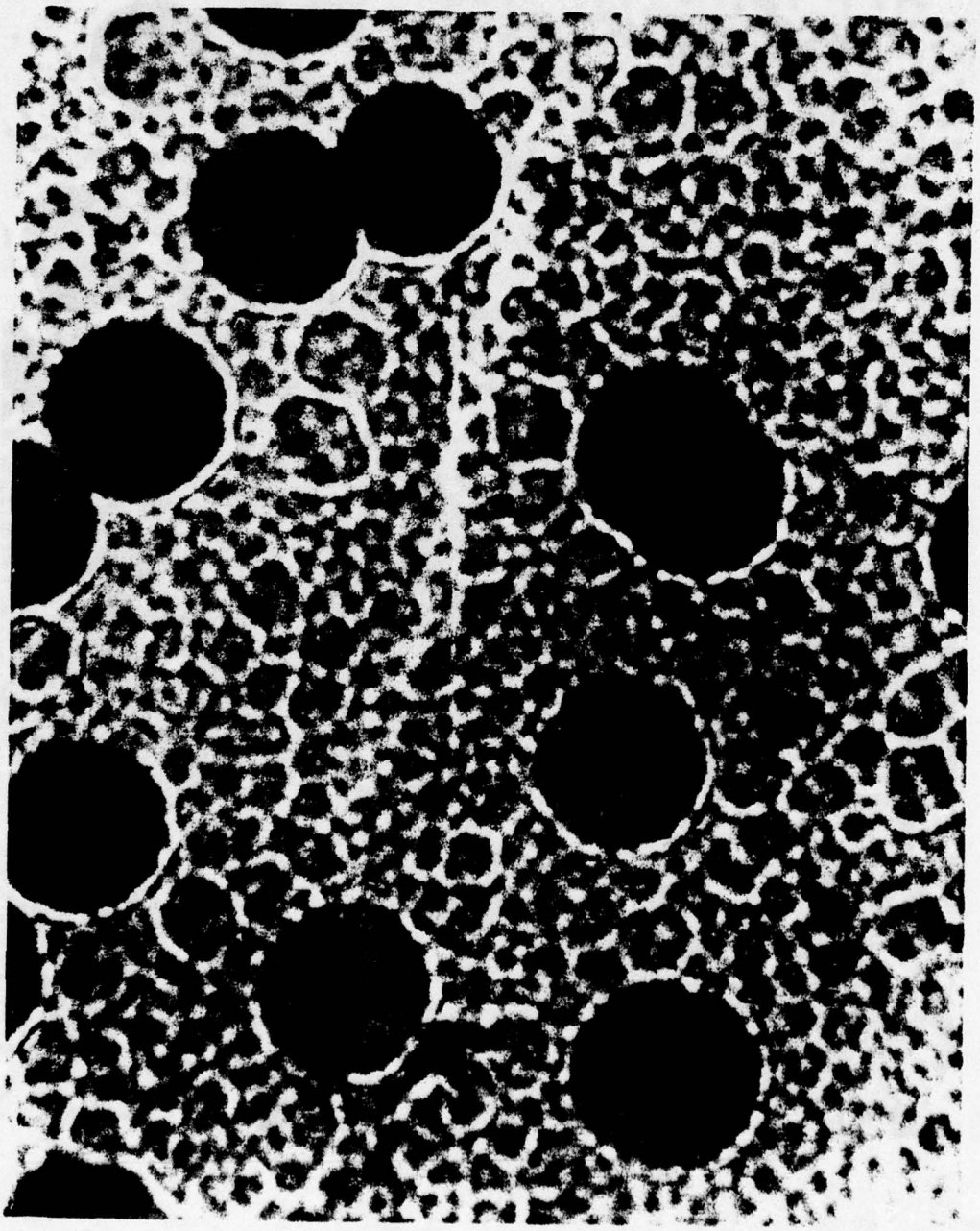

Fig. 6.5

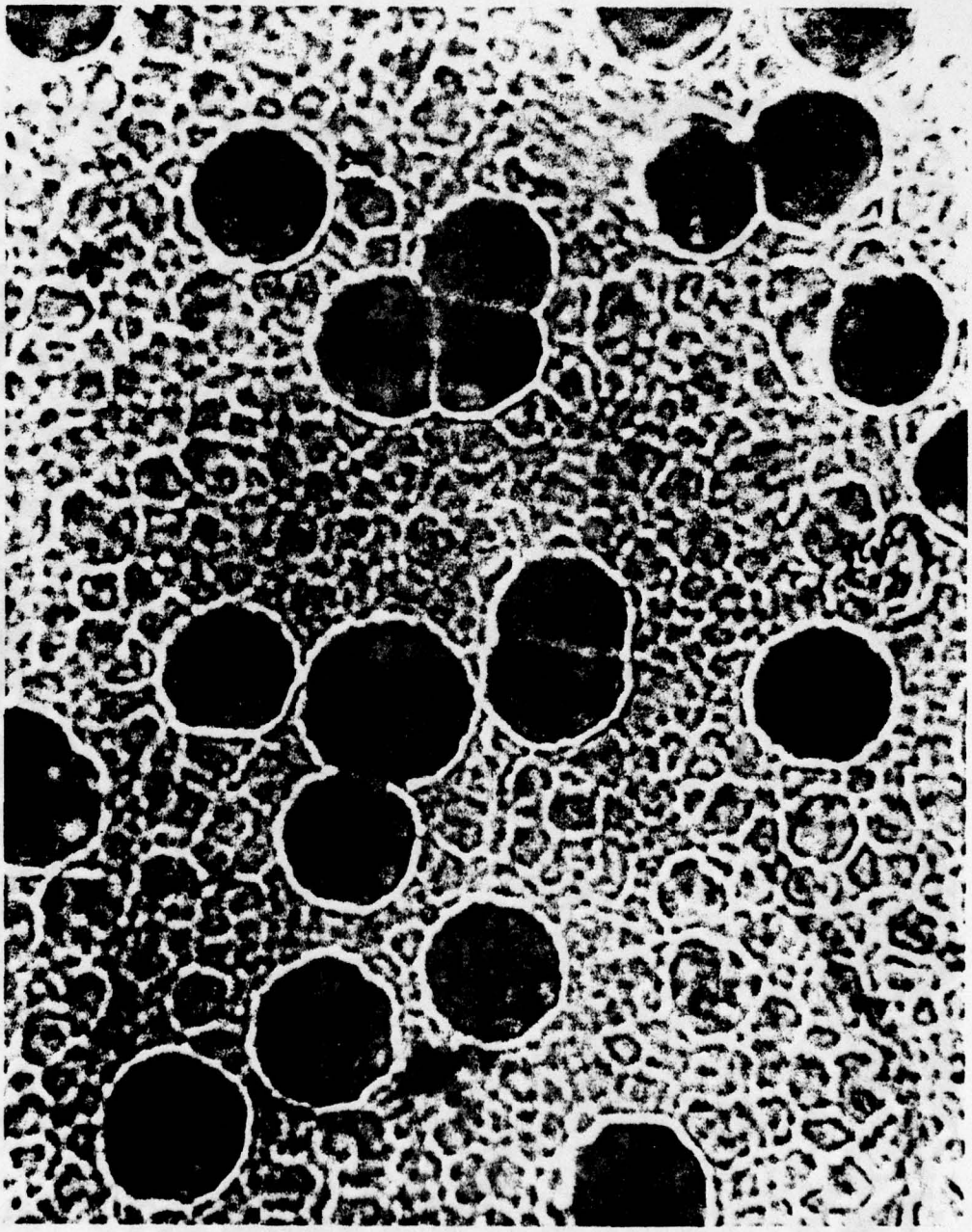

Fig. 6.6

7. MAGAF SYSTEM

7.1 Systems Generation

Initial preparations have been made to do another systems generation (sysgen) on the Univac minicomputer which services the AFGL Magnetometer Network. The purpose of this sysgen is: 1) to allow the use of both the teletype and the Tektronix CRT at the same time, 2) to incorporate the DEC printer into the system, 3) to incorporate the new drivers into the system, i.e., the magnetic tape and DDU drivers, and 4) to incorporate the existing patches contained in the patch file into the system.

To accomplish this the following things must be done: 1) update the current systems tape to reflect the new drivers and to include dummy drivers and controller tables in order to do the necessary diagnostic testing, 2) update the sysgen directives, and 3) dissassemble the patch file.

The two new drivers have been modified and the dummy controller tables and drivers have been made, and these need now to be added to the system tape. The controller tables for the DEC printer and the teletype have also been written.

7.2 Documentation of Minicomputer Software

Programs written for use on the Univac minicomputer which services the AFGL magnetometer network are in the process of documentation and, in some cases, overhauling. Descriptions and use of those documented to date are given in this section.

For all minicomputer programs described, operator communication with the minicomputer, is through the Tektronix CRT. Similarly all output from the minicomputer is received on the CRT. With each program

is provided the commands supplied by the operator and the output from the minicomputer, both of which appear on the CRT screen. Hard copy of the CRT screen is made by means of the Tektronix Hard Copy Unit, which is connected to the CRT, and it is these copies which are used to illustrate the programs.

Some programs have more than one mode of operation. Different options can be selected by responding at the CRT to prompts made by the program. Other options are selected by means of the sense switches, referred to as SS1, SS2, and SS3, respectively, which are on the front panel of the minicomputer. Each will be set on, off, or ignored depending on the particular program and the option desired. At other times the sign switch on the front panel can be used to signal the minicomputer. These variations are explained for each program in this section.

In this section are included descriptions of the following programs and procedures: A) TAPLOG, B) TAPDUP, C) Procedure to reconstitute the system from tape (DISKNU), and D) NUFILE. Examples and listings are also provided.

7.2.1 Program Descriptions and Procedures

TAPLOG

Program TAPLOG reads an ARCHIV tape, looks at the time of the first frame of each record, and may print it depending on criteria explained below. Some diagnostics are also printed in the case of defective records. This program is useful for finding out what time period is on a particular tape, what records are defective, and , in conjunction with other programs, for finding where a particular time period on a tape begins.

The program has two modes of operation, the difference between them being the amount of output produced by the minicomputer. The modes are selected by means of sense switches, and the mode can be changed while the program is running.

With SS3 on, the time of the first frame of every record is printed whether that time is good or bad. This option does, however, produce a lot of output since there are usually about 4000 records per tape, equivalent to 4000 lines of output.

With SS2 on and SS3 off, the time of the first frame of a record is printed only if one of the following conditions is fulfilled:

a) The time of the first record is always printed.

b) The time is printed if a new day is started, i.e., the time just passed midnight on that record.

c) All ends of file (EOF's) are printed.

d) The first time after an EOF is printed.

e) At any point where there is a logical gap in the data, the time is printed.

f) Bad times, i.e., times which make no sense, are also printed, e.g., the day is greater than 366, the time contains all 0's, etc.

If, while running with only SS2 on, the operator desires to know what the frame time is at that point in the tape, pressing the sign switch on the front panel will produce the current time being processed. This feature is handy in positioning a tape at a particular time for another program.

Operator commands and minicomputer output are shown in Figure 7.1. The operator starts the program by typing '/TAPLOG'. The program asks which magnetic tape drive contains the input tape, "ENTER INPUT UNIT :

1,2,3 FOR M1, M2, M3." The operator responds accordingly. The next line reminds the operator of the use of the sense and sign switches with this program.

Following this the times are printed when required. The format of a line reading across is:

a) 'SEQ' means sequence;

b) the time of the current record,

c) 'FOLLOWS',

d) the time of the previous record,

e) the number of the previous record (or the number of the current record if you count from 0).

The previous record is printed because in the event of a bad time one wants to know where on the tape it occurred. The format of the times is best explained by example. In Figure 7.1, the time of the first record is '8 94 15:25:40', which is year 1978, Julian day 94, 15 hours, 25 minutes, and 40 seconds.

Diagnostics are printed in the case of defective records. 'PAR' indicates a parity error on that record. Note that this could be due to a hardware problem as well as a bad record.

'BUM', meaning a 'bum' record, indicates that the consistency check made on the record failed, i.e., the program could make no sense of the record. In the consistency check the program reads through the record frame by frame, reading from each frame the length of that frame, and proceeding to the next frame. If, at the end of the record the count does not make sense, the record is declared bad, or 'BUM'. Note that TAPLOG does not check each frame time within a record, i.e., it is possible to have bad frame times within a record which TAPLOG

considers as 'good'.

Looking at Figure 7.1, we see that the tape started at the time just described above. Midnight was passed after record #859 and again after record #3203. There are bad times on records #1824 and #3162. An EOF follows record #2727. The rest of the times represent small gaps (logical gaps) in the data.

A listing of TAPLOG is shown in Figure 7.2.

TAPDUP

Program TAPDUP is used to copy selective records of an ARCHIV tape on to another tape. It is usually used in conjunction with TAPLOG since it distinguishes records on the input tape by their record number on that tape rather than by their frame times. However, no TAPLOG is needed if one wants, for example, to duplicate the whole or a part of a tape. Selective portions of many tapes e.g., magnetic storm commencements, can thus be merged on to one tape.

Operator commands and minicomputer output for TAPDUP are shown in the example given in Figure 7.3. The operator starts the program by typing '/TAPDUP'. The programs asks which magnetic tape drive contains the input tape, in a manner like TAPLOG. When the operator has responded, the program asks which magnetic tape drive contains the output tape. After the operator has responded, the program is ready to receive commands, whose descriptions and formats are explained below:

C Copies one physical record.

S Skips one physical record.

Cn Copies through record n.

C9999 Copies to the end of tape.

Sn Skips through record n.

W Writes an EOF (unless the last record written is an EOF, i.e., it will avoid a double EOF).

T Terminates, i.e., it writes a double EOF and exits.

Q Quits, i.e., it exits letting the next input tape be mounted. This is used when parts of two different tapes are to be merged on to one tape. TAPDUP must then be reinitiated as explained above.

Note that 'n' denotes the record number through which one copies or skips (not the number of records). Note that the record number corresponds to the record numbers provided in the right-hand column of TAPLOG, where this record number corresponds to the frame time given by the rightmost time, i.e., the time of the previous record. For example, in Figure 7.1 record number 859 starts at 23:59:30.

In this hypothetical example of TAPDUP shown in Figure 7.3 we want to merge parts of two different tapes to make one tape. Consider Figure 1 in which ARCHIV tape #8094 was run on TAPLOG. Suppose we want to combine everything after the first EOF (at record #2728) with the first 50 or so records on the next ARCHIV tape, #8096 whose TAPLOG is not shown. We also want to delete the bad time at record #3162. Note that if, in trying to copy a specified period of time, we want to be more precise as to what frame times we copy, we would have to use the sign switch or SS3 to find out exactly at what records the beginning and end times are.

An explanation of the procedure for this example is outlined below:

S2728 Skip through the EOF.

C3161 Copy up to the bad time.

S Skip one record, i.e., the bad time.

C4007 Copy up to the EOF.

Q TAPDUP exits; no EOF is written. Control returns to JCP.

/REW,M3 Rewind unit M3.

Dismount tape

Mount new tape, #8096, on the same tape drive.

/TAPDUP Re-enter TAPDUP, specifying input and output units.

C50 Copy the first 50 records.

T TAPDUP writes a double EOF and exits.

The finished tape was run on TAPLOG, and the result is shown in Figure 7.4.

A listing of TAPDUP is shown in Figure 7.5.

DISKNU

DISKNU is a restoration of the system from tape.

In the event that the operating system has to be put back on the disc from magnetic tape, a specified procedure must be followed. This procedure is shown step by step in Figure 7.6.

Note that in the present configuration the operating system resides on the bottom platter of the disc. The normal boot procedure is, with the switch above the front panel set to 'DISC BOOT', to press successively 'RESET', 'STEP/RUN', and 'BOOT' on the front panel.

NUFILE

Program NUFILE is a utility program which allows the user to go easily from magnetic tape to disc and vice versa. It dumps out or reads in partitions, file by file, thereby allowing selective additions. Merging and garbage collection can also be done.

NUFILE can be used to back up the disc, including the bottom

platter on which resides the system. (See the system recovery procedure included in this section.) A backup copy on magnetic tape of the whole disc is now routinely kept.

The commands which NUFILE provides are listed below. The following nomenclature is used to specify the command structure:

a) 'unit' or '$unit_1$' is always a disc-partition logical-unit name or number. (It is recommended that one not mix logical-unit names and numbers.)

b) 'key' is the protection key, if any, of that disc partition.

c) '$unit_2$' actually refers to the tape unit, but it is specified by the logical-unit name or number of the disc partition which was specified when that part of the tape was made. Note that to go from tape to disc the tape must have been previously created by NUFILE.

The commands are as follows:

T This specifies the magnetic tape unit for dumping or partition loading. The default is unit 39, DU.

R Rewind the tape unit.

D D,$unit_1$[,key[,$unit_2$]] dumps $unit_1$ to $unit_2$.

L L,$unit_1$[,key[,$unit_2$]] loads $unit_1$ from $unit_2$, with garbage collection, e.g., if we want to load disc partition D0 from that partition named D2 on the tape, we would type 'L,D0,,D2'.

G This does garbage collection on a disc partition; the magnetic tape is used as a buffer. 'G,unit[,key]' is equivalent to:

```
D,unit[,key]
R
L,unit[,key]
```

M This merges files on $unit_2$ on to $unit_1$, if they are not already there. The format is: M,$unit_1$[,key[,$unit_2$]].

A This adds files from $unit_2$ to $unit_1$. It prompts operation for the file list. Files to be added must not have names which correspond to files already on $unit_1$. If a file name is used which conflicts, the program will print 'ALREADY THERE' and ignore the request. The format is: A,$unit_1$,key ,$unit_2$.

Q Quit, i.e., exit program NUFILE. Note that a '/' will not bring you back to JCP; NUFILE considers this a bad request.

NUFILE can be used to retain object modules across systems generations (sysgens). Note that in the sysgen software provided by Univac, each module must be run through LMGEN every time a new sysgen is done. After the tape unit has been specified etc., the necessary commands are:

```
D,OM,D
D,BL,E
D,FL,F
```

When the new sysgen is done, these partitions are reloaded through NUFILE by typing 'L,OM,D', etc.

The program listing for NUFILE is shown in Figure 7.7.

7.3 Software Written for the CDC 6600

Three subroutines relating to the ARCHIV tapes have been written in Fortran for use on the CDC 6600. They were written to be used with, and as an enhancement for the existing software. The listings are included in Figures 7.8, 7.9 and 7.10.

The first routine called TIMECHK will check the time and station numbers of each frame and will print appropriate diagnostics if any time is incorrect or if there is a large time gap between frames.

The second routine called TOTDAT is used in conjunction with TIMECHK. It constructs the year, Julian day, hour, minute, second, and second within that year for each frame from the array IDATE which is provided by the existing software. For each record the frame time is stored in a series of arrays called YEAR, JDAY, etc. by an index whose value corresponds to that frame's position in that record. For

example, for frame #4 in a given record, the time is found in YEAR(4), JDAY(4), etc.

The third routine DUMP2T takes the frame data which is in a 245 word array and prints it in a format which is the same as that produced by program DUMP2T on the Univac minicomputer. The purpose of writing this routine was that people looking at the data would not be required to get acquainted with another format.

```
/TAPLOG

 ENTER INPUT UNIT: 1,2,3 FOR M1,M2,M3.
3

 SIGN FOR SINGLE PRINT SS3 FOR ALL PRINT, SS2 TO LOG GAPS.

 SEQ    8 94 15:25:40 FOLLOWS  0  0  0: 0: 0      0
 SEQ    8 95  0: 0:10 FOLLOWS  8 94 23:59:30    859
 SEQ    5100  2:53:40 FOLLOWS  8 95  9:59:40   1823
 SEQ    8 95 10: 0:50 FOLLOWS  5100  2:53:40   1824
 EOF                  FOLLOWS  8 95 19: 8: 0   2727
 SEQ    8 95 19:13: 0 FOLLOWS  8 95 19: 8: 0   2728
 SEQ    5236 31:53:40 FOLLOWS  8 95 23:34:50   3161
 SEQ    8 95 23:36: 0 FOLLOWS  5236 31:53:40   3162
 SEQ    8 96  0: 0:30 FOLLOWS  8 95 23:59:50   3203
 EOF                  FOLLOWS  8 96  8:13:50   4007
 EOF                  FOLLOWS  8 96  8:13:50   4008
  TAPLOG  STOP
  JC**
```

Fig. 7.1

```
0001            DIMENSION IA(2561,2)
0002            INTEGER $BUFF,$WITCH
0003            DIMENSION ITIME(5),JTIME(5)
0004            IEOF=0
0005  165       WRITE(1,1055)
0006            READ(2,106)INUNIT
0007  1055      FORMAT(' ENTER INPUT UNIT: 1,2,3 FOR M1,M2,M3.')
0008  106       FORMAT(I1)
0009            IF(INUNIT.LT.1.OR.INUNIT.GT.3)GO TO 165
0010            INUNIT=INUNIT+20
0011            IREC=-1
0012            WRITE(1,1056)
0013  1056      FORMAT(
0014           1'0SIGN FOR SINGLE PRINT SS3 FOR ALL PRINT, SS2 TO LOG GAPS.'/)
0015  11        IYR=99
0016            NL=32767
0017  1         CALL STZ(ITIME,5)
0018            IF(I$TSA(ITSA).LT.0)GO TO 11
0019            IF($WITCH(4).NE.0)IYR=99
0020            IST=IDBUFF(INUNIT,IA,IW)
0021            IREC=IREC+1
0022            IF(IST.EQ.-3)GO TO 56
0023            IF(IST.LT.0)GO TO 99
0024            IEOF=0
0025            NN=1
0026  2         IF(IA(NN,IW).NE.1)GO TO 3
0027            NN1=IA(NN+2,IW)
0028            NN=NN+NN1
0029            GO TO 2
0030  3         IF(IA(NN,IW).NE.4095)GO TO 55
0031            NN1=IA(3,IW)
0032            IF(NN1.NE.7)CALL $TCT1(IA(NN1-2,IW),ITIME)
0033            NL1=360*ITIME(3)+6*ITIME(4)+ITIME(5)/10
0034            IF($WITCH(6).NE.0)GO TO 123
0035            IF(IYR*ITIME(1).EQ.0.AND.IYR.NE.99)GO TO 59
0036  123       IF(IYR.NE.ITIME(1).OR.IDAY.NE.ITIME(2))GO TO 57
0037            IF(NL-NL1)61,62,57
```

Fig. 7.2

```
0038  62      IF(IYR)57,59,57
0039  61      IF((NL1-NL).GT.60)GO TO 57
0040  59      NL=NL1
0041          DO 105 J=1,5
0042  105     JTIME(J)=ITIME(J)
0043          IYR=ITIME(1)
0044          IDAY=ITIME(2)
0045          GO TO 1
0046  57      CALL OTMSG(3HSEQ,2,ITIME,JTIME,IREC)
0047          GO TO 59
0048  55      CALL OTMSG(3HBUM,1,ITIME,JTIME,IREC)
0049          GO TO 11
0050  56      CALL OTMSG(3HPAR,1,JTIME,JTIME,IREC)
0051          GO TO 11
0052  99      CALL OTMSG(3HEOF,1,ITIME,JTIME,IREC)
0053          IF(IST.EQ.-1.OR.IEOF.GT.0)STOP
0054          IEOF=1
0055          GO TO 11
0056          END
0057
0058
0059          SUBROUTINE OTMSG(IA,IW,IT,JT,IREC)
0060          DIMENSION IA(2),IT(5),JT(5)
0061          IF(IW.EQ.1)WRITE(12,100)IA,JT,IREC
0062          IF(IW.EQ.2)WRITE(12,101)IA,IT,JT,IREC
0063          RETURN
0064  100     FORMAT(1X,2A2,15X,' FOLLOWS',3I3,2(1H:,I2),5I6)
0065  101     FORMAT(1X,2A2,3I3,2(1H:,I2),' FOLLOWS',3I3,2(1H:,I2),5I6)
0066          END
0067
0068
0069          FUNCTION IDBUFF(IUNIT,IA,IW)
0070          DIMENSION IA(2561,2)
0071          IF(IW.NE.0)GO TO 1
0072          NN=2560
0073          IST1=IWBUFF(IUNIT,IA,NN,0,4,0)
0074          IW=2
0075  1       IST1=ISTCHK(IA)
```

Fig. 7.2 (cont.)

```
0076            IDBUFF=IST1
0077            IF(IST1)2,11,3
0078   11       CALL $BUFF(1,0,1,1,4)
0079            GO TO 1
0080   2        IF(IST1.EQ.-3)GO TO 3
0081            IW=0
0082            RETURN
0083   3        MM=NN
0084            NN=2560
0085            IST1=IWBUFF(IUNIT,IA(1,IW),NN,0,4,1)
0086            IW=3-IW
0087            N=2561-MM
0088            CALL STZ(IA(MM+1,IW),N)
0089            RETURN
0090            END
BOT:
ED**
```

Fig. 7.2 (cont.)

```
/TAPDUP
 ENTER INPUT UNIT: 1,2,3 FOR M1,M2,M3.
3
 ENTER OUTPUT UNIT 1,2,3; BUT NOT INPUT
1
S2723
 S,2728
C3161
 C,3161
S
 S,
C4007

 C,4007
Q
 Q,
  TAPDUP  STOP
  JC**
/REW,M3
  JC**
/TAPDUP
 ENTER INPUT UNIT: 1,2,3 FOR M1,M2,M3.
3
 ENTER OUTPUT UNIT 1,2,3; BUT NOT INPUT
1
C50
 C,50
T
 T,
  TAPDUP  STOP
  JC**
```

Fig. 7.3

```
/TAPLOG

 ENTER INPUT UNIT: 1,2,3 FOR M1,M2,M3.
1

 SIGN FOR SINGLE PRINT SS3 FOR ALL PRINT, SS2 TO LOG GAPS.

 SEQ    8 95 19:13: 0 FOLLOWS  0  0  0: 0: 0     0
 SEQ    8 96  0: 0:30 FOLLOWS  8 95 23:59:50   474
 SEQ    8 96  8:32:40 FOLLOWS  8 96  8:13:50  1278
 EOF                  FOLLOWS  8 96  9: 4:30  1328
 EOF                  FOLLOWS  8 96  9: 4:30  1329
  TAPLOG  STOP
  JC**
```

Fig. 7.4

```
0001            DIMENSION IA(2561)
0002            COMMON IA,OUNIT,NN
0003            INTEGER OUNIT,$BUFF
0004            DIMENSION IWH1(6),IDIG(4)
0005            DATA IWH1,IBL/1HQ,1HT,1HW,1HS,1HC,0,1H /
0006            IEOF=0
0007  165       WRITE(1,1055)
0008            READ(2,106)INUNIT
0009  1055      FORMAT(' ENTER INPUT UNIT: 1,2,3 FOR M1,M2,M3.')
0010            IF(INUNIT.LT.1.OR.INUNIT.GT.3)GO TO 165
0011            INUNIT=INUNIT+20
0012  166       WRITE(1,105)
0013  105       FORMAT(' ENTER OUTPUT UNIT 1,2,3; BUT NOT INPUT')
0014            READ(2,106)OUNIT
0015  106       FORMAT(I1)
0016            IF(OUNIT.LT.1.OR.OUNIT.GT.3)GO TO 166
0017            OUNIT=OUNIT+20
0018            IF(INUNIT.EQ.OUNIT)GO TO 166
0019            IREC=-1
0020  12        READ(2,107)IWHAT,IDIG
0021            WRITE(1,123)IWHAT,IDIG
0022  123       FORMAT(1X,A1,1H,,5A1)
0023  107       FORMAT(5A1)
0024            DO 112 IN=1,20
0025            IF(IWH1(IN).EQ.0)GO TO 12
0026            IF(IWH1(IN).EQ.IWHAT)GO TO 13
0027  112       CONTINUE
0028  13        GO TO (201,202,203,204,204),IN
0029  202       END FILE OUNIT
0030            END FILE OUNIT
0031  201       STOP
0032  203       CALL WRITR(0)
0033            GO TO 12
0034  204       IN=IN-4
0035            INREC=0
0036            DO 15 I=1,4
0037            IQQ=ISWAB(IDIG(I))
```

Fig. 7.5

```
0038            IF(IQQ.EQ.IBL)GO TO 177
0039            IQQ=IAND(IQQ,255)-176
0040            IF(IQQ.LT.0.OR.IQQ.GT.9)GO TO 12
0041            INREC=10*INREC+IQQ
0042   15       CONTINUE
0043   177      IF(INREC.EQ.0)INREC=IREC+2
0044            INREC=INREC-1
0045   17       IF(INREC-IREC)12,12,16
0046   16       NN=2560
0047            IST=IWBUFF(INUNIT,IA,NN,0,4,0)
0048            MM=NN
0049            IREC=IREC+1
0050            IF(IST.EQ.-3)GO TO 56
0051            IF(IST.LT.0)GO TO 99
0052   56       IEOF=0
0053            IF(IN.EQ.0)GO TO 17
0054            N=2561-MM
0055            CALL STZ(IA(MM+1),N)
0056            NN=1
0057   2        IF(IA(NN).NE.1)GO TO 3
0058            NN1=IA(NN+2)
0059            IF(NN1.LE.0)GO TO 55
0060            NN=NN+NN1
0061            IF(NN-MM)2,3,55
0062   3        IF(IA(NN).NE.4095)GO TO 55
0063            CALL WRITR(1)
0064            GO TO 17
0065   55       CALL WRITR(0)
0066            GO TO 17
0067   99       IF(IN.EQ.1)CALL WRITR(0)
0068            IF(IEOF.EQ.1.OR.IST.EQ.-1)GO TO 202
0069            IEOF=1
0070            GO TO 17
0071            END
0072
0073
ED**
```

Fig. 7.5 (cont.)

```
0073
0074          SUBROUTINE WRITR(IEOF)
0075          COMMON IA(2561),IOUT,NN
0076          IF(JJ+IEOF.EQ.0)GO TO 1
0077          IF(IEOF.EQ.0)END FILE IOUT
0078          IF(IEOF.EQ.1)CALL IWBUFF(IOUT,IA,NN,1,4,0)
0079    1     JJ=IEOF
0080          RETURN
0081          END
BOT:
ED**
```

Fig. 7.5 (cont.)

TO RESTORE THE BOTTOM DISC FROM TAPE

1. Mount the magnetic tape labeled "SAVED SYSTEM BOTTOM DISC 5/4/79" on logical unit DU.

2. Set the switch above the CPU to "TTY BOOT". (It is normally on the "DISC BOOT" position.)

3. On the CPU console, press RESET, STEP/RUN, and BOOT. The system will now hang waiting for the teletype to come ready.

4. Make sure that the teletype is connected to the back of the console, is turned on, and is on line. Mount the paper tape labeled "SYSTEM" RECOVERY BOOT" (about 18 inches long) so that the first frame is exactly at the read point.

5. Turn on the paper tape switch. The paper tape will be read and the Tektronix will beep. A small part of the magnetic tape will be read. The CRT display will show

```
001032  (001000)  001000  000004  007020  000000
DG**  DISKNU
```

6. On the Tektronix, enter: G1032. RETURN. The program will halt with the program counter = 01513

7. Press START on the CPU. About 1/2 to 1 inch thickness of magnetic tape will then be read in; program DISKNU is reading in from tape. When this is finished, the CPU will be in blinking run.

8. Turn the switch above the CPU to the "DISK BOOT" position.

9. Boot the system in the usual way by pressing RESET, STEP/RUN, and BOOT. The teletype will print out"PATCHING COMPLETED".

10. The system will come up in the usual way, making the query:

```
UNIT 1 OR 2? (0 FOR NO ARCHIV)
```

    Resume archiving if desired; restoration is complete.

11. Turn off the teletype and dismount the saved-system tape.

Fig. 7.6

```
0001            DIMENSION IBUFF(80),JBUFF(20),IA(9),IDV(2,2)
0002            EXTERNAL V$PED,V$JPBF
0003            COMMON ITAPE,IUNIT,IPROT,NFILES,NTRY,IUN1,IJNK(19)
0004            COMMON /M$XES/IMXS(3),IDAT(120),IFCB(13)
0005            COMMON /NMX/NMAX
0006            DATA IDV/2H 1,2HST,2H 2,2HND/
0007            DATA IA/1HR,1HT,1HG,1HD,1HL,1HM,1HA,1HQ,1H//
0008            ITAPE=39
0009  1         NTYPE=1
0010            WRITE(3,100)
0011  100       FORMAT(' F**')
0012            READ(3,101)IBUFF
0013  101       FORMAT(80A1)
0014            N=0
0015            IF(INUM(IBUFF,N,JBUFF).NE.1)GO TO 99
0016            ITYPE=JBUFF(1)
0017            IF(ITYPE.EQ.IA(8))CALL EXIT
0018            DO 2 I=1,7
0019            NN=I
0020            IF(ITYPE.EQ.IA(I))GO TO 3
0021  2         CONTINUE
0022  99        WRITE(3,105)
0023  105       FORMAT(' BAD REQUEST')
0024            GO TO 1
0025  3         IF(NN.NE.1)GO TO 4
0026            REWIND ITAPE
0027            GO TO 1
0028  4         NCHR=INUM(IBUFF,N,JBUFF)
0029            IF(NCHR.GT.2.OR.NCHR.LT.-3)GO TO 98
0030            IUNIT=I$DVCE(JBUFF(1))
0031            IF(NN.NE.2)GO TO 5
0032            IF(IUNIT.GE.0)GO TO 98
0033            ITAPE=-IUNIT
0034            GO TO 1
0035  5         IF(IUNIT.LE.0)GO TO 98
0036            NCHR=INUM(IBUFF,N,JBUFF)
0037            IF(NCHR.LT.0.OR.NCHR.GT.1)GO TO 97
```

Fig. 7.7

```
0038            IPROT=JBUFF(1)
0039            NTYPE=2
0040            IUN1=IUNIT
0041            NCHR=INUM(IBUFF,N,JBUFF)
0042            IF(N.LT.NMAX.AND.NN.LE.4)GO TO 98
0043            IF(NCHR.EQ.0)GO TO 7
0044            IF(NCHR.LT.-3.OR.NCHR.GT.2)GO TO 98
0045            IUN1=JBUFF(1)
0046            IF(NCHR.GT.0)IUN1=I$DVCE(IUN1)
0047            IUN1=IABS(IUN1)
0048            IF(IUN1.EQ.0)GO TO 98
0049  7         NN=NN-4
0050            IF(NN)8,9,10
0051  8         REWIND ITAPE
0052  9         CALL DUMPIT(V$PED,1,NFILES,NTRY)
0053            IF(NN.EQ.0)GO TO 1
0054            REWIND ITAPE
0055  10        IT=IPROT
0056            IT1=IUNIT
0057            IF(IPOST(IUN1).NE.0)GO TO 11
0058            WRITE(3,102)
0059  102       FORMAT(' HIT END OF TAPE')
0060            GO TO 1
0061  11        IPROT=IT
0062            IUNIT=IT1
0063            IF(NN-2)12,13,14
0064  12        CALL LOADIT(V$PED,1,NFILES,NTRY)
0065            GO TO 1
0066  13        CALL MERGIT(V$PED)
0067            GO TO 1
0068  14        CALL ADDIT(V$PED)
0069            GO TO 1
0070  98        WRITE(3,106)(IDV(I,NTYPE),I=1,2)
0071  106       FORMAT(A3,A2,' DEVICE BAD')
0072            GO TO 1
0073  97        WRITE(3,107)
0074  107       FORMAT(' PROTECTION CODE BAD')
0075            GO TO 1
```

Fig. 7.7 (cont.)

```
0076            END
0077
0078
0079
0080            FUNCTION INUM(IBUFF,N,JBUFF)
0081            COMMON /NMX/NMAX
0082            DIMENSION IBUFF(80),JBUFF(20),IFMT(3)
0083            DATA IMN,IBL,ICOM,IZERO,I9,LHW/1H-,1H ,1H,,1H0,1H9,ZFF00/
0084            IF(N.NE.0)GO TO 2
0085            NMAX=81
0086            DO 1 I=1,80
0087            NMAX=NMAX-1
0088            IF(IBUFF(NMAX).NE.IBL)GO TO 2
0089    1       CONTINUE
0090            NMAX=0
0091    2       INUM=0
0092            JBUFF(1)=0
0093            JBUFF(2)=IBL
0094            JBUFF(3)=IBL
0095            N=N+1
0096            IF(N.GT.NMAX)RETURN
0097            IALPH=0
0098            DO 3 I=1,20
0099            DO 4 J=1,2
0100            ICHR=IBUFF(N)
0101            IF(ICHR.EQ.ICOM)GO TO 5
0102            IF(ICHR.EQ.IBL.OR.ICHR.EQ.IMN)GO TO 44
0103            IF(ICHR.LT.IZERO.OR.ICHR.GT.I9)IALPH=1
0104    44      IF(J.EQ.1)GO TO 45
0105            JBUFF(I)=IOR(JBF,ISWAB(IAND(ICHR,LHW)))
0106            GO TO 46
0107    45      JBUFF(I)=ICHR
0108            JBF=IAND(ICHR,LHW)
0109    46      N=N+1
0110            INUM=INUM+1
0111            IF(N.GT.NMAX)GO TO5
0112    4       CONTINUE
```

Fig. 7.7 (cont.)

```
0113  3       CONTINUE
0114  5       IF(IALPH.EQ.1.OR.INUM.EQ.0)RETURN
0115          ENCODE(6,101,IFMT)INUM
0116  101     FORMAT(2H(I,I2,2H) )
0117          DECODE(INUM,IFMT,JBUFF)JBUFF(1)
0118          INUM=-INUM
0119          RETURN
0120          END
0121
0122
0123          FUNCTION I$DVCE(IUN)
0124          EXTERNAL V$LUNT,V$LUT1,V$LUT2,V$LUT3,V$DSTB
0125          DIMENSION ITYPE(3)
0126          DATA MT,IFF,ID0/2HMT,ZFFF0,2HD0/
0127          IDV= ID$CHK(IUN,V$LUNT,V$LUT1,V$LUT2,V$LUT3,V$DSTB,ITYPE)
0128          I$DVCE=0
0129          IF(ITYPE(2).EQ.MT)I$DVCE=-IDV
0130          IF(IAND(ITYPE(2),IFF).EQ.ID0)I$DVCE=IDV
0131          RETURN
0132          END
0133
0134
0135          FUNCTION ID$CHK(IUN,LUNT,LUT1,LUT2,LUT3,IDST,ITYPE)
0136          DIMENSION IDST(1),LUNT(1),LUT1(1),LUT2(1),LUT3(1)
0137          DIMENSION ITYPE(3)
0138          ID$CHK=0
0139          JUN=IUN
0140          LUN=JUN
0141          IF(IUN)1,2,3
0142  2       RETURN
0143  1       DO 4 I=1,1000,2
0144          JUN=LUNT(I+1)
0145          LUN=JUN
0146          IF(LUNT(I).EQ.0)RETURN
0147          IF(LUNT(I).EQ.IUN)GO TO 3
0148  4       CONTINUE
0149  3       IF(JUN.GT.100)GO TO 5
```

Fig. 7.7 (cont.)

```
0150            IF(JUN.GT.LUT1(1))RETURN
0151            INX=IAND(LUT1(JUN+1),255)
0152            GO TO 7
0153  5         JUN=JUN-100
0154            IF(JUN.GT.79)GO TO 6
0155            IF(JUN.GT.LUT2(1))RETURN
0156            INX=IAND(LUT2(JUN+1),255)
0157            GO TO 7
0158  6         JUN=JUN-79
0159            IF(JUN.GT.LUT3(1))RETURN
0160            INX=IAND(LUT3(JUN+1),255)
0161  7         IF(INX.EQ.0)RETURN
0162            INX=3*INX-2
0163            DO 8 I=1,3
0164            ITYPE(I)=IDST(INX)
0165  8         INX=INX+1
0166            ID$CHK=LUN
0167            RETURN
0168            END
0169
0170
0171            FUNCTION IPOST(ICHEK)
0172            COMMON ITAPE,IUNIT,IPROT,NFILES,NTRY,IUN1(20)
0173            INTEGER$BUFF
0174            JCHEK=ICHEK
0175            IPOST=ICHEK
0176            NEOF=2
0177  1         IST=$BUFF(ITAPE,IUNIT,6,0,1)
0178            IF(IST.EQ.-2)GO TO 2
0179            IF(NEOF.EQ.2)GO TO 3
0180  4         NEOF=0
0181            GO TO 1
0182  2         NEOF=NEOF+1
0183            IF(NEOF.NE.3)GO TO 1
0184            IPOST=0
0185            RETURN
0186  3         IF(JCHEK*(JCHEK-IUNIT).NE.0)GO TO 4
0187            RETURN
```

Fig. 7.7 (cont.)

```
0188            END
0189
0190
0191            SUBROUTINE DUMPIT(IDIR,IGO,NFILES,NTRY)
0192            COMMON /M$XES/IMXS(3),IDAT(120),IFCB(13)
0193            DIMENSION IWHERE(3),IDIR(7,2)
0194            COMMON ITAPE,IUNIT,IPROT,NJNQ(22)
0195            NFILES=0
0196           IMXS(3)=I$NFLO(IUNIT,IPROT,IFCB(8))
0197  2        IF(I$NFL(IWHERE))11,2,3
0198  3         CONTINUE
0199            WRITE(59,101)(IFCB(I),I=8,10),IWHERE
0200            CALL ADDER(IFCB(8),IWHERE,IDIR,NFILES,NTRY)
0201            GO TO 2
0202  11        CONTINUE
0203            IF(NFILES.EQ.0)GO TO 1
0204            IF(IGO.EQ.0)RETURN
0205            IST=$BUFF(1,6924,1,1,4)
0206            WRITE(5,105)IUNIT,IPROT
0207  105       FORMAT(' UNIT=',I3,1H,,A1/)
0208            WRITE(5,101)((IDIR(I,J),I=1,7),J=1,NTRY)
0209  101       FORMAT(1X,3A2,4I6)
0210            IST=$BUFF(ITAPE,IUNIT,120,1,3)
0211            DO 222 I=1,NTRY,19
0212  222       CALL $BUFF(ITAPE,IDIR(1,I),133,1,3)
0213            END FILE ITAPE
0214            J=1
0215            DO 12 I=1,NFILES
0216            MAX=0
0217  14        IFILE=IDIR(7,J)
0218            IF(IFILE.NE.I)GO TO 13
0219            MAX=MAX0(MAX,IDIR(5,J))
0220            J=J+1
0221            IF(J.LE.NTRY)GO TO 14
0222  13        J=J-1
0223            DO 15 K=1,3
0224  15        IFCB(K+7)=IDIR(K,J)
0225            IFCB(3)=IAND(ISWAB(IPROT),255)
```

Fig. 7.7 (cont.)

```
0226            CALL V$OPEN(99,IUNIT,IFCB,0)
0227            DO 16 K=1,MAX
0228            READ(99)IDAT
0229    16      IST=$BUFF(ITAPE,IDAT,120,1,1)
0230            CALL V$CLOS(99,0)
0231            END FILE ITAPE
0232    12      J=J+1
0233            END FILE ITAPE
0234            END FILE ITAPE
0235            BACKSPACE ITAPE
0236            RETURN
0237    1       WRITE(3,100)
0238    100     FORMAT(' VACUOUS PARTITION')
0239            RETURN
0240            END
0241
0242
0243            SUBROUTINE ADDER(INAME,IWHERE,IDIR,NFILES,NTRY)
0244            DIMENSION INAME(3),IWHERE(3)
0245            DIMENSION IDIR(7,10)
0246            IF(NFILES.NE.0)GO TO 11
0247            M=1
0248            INEW=1
0249            NTRY=0
0250            IENTRY=1
0251    15      DO 1 I=1,3
0252    1       IDIR(I,M)=INAME(I)
0253            IDIR(4,M)=IWHERE(2)
0254            ITMP=IWHERE(1)-IWHERE(2)
0255            IDIR(5,M)=ITMP
0256            IDIR(6,M)=IWHERE(3)-IWHERE(2)
0257            IDIR(7,M)=IENTRY
0258            NFILES=NFILES+INEW
0259            NTRY=NTRY+1
0260            RETURN
0261    11      IF(IWHERE(2)-IDIR(4,NTRY))12,13,14
0262    14      INEW=1
0263            GO TO 17
```

Fig. 7.7 (cont.)

```
0264   13      INEW=0
0265   17      MM=NTRY
0266           M=NTRY+1
0267   16      IENTRY=IDIR(7,MM)+INEW
0268           GO TO 15
0269   12      INEW=1
0270           DO 20 I=1,NTRY
0271           IF(IWHERE(2)-IDIR(4,I))21,22,20
0272   22      INEW=0
0273           GO TO 20
0274   21      JJ=NTRY+1
0275           DO 26 J=I,NTRY
0276           DO 27 K=1,6
0277   27      IDIR(K,JJ)=IDIR(K,JJ-1)
0278           IDIR(7,JJ)=IDIR(7,JJ-1)+INEW
0279   26      JJ=JJ-1
0280           MM=MAX0(1,I-1)
0281           M=I
0282           GO TO 16
0283   20      CONTINUE
0284           STOP 77
0285           END
0286
0287
0288           SUBROUTINE LOADIT(IDIR,IGO,NFILES,NTRY)
0289           INTEGER $BUFF
0290           DIMENSION IWHERE(3),IDIR(7,2)
0291           COMMON ITAPE,IUNIT,IPROT,NJNQ(22)
0292           COMMON /M$XES/IMXS(3),IDAT(120),IFCB(13)
0293           DO 1 I=1,NTRY,19
0294   1       CALL $BUFF(ITAPE,IDIR(1,I),133,0,3)
0295           CALL $BUFF(ITAPE,IJUNK,1,4,0)
0296           IF(IGO.EQ.0)RETURN
0297           NMAX=0
0298           NF=0
0299           DO 7 I=1,NTRY
0300           IF(IDIR(7,I).EQ.NF)GO TO 7
0301           NMAX=NMAX+IDIR(6,I)
```

Fig. 7.7 (cont.)

```
0302            NF=NF+1
0303    7       CONTINUE
0304           IMAX=I$NFLO(IUNIT,IPROT,IFCB(8))
0305            IRM=(NTRY+18)/19
0306            IF(IRM+NMAX.LE.IMAX)GO TO 2
0307            WRITE(2,101)
0308    101     FORMAT(' NOT ENOUGH ROOM')
0309            RETURN
0310    2       IRM1=IRM+1
0311            NT=0
0312            NF=1
0313            DO 3 JDIR=1,IRM
0314            M=6
0315            CALL STZ(IDAT,120)
0316            DO 4 I=1,19
0317            IDAT(1)=I
0318            NT=NT+1
0319            DO 6 J=1,3
0320            IDAT(M)=IDIR(J,NT)
0321    6       M=M+1
0322            IDAT(M+1)=IRM1
0323            IDAT(M+2)=IRM1+IDIR(6,NT)
0324            IDAT(M)=IRM1+IDIR(5,NT)
0325            M=M+3
0326            IDAT(M)=1
0327            IF(NT.EQ.NTRY)GO TO 33
0328            NF1=IDIR(7,NT+1)
0329            IF(NF.EQ.NF1)GO TO 4
0330            NF=NF1
0331            IRM1=IRM1+IDIR(6,NT)
0332    4       CONTINUE
0333            IDAT(120)=JDIR+1
0334    33      CALL OUTDIR(JDIR,IDAT)
0335            WRITE(5,105)IDAT(M),IDAT
0336    105     FORMAT(6I5/(1X,3A2,3I6))
0337    3       CONTINUE
0338            CALL BORDIT(IDIR,IDIR(1,NTRY+1),NTRY)
0339            CALL OUTIT(IDIR,IDIR(1,NTRY+1),NFILES)
```

Fig. 7.7 (cont.)

```
0340            RETURN
0341            END
0342
0343
0344            SUBROUTINE MERGIT(IDIR)
0345            COMMON/NMX/NMAX
0346            COMMON/M$XES/IMXS(3),IDAT(133)
0347            DIMENSION IBUFF(80),JBUFF(3)
0348            EQUIVALENCE (JBUFF(1),IDAT(82),IBUFF(82))
0349            DIMENSION IDIR(2)
0350            COMMON ITAPE,IUNIT,IPROT,NFILES,NTRY,IJUNK(20)
0351            IADD=0
0352  1         NFLZ=NFILES
0353            NTRY1=NTRY
0354            CALL DUMPIT(IDIR,0,NFILES,NTRY)
0355            NX=7*NTRY+1
0356            CALL LOADIT(IDIR(NX),0,NFLZ,NTRY1)
0357            NY=NX+7*NTRY1
0358            CALL BORDIT(IDIR(NX),IDIR(NY),NTRY1)
0359            IF(IADD.NE.0)GO TO 3
0360  33        CALL MERGER(IDIR(NX),NFLZ,NTRY1,IDIR,NFILES,NTRY,IDIR(NY),IADD)
0361            RETURN
0362            ENTRY ADDIT(IDIR)
0363            IADD=1
0364            GO TO 1
0365  3         WRITE(3,101)
0366  101       FORMAT(' ADDITIONS')
0367            READ(2,100)IBUFF
0368  100       FORMAT(80A1)
0369            N=0
0370  8         NCHR=INUM(IBUFF,N,JBUFF)
0371            IF(NMAX.EQ.0)GO TO 4
0372            IF(NCHR)5,6,7
0373  6         IF(N.GT.NMAX)GO TO 3
0374            GO TO 8
0375  7         IF(NCHR.LE.6)GO TO 9
0376            NN=(NCHR+1)/2
0377            WRITE(3,102)(JBUFF(I),I=1,NN)
```

Fig. 7.7 (cont.)

```
0378  102     FORMAT(' ERROR ',20A2)
0379          GO TO 6
0380  9       JBUFF(6)=99
0381          IMAX=IAD(JBUFF,IDIR(NX),NTRY1,1)
0382          IF(IMAX.GT.0)GO TO 10
0383          IMAX=-IMAX
0384          NS1=1
0385          DO 12 I=1,NFLZ
0386          NN=NY+I-1
0387          NN=IDIR(NN)
0388          NS2=NS1+NN-1
0389          IF(IMAX.LT.NS1.OR.IMAX.GT.NS2)GO TO 12
0390          INX=NX+7*(NS1-1)
0391          CALL IAD(IDIR(INX),IDIR(INX),NN,NN)
0392          GO TO 6
0393  12      NS1=NS2+1
0394          STOP 1111
0395  10      WRITE(3,105)JBUFF
0396  105     FORMAT(A3,2A2, 'NOT FOUND')
0397          GO TO 6
0398  5       WRITE(3,106)
0399  106     FORMAT(' ERROR, NUMERIC')
0400          GO TO 6
0401  4       INX=NX-1
0402          DO 111 I=1,NTRY1
0403          INX=INX+7
0404  111     IDIR(INX)=-IDIR(INX)
0405          GO TO 33
0406          END
0407
0408
0409          SUBROUTINE BORDIT(IA,IBORD,N)
0410          DIMENSION IA(7,2),IBORD(2)
0411          IBORD(1)=0
0412          NN=1
0413          INXT=IA(7,1)
0414          DO 1 I=1,N
0415          IST=INXT
```

Fig. 7.7 (cont.)

```
0416            INXT=IA(7,I)
0417            IF(IST.EQ.INXT)GO TO 1
0418            NN=NN+1
0419            IBORD(NN)=0
0420    1       IBORD(NN)=IBORD(NN)+1
0421            RETURN
0422            END
0423
0424
0425            SUBROUTINE MERGER(IA,NNEW,NTRY1,IB,NOLD,NTRY,IC,IP)
0426            DIMENSION IA(7,2),IB(7,2),IC(2)
0427            COMMON /MSXES/LASMAX,MAXDIR,MAXPAR,IDAT(120),IFCB(13)
0428            DATA INO,IYES/1HN,1HY/
0429            LASNUM=INDIR(IDAT)
0430            IDRADD=0
0431            NADD=0
0432            LASMAX=MAX0(LASMAX,MAXDIR)
0433            ISTADD=LASMAX
0434            MXDIR=MAXDIR
0435            NS1=1
0436            DO 1 I=1,NNEW
0437            NN=IC(I)
0438            NS2=NS1+NN-1
0439            IF(IA(7,NS1).LE.0)GO TO 1
0440            IMAX=IAD(IA(1,NS1),IB,NTRY,NN)
0441            IF(IMAX.GT.0)GO TO 12
0442            IF(IP.EQ.1)WRITE(1,110)((IA(J,NQ),J=1,3),NQ=NS1,NS2)
0443    110     FORMAT(A3,2A2,' ALREADY THERE')
0444            GO TO 1
0445    12      IDRAD=0
0446            NEWNUM=LASNUM+NN
0447            IF(NEWNUM.LE.19)GO TO 3
0448            IDRAD=NEWNUM/19
0449            NEWNUM=MOD(NEWNUM,19)
0450    3       NEWMAX=LASMAX+IMAX+IDRAD
0451            IF(NEWMAX.LE.MAXPAR)GO TO 5
0452    6       WRITE(3,100)
0453    100     FORMAT(' NOT ENOUGH ROOM, PROCEED ?(Y,N)')
```

Fig. 7.7 (cont.)

```
0454            READ(2,101)IPRO
0455    101     FORMAT(A1)
0456            IF(IPRO.EQ.INO)RETURN
0457            IF(IPRO.NE.IYES)GO TO 6
0458            DO 111 J=NS1,NTRY1
0459    111     IA(7,J)=-IABS(IA(7,J))
0460            GO TO7
0461    5       LASMAX=NEWMAX
0462            LASNUM=NEWNUM
0463            IDRADD=IDRADD+IDRAD
0464            NADD=NADD+NN
0465            IF(IP.EQ.0)WRITE(1,109)((IA(J,NQ),J=1,3),NQ=NS1,NS2)
0466    109     FORMAT(A3,2A2)
0467    1       NS1=NS1+NN
0468    7       IF(NADD.EQ.0)RETURN
0469            ISF=ISTADD+IDRADD
0470            NXDIR=ISTADD
0471            NS1=1
0472            DO 8 I=1,NNEW
0473            NN=IC(I)
0474            IF(IA(7,NS1).LT.0)GO TO 8
0475            NS2=NS1
0476            DO 9 J=1,NN
0477            CALL DIRAD(IDAT,ISF,NXDIR,IA(1,NS2),NADD,MXDIR)
0478    9       NS2=NS2+1
0479            IF(NADD.EQ.0)GO TO 10
0480            ISF=ISF+IA(6,NS1)
0481    8       NS1=NS1+NN
0482    10      CALL OUTIT(IA,IC,NNEW)
0483            RETURN
0484            END
0485
0486
0487            FUNCTION IAD(IA,IB,NTRY,N)
0488            DIMENSION IA(7,N),IB(7,NTRY)
0489            IAD=0
0490            DO 1 I=1,N
0491            DO 2 J=1,NTRY
```

Fig. 7.7 (cont.)

```
0492            DO 3 K=1,3
0493            IF(IA(K,I).NE.IB(K,J))GO TO 2
0494    3       CONTINUE
0495            IAD=-J
0496            GO TO 4
0497    2       CONTINUE
0498    1       IAD=IA(6,1)
0499            RETURN
0500    4       DO 5 I=1,N
0501    5       IA(7,I)=-IABS(IA(7,I))
0502            RETURN
0503            END
0504
0505
0506            SUBROUTINE DIRAD(IDAT,ISF,NXT,IADD,NADD,MXDIR)
0507            DIMENSION IDAT(120),IADD(7)
0508            IWHR=IDAT(1)
0509            IF(IWHR.EQ.19)GO TO 11
0510    12      IWHR=IWHR+1
0511            INX=6*IWHR
0512            DO 1 I=1,3
0513            IDAT(INX)=IADD(I)
0514    1       INX=INX+1
0515            IDAT(INX)=ISF+IADD(5)
0516            IDAT(INX+1)=ISF
0517            IDAT(INX+2)=ISF+IADD(6)
0518            INX=INX+3
0519            IDAT(1)=IWHR
0520            NADD=NADD-1
0521            IDAT(INX)=1
0522            IF(NADD.EQ.0)GO TO 3
0523            IF(IWHR.NE.19)RETURN
0524    4       IDAT(120)=NXT
0525    3       CALL OUTDIR(MXDIR,IDAT)
0526            MXDIR=NXT
0527            NXT=NXT+1
0528            IDAT(1)=0
0529            IF(IWHR.EQ.0)GO TO 12
```

Fig. 7.7 (cont.)

```
0530            RETURN
0531   11       IWHR=0
0532            GO TO 4
0533            END
0534
0535
0536            SUBROUTINE OUTIT(IDIR,INUM,NFILES)
0537            INTEGER $BUFF
0538            COMMON /M$XES/IMXS(3),IDAT(120),IFCB(13)
0539            COMMON ITAPE,IUNIT,IPROT,NJNQ(22)
0540            DIMENSION IDIR(7,2),INUM(2)
0541            NS1=1
0542            DO 1 I=1,NFILES
0543            IDO=IDIR(7,NS1)
0544   X        WRITE(1,100)IDO,I,NFILES,(IDIR(K,NS1),K=1,7)
0545   X100      FORMAT(1X,3I5,1X,3A2,4I5)
0546            IF(IDO.LT.0)GO TO 4
0547            DO 3 K=1,3
0548   3        IFCB(K+7)=IDIR(K,NS1)
0549            IFCB(3)=IAND(ISWAB(IPROT),255)
0550   X        WRITE(1,101)IUNIT,IPROT,IFCB
0551   X101     FORMAT(I5,A2,7I5,1X,3A2,7I5)
0552            CALL U$OPEN(99,IUNIT,IFCB,0)
0553   X        WRITE(1,101)IUNIT,IPROT,IFCB
0554   4        IST=$BUFF(ITAPE,IDAT,120,0,3)
0555            IF(IST.EQ.-1.OR.IST.EQ.-2)GO TO 2
0556            IF(IDO.GT.0)WRITE(99)IDAT
0557            GO TO 4
0558   2        IF(IDO.GT.0)CALL U$CLOS(99,0)
0559   1        NS1=NS1+INUM(I)
0560            CALL $BUFF(ITAPE,IDAT,1,4,0)
0561            RETURN
0562            END
0563
0564
BOT:
ED**
```

Fig. 7.7 (cont.)

```
2170=      SUBROUTINE DUMP2T(ID,IDAY,IMS,ISET,IPACK)
2180=C
2190=C  SUBROUTINE TO OUTPUT PACKERS
2200=C   VERSION OF 1 FEB 1979
2210=C
2220=      INTEGER IUNPAK(51),IRRAY(10,25),IART(10,25),IDATE(11),ILET(
9)
2230=      COMMON /B2/ IUNPAK,IRRAY,IART,IDATE,ILET
2240=C
2250=      IF (ID .NE. 1) GO TO 100
2260=       PRINT(5,180) ISET,IRRAY(4,25),IRRAY(5,25)
2270=       PRINT (5,185) (IDATE(I),I=1,11),IDAY,IMS
2280=       PRINT(5,190)((IRRAY(I,J),IART(I,J),J=1,25),ILET(I),I=1,10)
2290=100   CONTINUE
2300=C
2310=180   FORMAT (//,1X,"SET NUMBER",I3,10X,"STN",I3,10X,"SN",I5)
2320=185   FORMAT (/," DATE AND TIME  ",I2,3I1,"/",2(2I1,":"),I1,"0",
          +10X,I1,".",I3,10X,2I14)
2340=190   FORMAT (10(/,1X,I1,A1,24(I4,A1),2X,A2))
2350=C
2360=      RETURN
2370=      END
..
```

Fig. 7.8

```
  3020=      SUBROUTINE TOTDAT(IDATE,I)
  3030=C
  3040=C  VERSION OF 13 FEB 1979.
  3050=C
  3060=      INTEGER IDATE(9),YEAR(30),JDAY(30),HOUR(30),MINUTE(30),SECO
ND(30)
  3070=      INTEGER TSEC(30)
  3080=      COMMON /B3/ YEAR,JDAY,HOUR,MINUTE,SECOND,TSEC
  3090=C
  3100=      YEAR(I) = IDATE(1)
  3110=      JDAY(I) = IDATE(2)*100 + IDATE(3)*10 + IDATE(4)
  3120=      HOUR(I) = IDATE(5)*10 + IDATE(6)
  3130=      MINUTE(I) = IDATE(7)*10 + IDATE(8)
  3140=      SECOND(I) = IDATE(9)*10
  3150=C
  3160=      TSEC(I) = 60*(60*(JDAY(I)*24+HOUR(I))+MINUTE(I))+SECOND(I)
  3170=C     WRITE (5,*) TSEC(I),YEAR(I),JDAY(I),HOUR(I),MINUTE(I),SECON
D(I)
  3180=C
  3190=      RETURN
  3200=      END
..
```

Fig. 7.9

```
2380=      SUBROUTINE TIMECHK(NSET,ID,IREC,OLD)
2390=C
2400=C   VERSION OF 14 FEB 1979.
2410=C
2420=      INTEGER YEAR(30),JDAY(30),HOUR(30),MINUTE(30),SECOND(30)
2430=      INTEGER TSEC(30),ISTA(30)
2440=      INTEGER BEGT,OLD,CURR,TDIFF
2450=      COMMON /B3/ YEAR,JDAY,HOUR,MINUTE,SECOND,TSEC,ISTA
2460=      DATA MTI/300/
2470=      IF (TSEC(NSET) .LT. 0) NSET = NSET - 1
2480=C     WRITE (5,*) NSET,ID,IREC,OLD
2490=C
2500=C  PHASE 1
2510=C    IS RECORD ALL ZEROS? IF YES, PRINT AND RETURN
2520=C
2530=      DO  20  I = 1,NSET
2540=         IF (TSEC(I) .GT. 0) GO TO 25
2550=20    CONTINUE
2560=       WRITE (5,22) IREC
2570=22    FORMAT (*0REC#*,I5,* IS ALL ZEROS*)
2580=       RETURN
2590=C
2600=C    IS THERE A LOGICAL GAP?
2610=C
2620=25    DO  30  I = 1,NSET
2630=         TDIFF = IABS(TSEC(I)-OLD)
2640=         IF (TDIFF .LE. MTI) GO TO 50
2650=30    CONTINUE
2660=C
2670=C    IF (LOGGAP), FIND FIRST NONZERO FRAME
2680=C
2690=      DO  40  I = 1,NSET
2700=         IF (TSEC(I) .GT. 0) GO TO 45
2710=40    CONTINUE
2720=45    BEGT = TSEC(I)
2730=      WRITE (5,47) IREC,YEAR(I),JDAY(I),HOUR(I),MINUTE(I),SECOND(
```

Fig. 7.10

```
I)
  2740=47    FORMAT (*ØRECORD #*,I5,* LOGICAL GAP AT*,5I5)
  2750=      GO TO 60
  2760=50    BEGT = TSEC(I)
  2770=      WRITE (5,52) IREC,YEAR(I),JDAY(I),HOUR(I),MINUTE(I),SECOND(
I)
  2780=52    FORMAT (*ØRECORD #*,I5,* STARTS AT*,5I5)
  2790=C
  2800=C   PHASE 2--CHECK RECORD LINE BY LINE
  2810=C
  2820=60    CONTINUE
  2830=      DO  100 I = 1,NSET
  2840=C       WRITE(5,*)I,TSEC(I),YEAR(I),JDAY(I),HOUR(I),MINUTE(I),SEC
OND(I)
  2850=C
  2860=          IF (TSEC(I)) 100,70,80
  2870=70           WRITE (5,75) I
  2880=75           FORMAT(* ZERO TIME IN SET#*,I3)
  2890=             GO TO 100
  2900=80         TDIFF = IABS(TSEC(I)-BEGT)
  2910=           IF (TDIFF .GT. MTI) WRITE (5,85)
  2920=     +I,YEAR(I),JDAY(I),HOUR(I),MINUTE(I),SECOND(I)
  2930=85    FORMAT (* INCORRECT TIME IN SET#*,I3,* RECORDED AS *,5I5)
  2940=C
  2950=          IF (TDIFF .LE. MTI) CURR = TSEC(I)
  2960=C
  2970=100   CONTINUE
  2980=C
  2990=      OLD = CURR
  3000=      RETURN
  3010=      END
 ..
```

Fig. 7.10 (cont.)

8. MICROPULSATION ACTIVITY

8.1 Micropulsation Events

The reader of this report is referred to AFGL-TR-78-0312 for a comprehensive treatment of Mathematical Analysis of data from the MAGAF Network including studies of Magnetic Pulsation Events and Micropulsation Events.

A study has been undertaken to determine how best to use data from the MAGAF Network to specify and predict status of the magnetosphere by means of micropulsations.

As a first step a number of magnetically quiet days on which all seven stations were active has been selected for study to establish the quiet time behavior of micropulsations. A list of these days below, and some representative magnetograms for 28 May 78 (Figures 8.1-8.8) are given.

9 April 78
15 April 78
16 April 78
27 May 78
28 May 78

Data have been taken from the Varian System and inputted to the CDC 6600 System at AFGL.

Modifications have been made to the existing program for filtering the data; this filtering is now in progress.

Maximum entropy program will be used to obtain the frequency spectrum of the filtered data.

After obtaining the frequency spectrum, results will be presented in the form of a dynamic spectrum.

A search was carried out of the network data on the 5 quietest days of the month up to December 1977. From this search 9 days were selected as promising: 4 May, 27 Apr, 26 May, 27 July, 5 Sept, 9 Oct, 23 Nov,

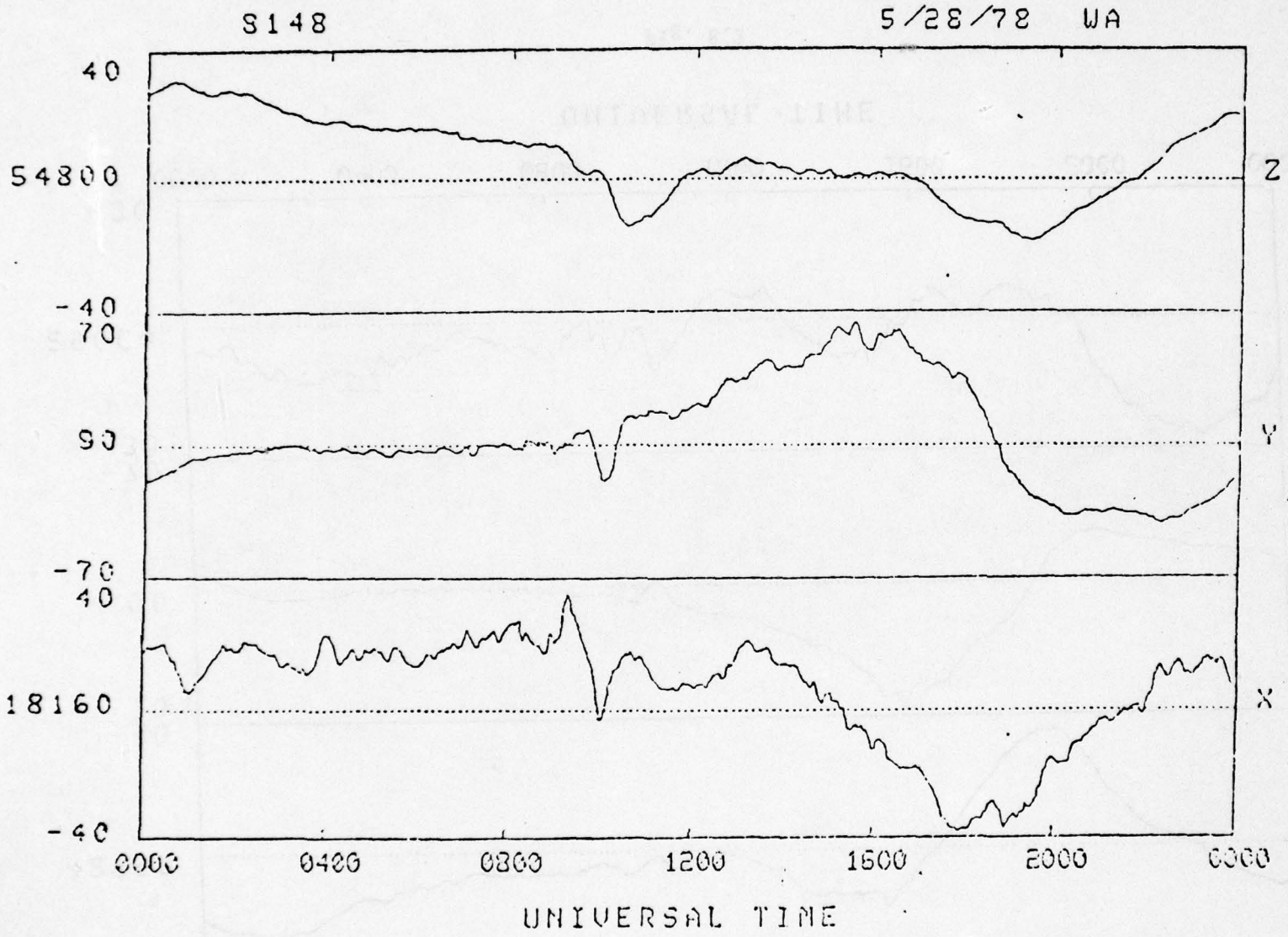

Fig. 8.1

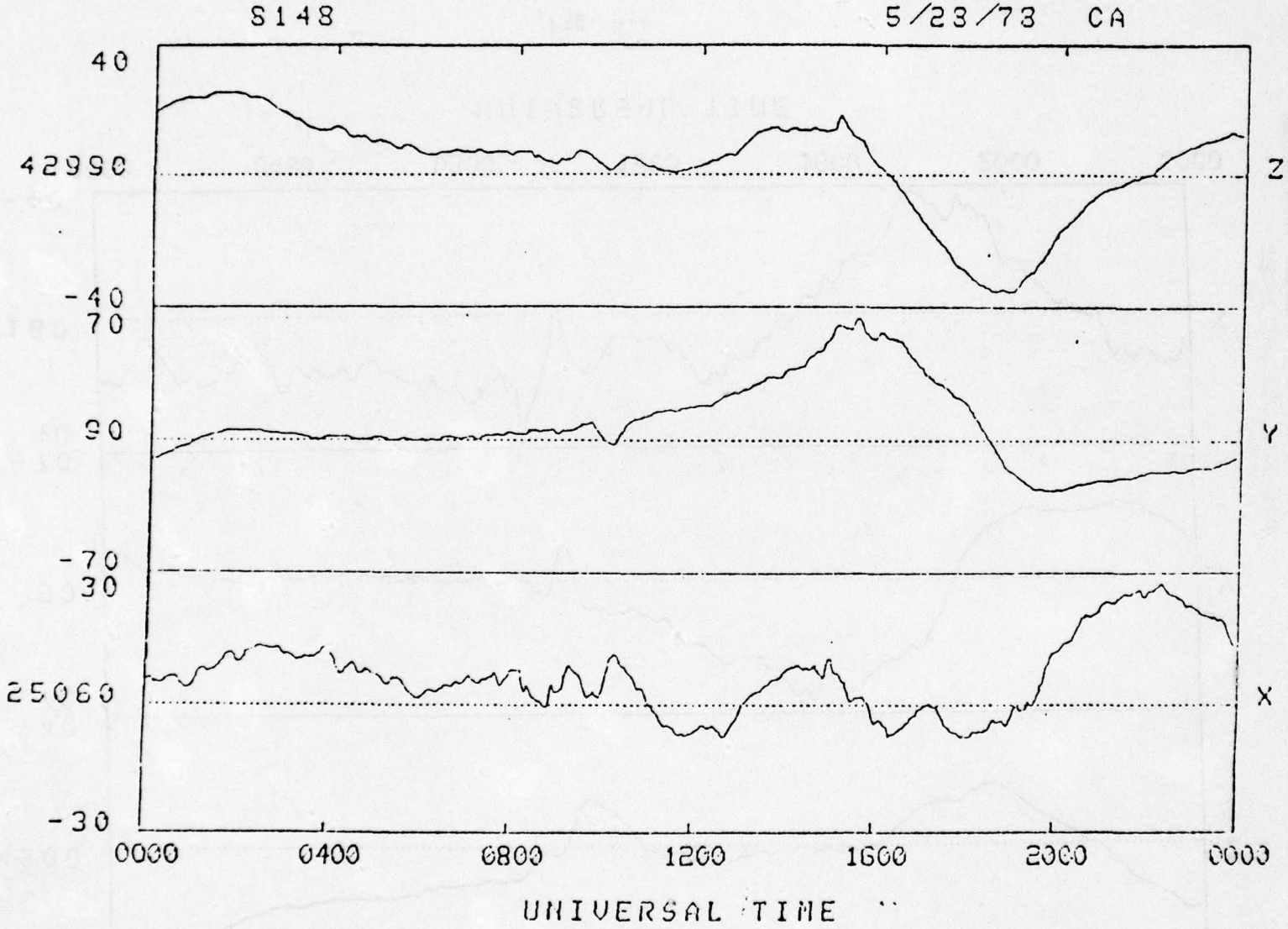
S148
5/23/73 CA
40
42990
-40
Z
70
90
-70
Y
30
25060
-30
X
0000
0400
0800
1200
1600
2000
0000
UNIVERSAL TIME

Fig. 8.2

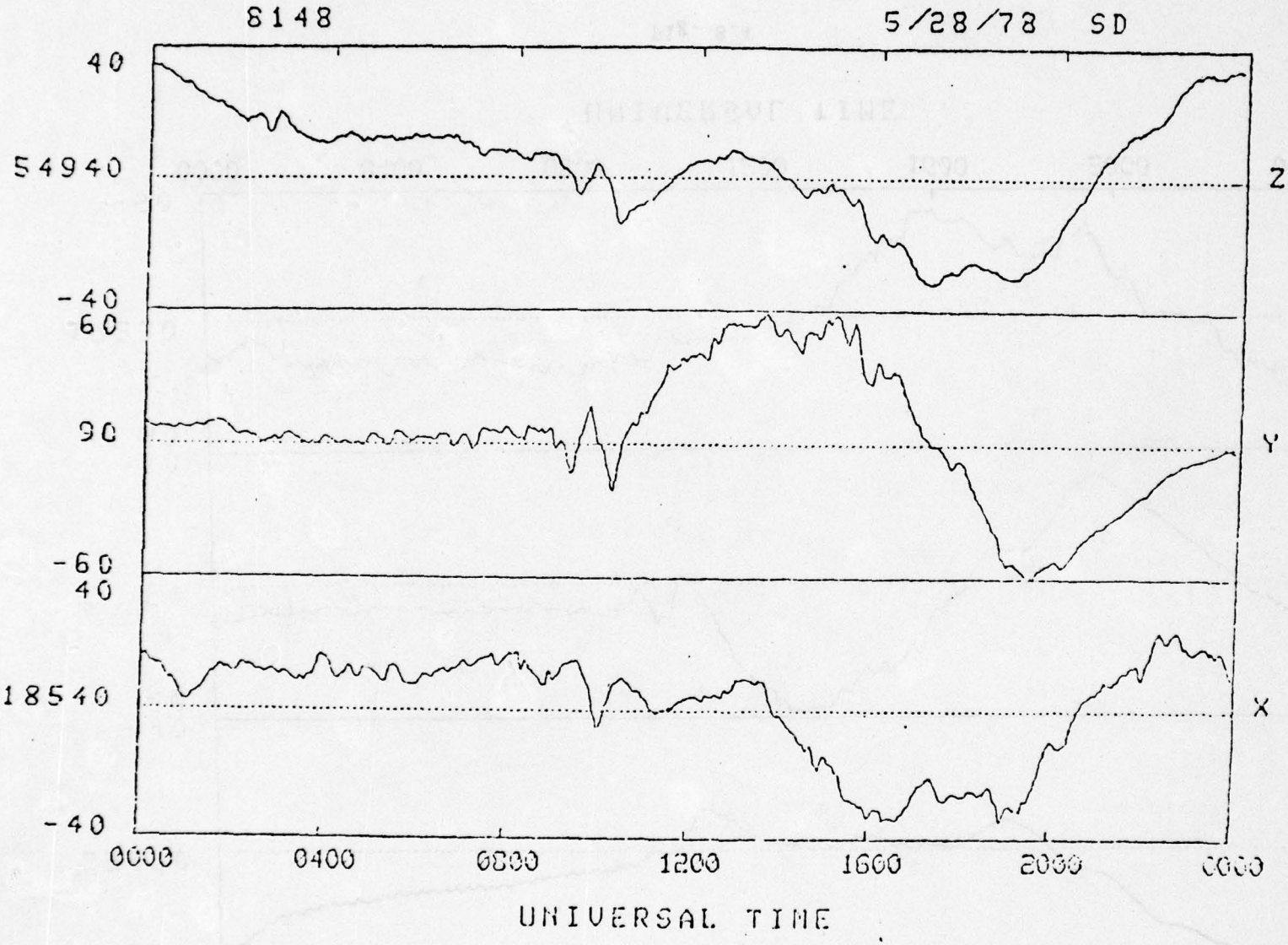

Fig. 8.3

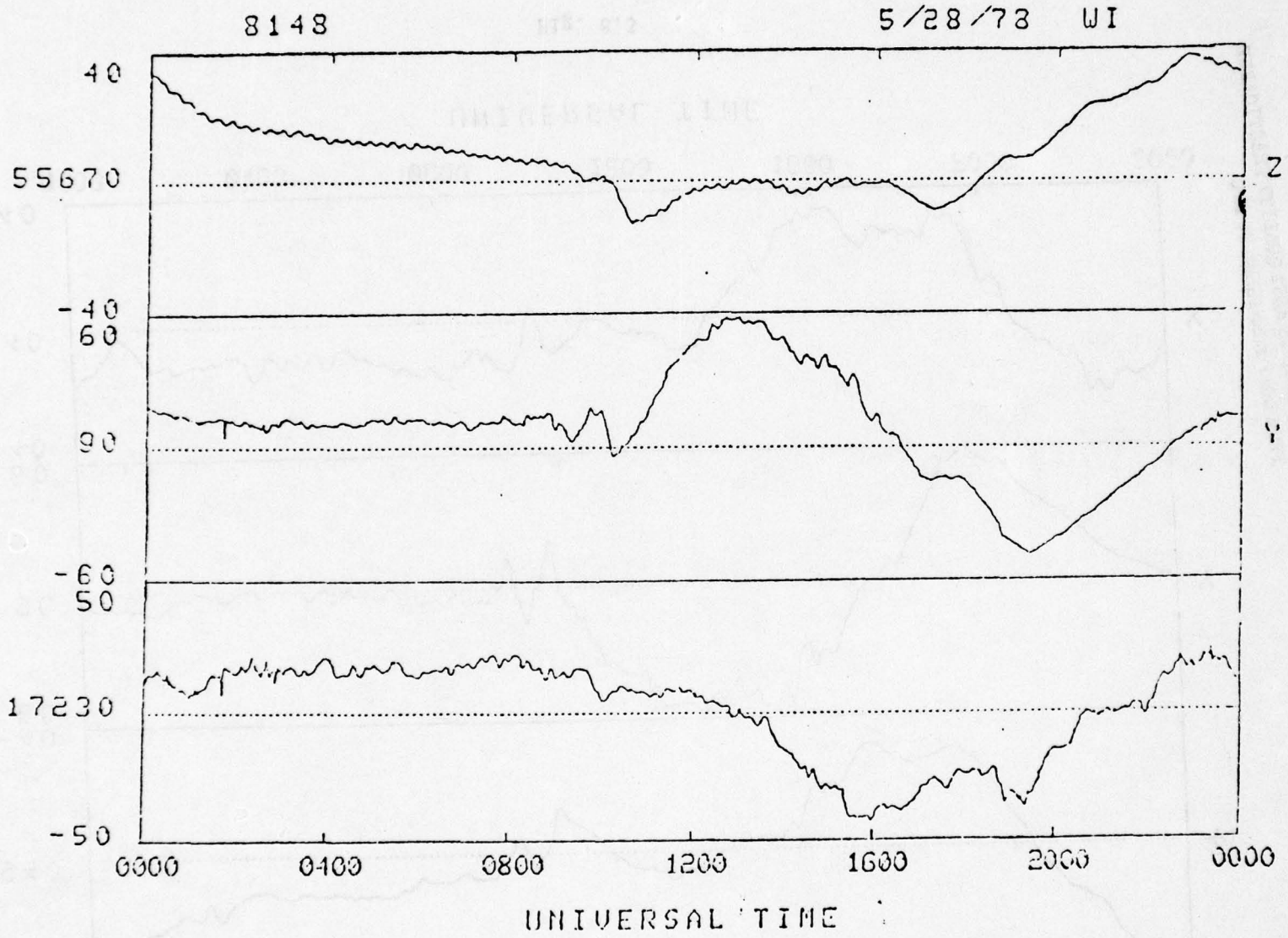

Fig. 8.4

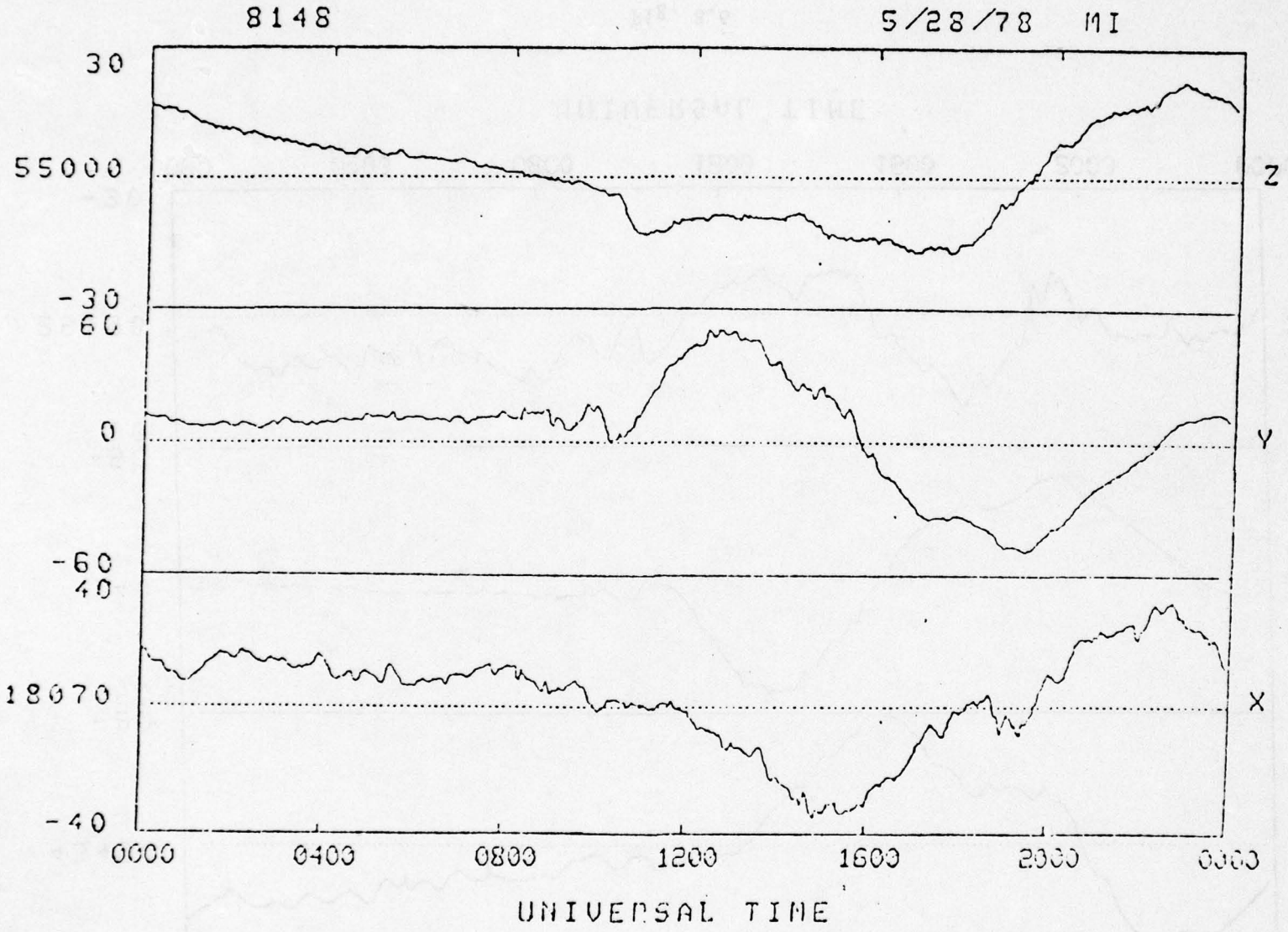

Fig. 8.5

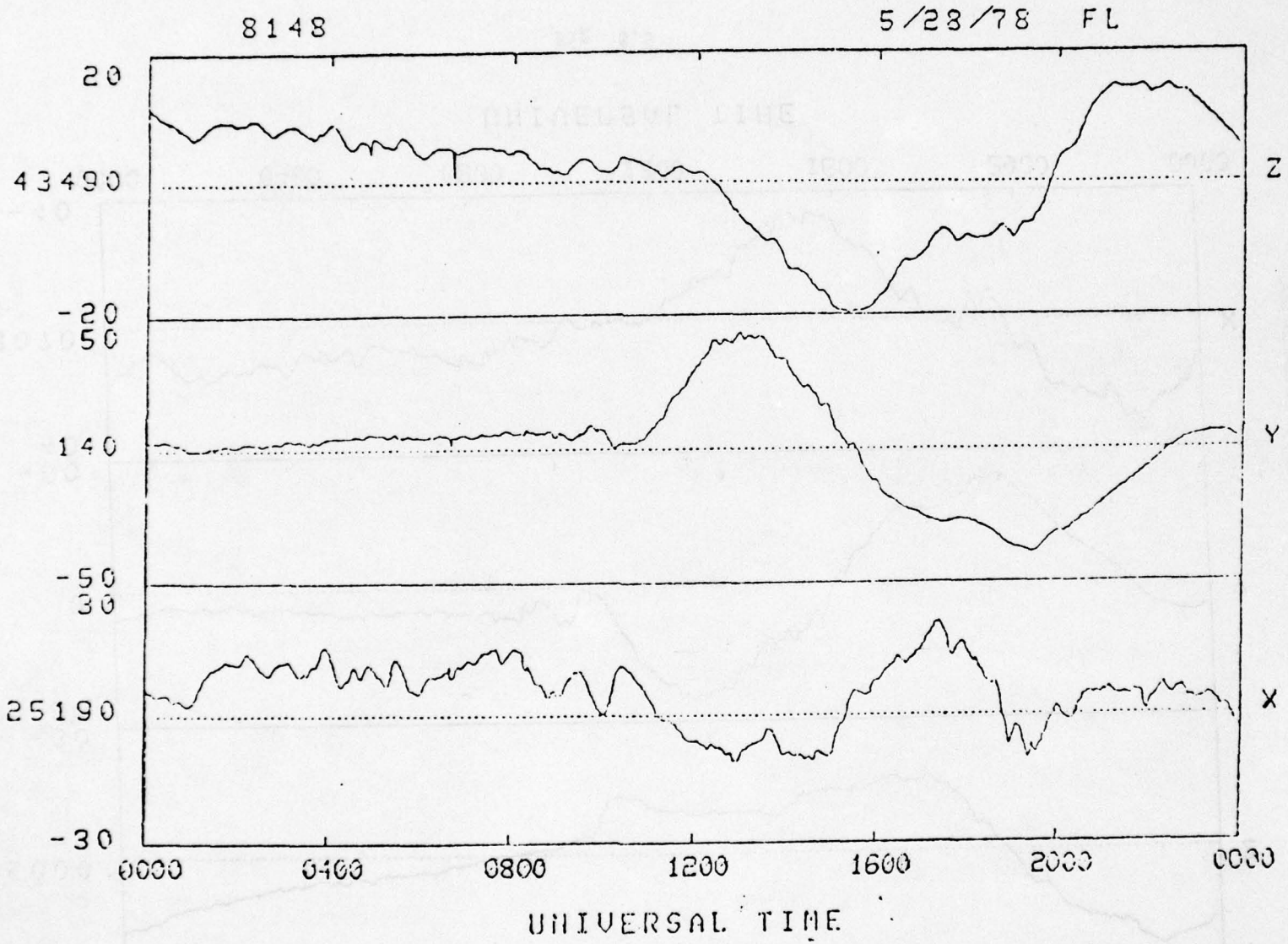

Fig. 8.6

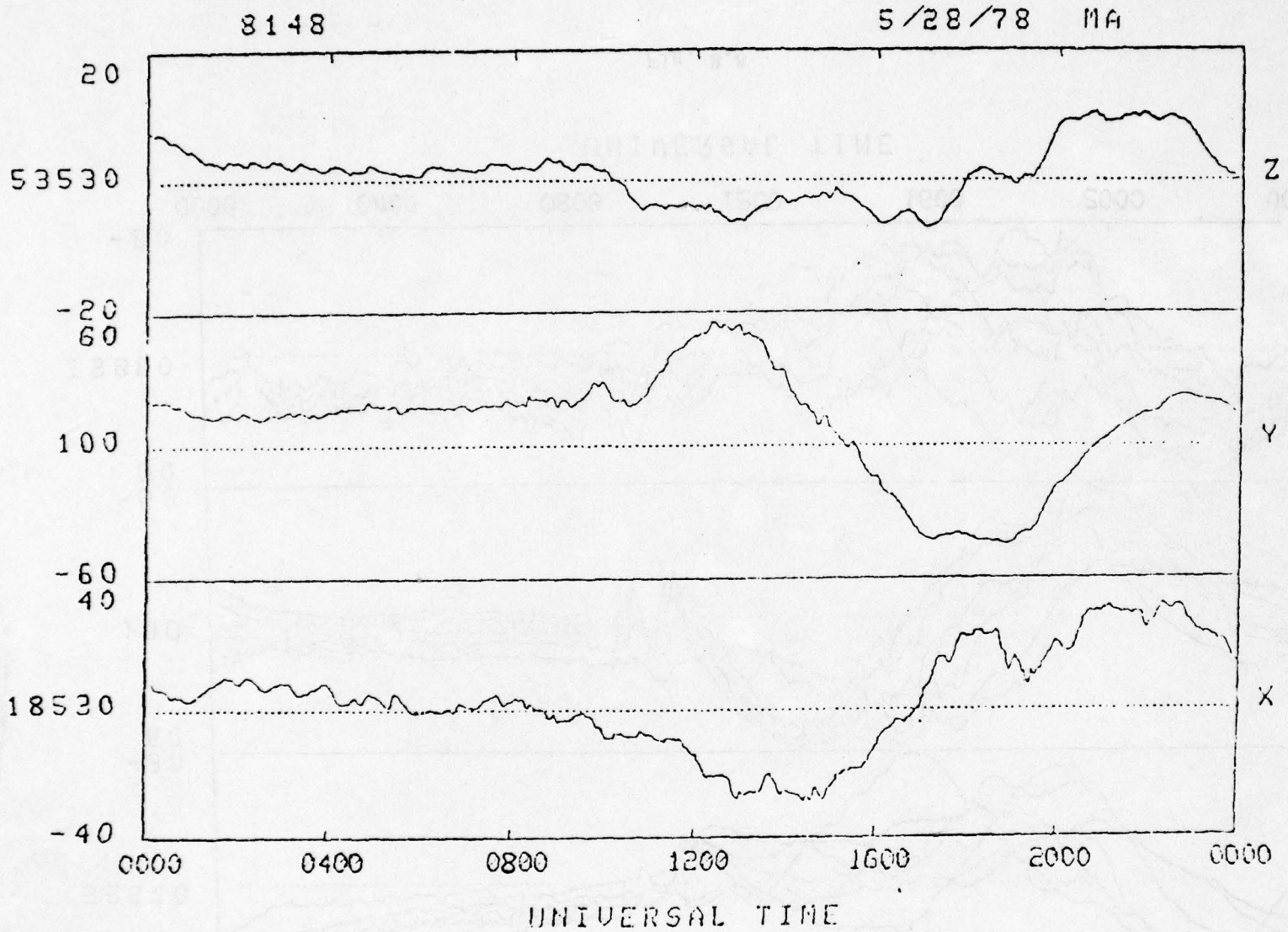

Fig. 8.7

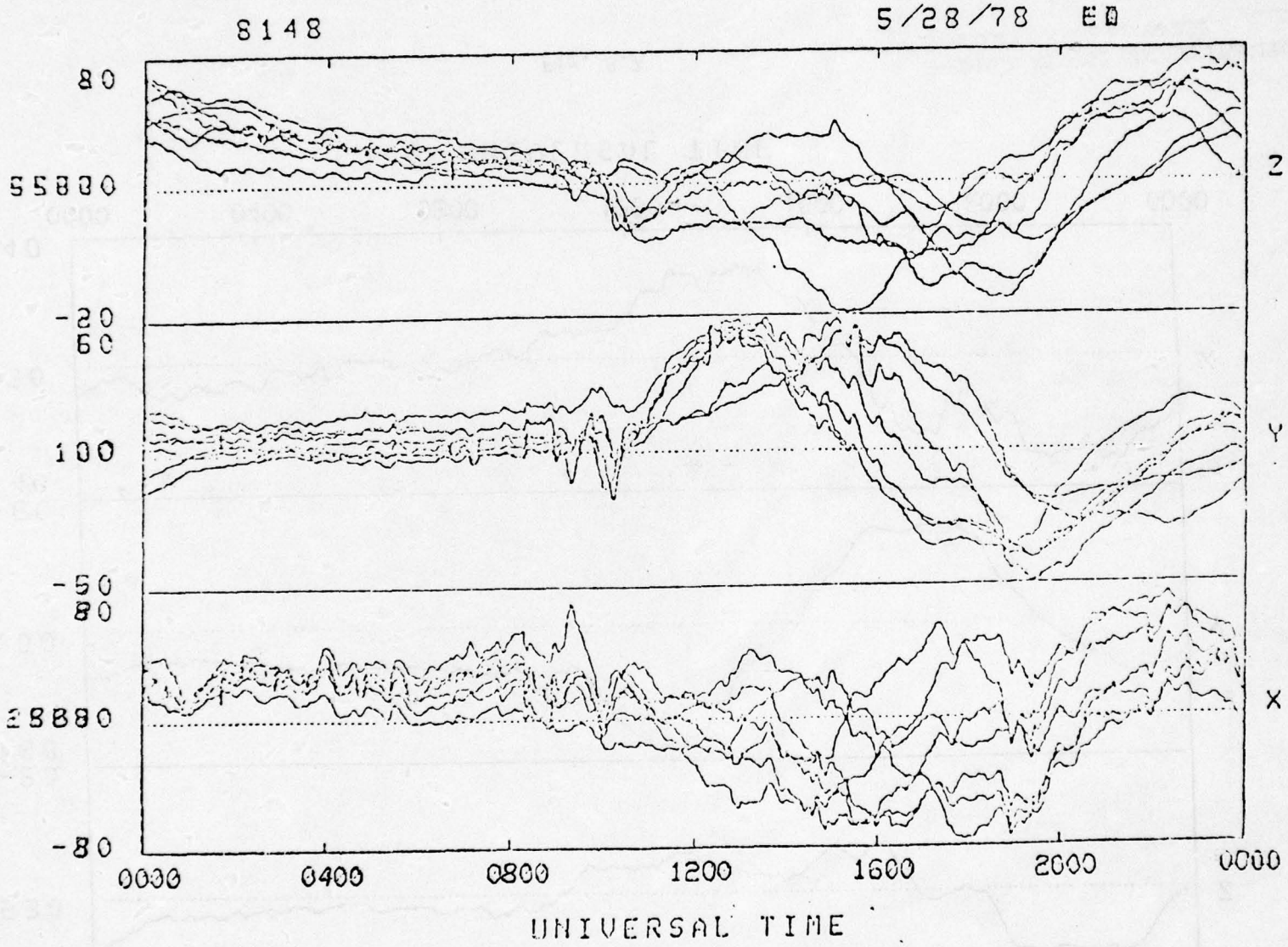

Fig. 8.8

24 Nov, 8 Dec and 18 December. However these proved unsatisfactory because of gaps in the data or noisy data. The search will be resumed for the period when all seven stations are operating.

A talk was given at the spring 1978 meeting of the AGU. The abstract is attached below.

LONGITUDINAL EXTENT OF OCCURRENCE OF Pc4 AND Pc5 GEOMAGNETIC PULSATIONS

W. Bellew (Physics Research Division, Immanuel College, Boston MA 02115)
V.L. Patel* (Dept. of Physics, Massachusetts Institute of Technology, Cambridge MA 02139)
P. Fougere (Air Force Geophysics Laboratory, Hanscom AFB MA 01731)

We have analyzed magnetic pulsation events from the AFGL magnetometer network located at ∿55°N geomagnetic latitude and covering 3 hours of local time sector. Pulsation events with period greater than 80s have been studied on June 3, 1977. The results indicate that the pulsations of Pc4 with small amplitudes (few gammas) are localized in a longitudinal sector of 1 or 2 hours extent. However, the pulsations woth large amplitudes ($\gtrsim 10\gamma$) and longer periods are observed over a longitudinal extent of 3 hours. Detailed results of wave characteristics will be presented and will be compared with theoretical models for the pulsations.

1. 023872 FOUGERE
2. 1978 Spring Meeting
3. Solar-Planetary Relations
4. Micropulsations
5. No
6. No
7. None
8. Bill to:
   Emmanuel College
   Physics Research Div.
   400 The Fenway
   Boston MA 02115
9. 1143

As a continuation of the study of Micropulsation Events, the program BINNER was written. This program divides the frequency range over which a frequency spectrum has been taken in to 18 bins, selects the 5 largest amplitudes and orders them according to frequency. If one of these amplitudes is found in a particular bin, its order is printed in that bin. For instance at Washington, (KST=1) at midnight UT (8148000000 i.e. day 148, 1978 at 0000 UT) from the output we see that the largest amplitude was in bin 5, the next largest in bin 9 and so on. If none

of the five largest ampliudes was found in a particular bin then a zero is entered. After the location of the amplitudes in their bins the power in the spectrum is printed out, followed by the magnitude of the top 5 amplitudes.

8.2 High Time Resolution

In order to study micropulsations with high time resolution we have undertaken writing a plotting routine that plots the search coil data. Using such plots it will be possible to pinpoint the time at which a change in the magnetic field occurs. Furthermore, since the search coils measure $\frac{dB}{dt}$, the low frequency component of the magnetic field is effectively filtered out. This feature is illustrated by a comparison of the following figures (Figures 8.9-8.14) which show 24 hours of search coil and fluxgate data for the same periods.

This program is flexible enough so that it will be able to plot for a period as small as 1 minute.

```
      PROGRAM MAIN     74/74   OPT=1                              FTN 4.7+476

 1                     PROGRAM MAIN(INPUT,OUTPUT,TAPE2)
                       DIMENSION F(50),A(50),AMP(50),FRE(50),NB(25),AVMP(25)
                       COMMON SUM(25),ISUM(25)
                       COMMON /SEP/ S,E,P
 5                     S=1.0
                       E=30.0
                       P=.1
                       N=5
                       KEOF=0
 10                    REWIND 2
                 11    PRINT 100
                100    FORMAT(1H1)
                       READ(2) KST
                       IF(EOF(2)) 4,1
 15              1     PRINT*,"  KST = ",KST
                 2     READ(2) NEW1,POWER,NP,(A(I),F(I),I=1,NP)
                       IF(EOF(2)) 4,5
                 5     IF(NEW1.GT.81482450) GO TO 2
                       CALL SORT(F,A,NP,N,FRE,AMP,NB,K)
 20              3     FORMAT(1PE13.4)
                       PRINT 6,NEW1,(NB(I),I=1,K),POWER,(AMP(I),I=1,N)
                 6     FORMAT(I16,16I2,1PE13.4,3X,9PE13.4)
                       GO TO 2
                 4     KEOF=KEOF+1
 25                    PRINT*,(SUM(I),I=1,K)
                       PRINT*,(ISUM(I),I=1,K)
                       DO 7 I=1,K
                       AVMP(I)=0
                       IF(ISUM(I).EQ.0) GO TO 7
 30                    AVMP(I)=SUM(I)/FLOAT(ISUM(I))
                 7     CONTINUE
                       PRINT*,(AVMP(I),I=1,K)
                       IF(KEOF.LT.7.OR.NEW1.LT.810000000) GO TO 10
                       STOP
 35                    END
```

```
      SUBROUTINE SORT(F,A,K,N,FRE,AMP,NB,KB)
      DIMENSION F(50),A(50),AMP(10),FRE(10),B(25)
     +,KNU(25),NB(25)
      COMMON SUM(25),ISUM(25)
      DATA INIT /0/
C
C     SELECT THE N LARGEST AMPLITUDES
C
      J=0
1     AM=0
      DO 4 I=1,K
      IF(J.EQ.0) GO TO 3
      DO 2 L=1,J
2     IF(I.EQ.KNU(L)) GO TO 4
3     IF(A(I).LT.AM) GO TO 4
      AM=A(I)
      NU=I
4     CONTINUE
      J=J+1
      KNU(J)=NU
      IF(J.LT.N) GO TO 1
      DO 10 I=1,N
      J=KNU(I)
      AMP(I)=A(J)
10    FRE(I)=F(J)
      GO TO 7
C
C        PLACE THE N LARGEST AMPLITUDES
C        IN FREQUENCY BINS
C
7     IF(INIT.NE.0) GO TO 12
      CALL BIN(B,KB)
      KB=KB-1
      INIT=1
      DO 11 I=1,KB
      SUM(I)=0.0
11    ISUM(I)=0
12    DO 13 I=1,KB
13    NB(I)=0
      DO 20 I=1,N
      DO 15 J=2,KB
      NU=KNU(I)
```

```
                      IF(FRE(I).LT.B(J-1).OR.FRE(I).GT.B(J)) GO TO 15
                      SUM(J-1)=SUM(J-1)+AMP(I)
   45                 ISUM(J-1)=ISUM(J-1)+I
                      NB(J-1)=NB(J-1)+I
                      GO TO 20
                15    CONTINUE
                20    CONTINUE
   50           C
                C
                C        ORDER THE N LARGEST AMPLITUDES
                C        ACCORDING TO FREQUENCY
                C
                      J=6
   55           5     AM=9999999
                      J=J+1
                      DO 6 I=J,N
```


SUBROUTINE SORT 74/74 OPT=1 FTN 4.7+476

```
                      IF(FRE(I).GT.AM) GO TO 6
                      AM=FRE(I)
   60                 BM=AMP(I)
                      NU=I
                6     CONTINUE
                      SF=FRE(J)
                      SA=AMP(J)
   65                 FRE(J)=AM
                      AMP(J)=BM
                      FRE(NU)=SF
                      AMP(NU)=SA
                      IF(J.EQ.N) RETURN
   70                 GO TO 5
                      END
```

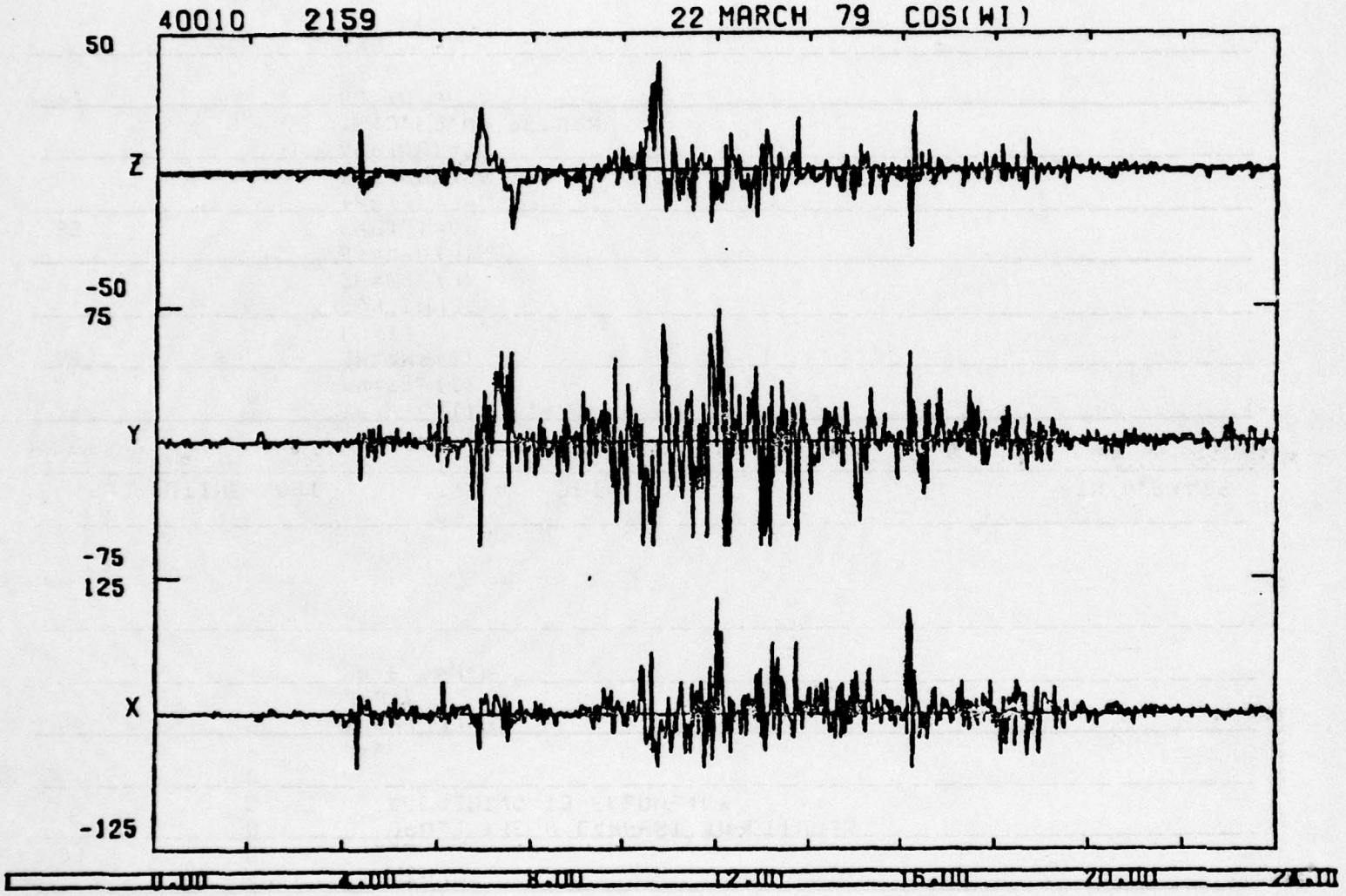
40010 2159
22 MARCH 79 COS(WI)
50
Z
-50
75
Y
-75
125
X
-125
0.000
4.000
8.000
12.000
16.000
20.000
24.00

Fig. 8.9

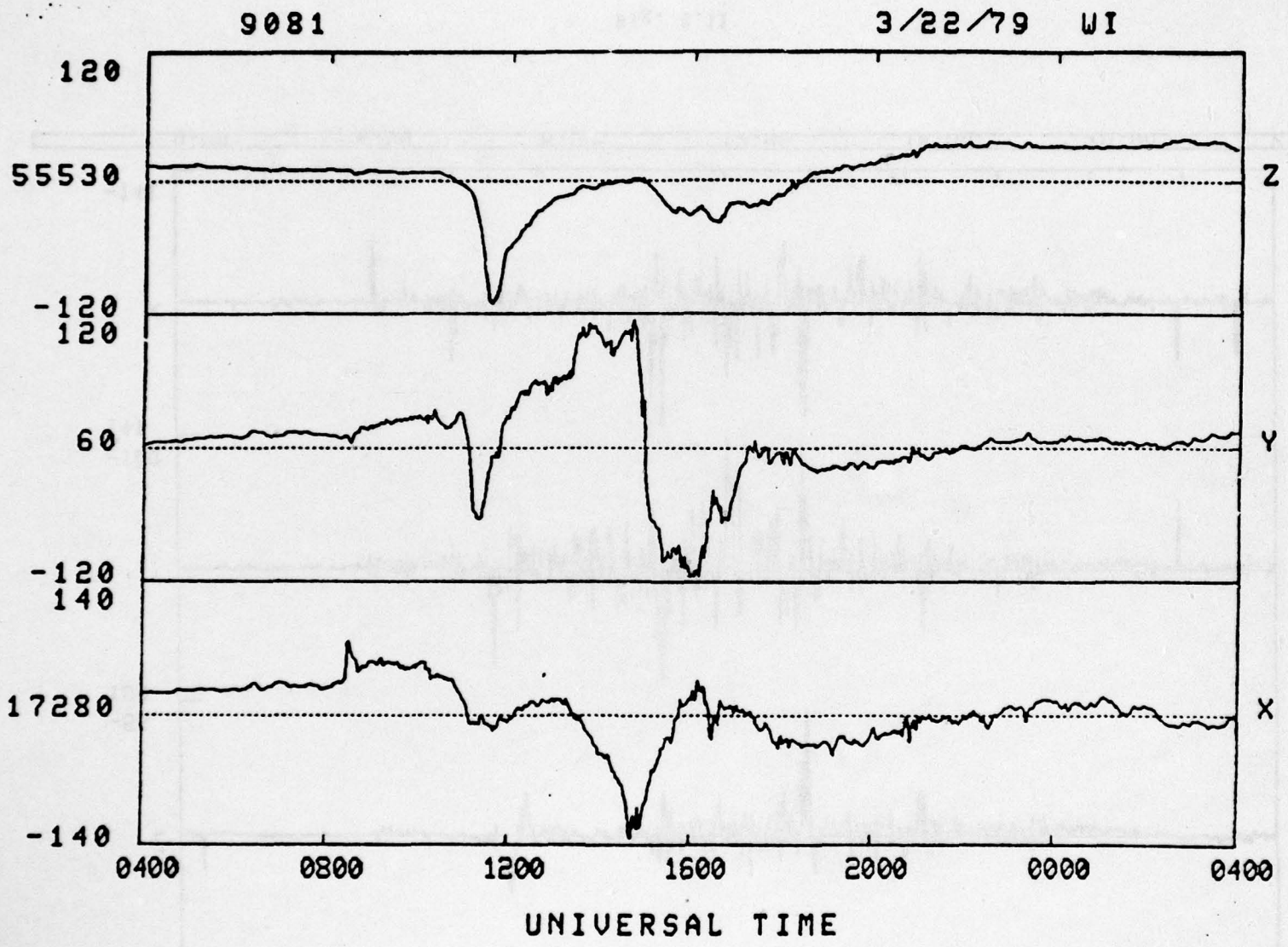
9081
3/22/79 WI
120
55530
-120
Z
120
60
-120
Y
140
17280
-140
X
0400
0800
1200
1600
2000
0000
0400
UNIVERSAL TIME

Fig. 8.10

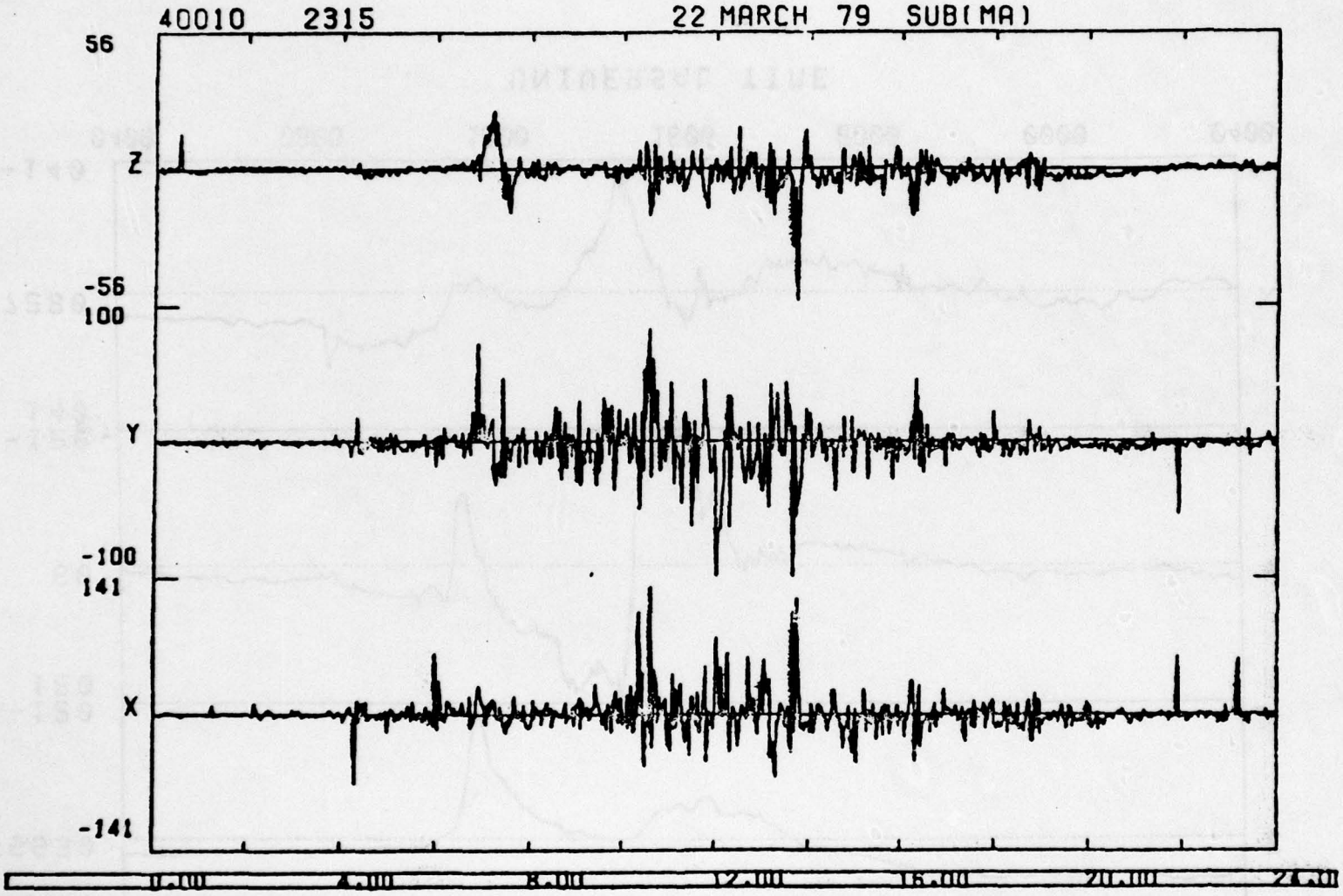
40010 2315
22 MARCH 79 SUB(MA)
56
Z
-56
100
Y
-100
141
X
-141
0.00
4.00
8.00
12.00
16.00
20.00
24.00

Fig. 8.11

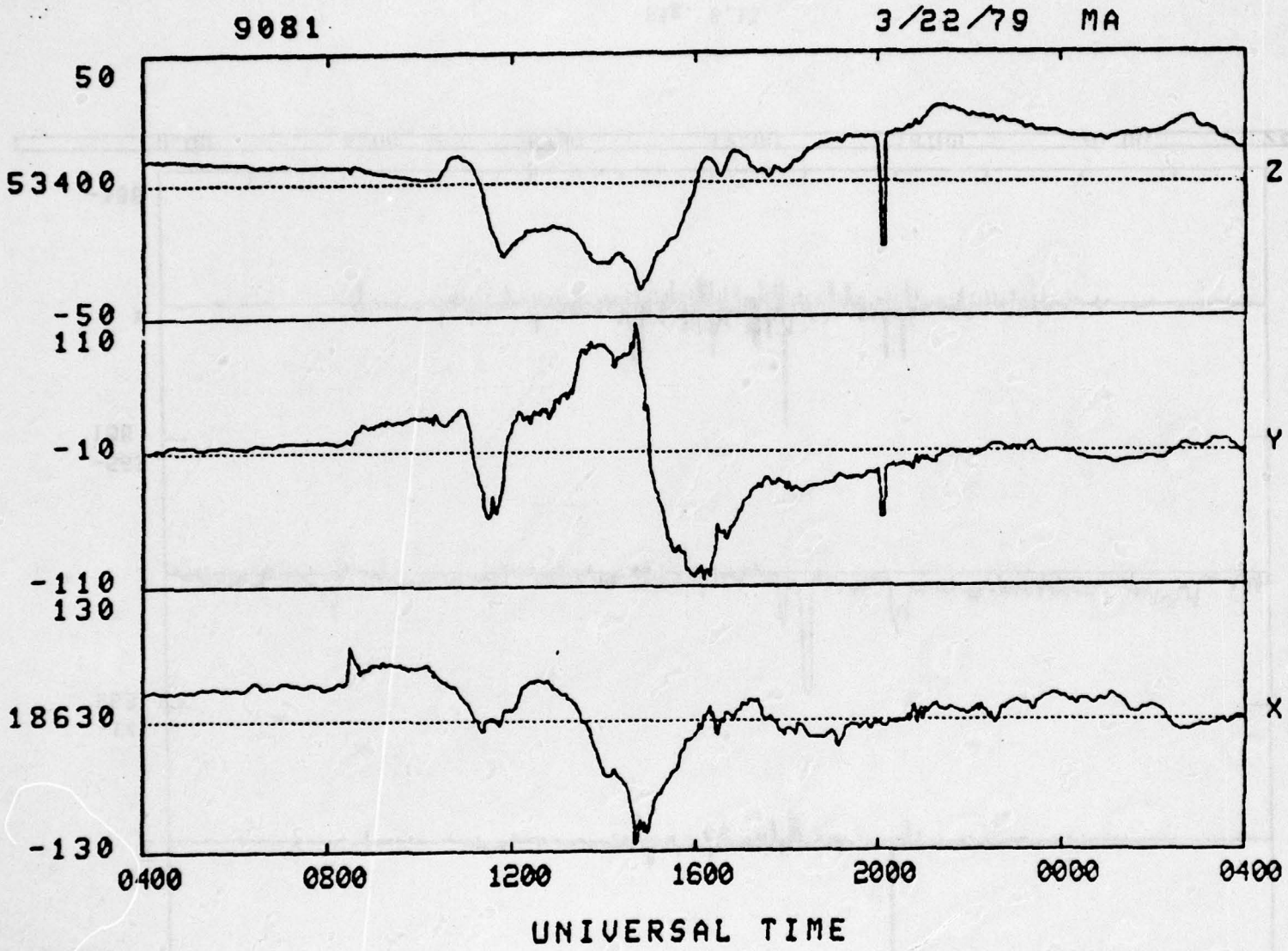
9081
3/22/79 MA
50
53400
-50
110
-10
-110
130
18630
-130
Z
Y
X
0400
0800
1200
1600
2000
0000
0400
UNIVERSAL TIME

Fig. 8.12

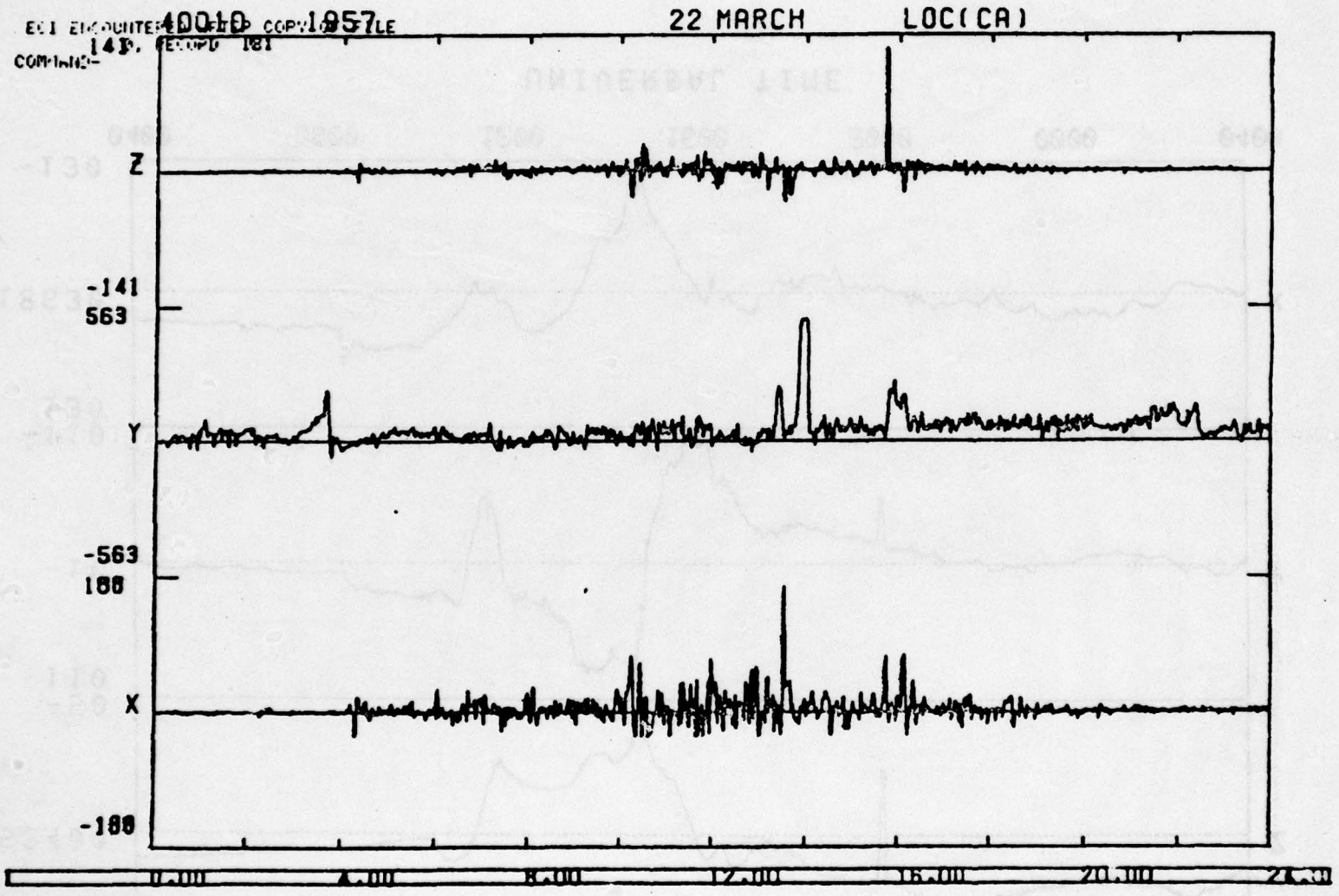
40010 1957
22 MARCH
LOC(CA)
Z
-141
563
Y
-563
188
X
-188
0.000
4.000
8.000
12.000
16.000
20.000

Fig. 8.13

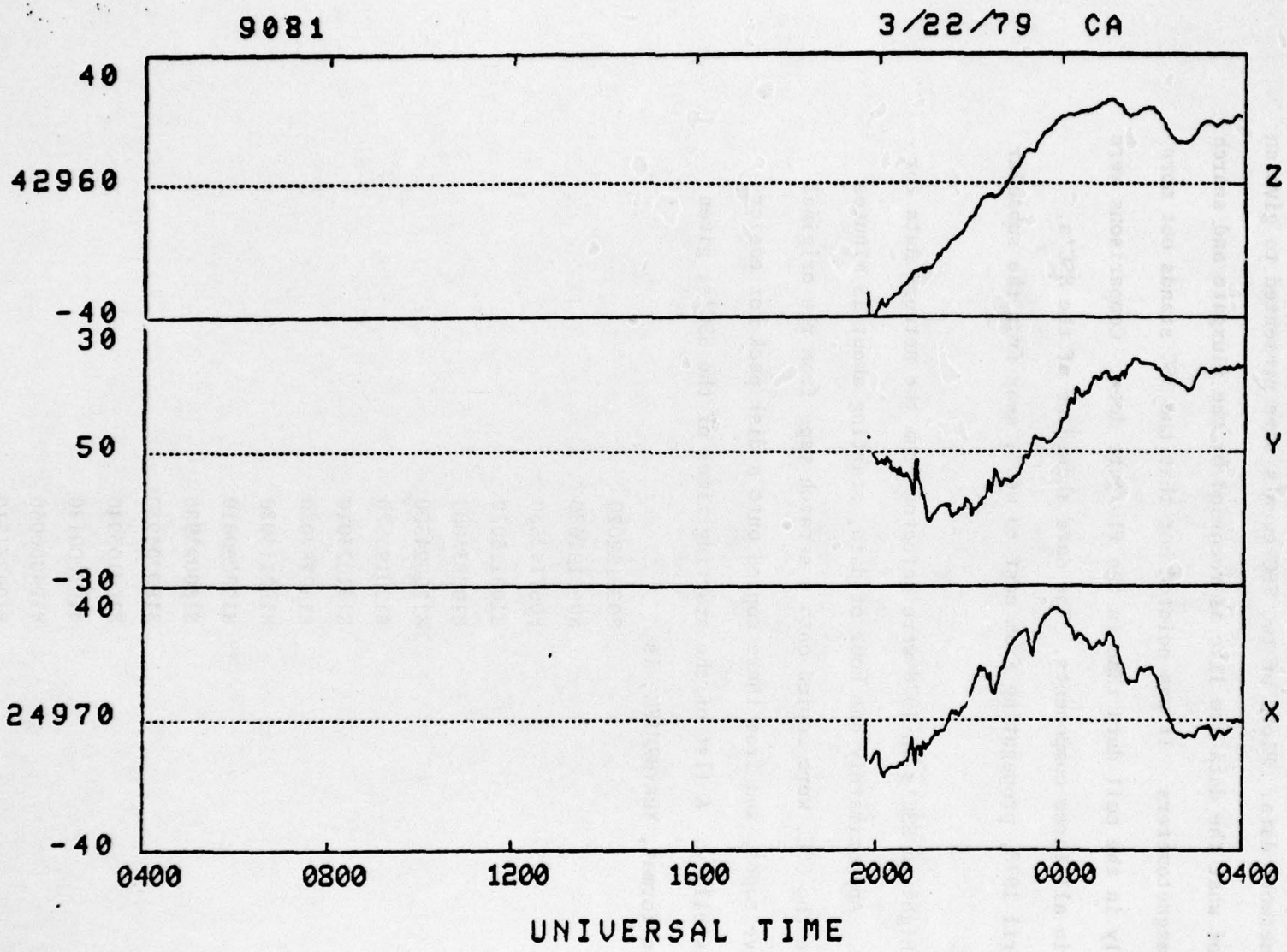
9081
3/22/79 CA
40
42960
-40
Z
30
50
-30
Y
40
24970
-40
X
0400
0800
1200
1600
2000
0000
0400
UNIVERSAL TIME

Fig. 8.14

8.3 Sudden Storm Commencement (SSC)

A talk was given at the AFGL Magnetometer Network Workshop on the AFGL network data. Plots of two SSC events were presented to give an idea of what the data are like as recorded by the fluxgate and search coil magnetometers. It was pointed out that the SSC stands out more clearly in the coil data than in the fluxgate data. Comparisons were made in all three components. The data showed on of the SSC's, 10 April 1978, propagating from east to west, away from the subsolar point.

Eighteen SSC's in 1978 were selected from the network data for study. Approximately one hour of data, starting about 15 minutes before the SSC, were copied onto a scratch tape from the original archive tapes, and from there copied onto a disk pack for easier accessibility. A list of the starting times of the SSC's, given in the format, YDAYHRMISC, is

8025152020
8056191630
8067142530
8100125020
8107233000
8120094300
8130195520
8141023010
8149182030
8152213020
8153090010
8180093950
8180204930
8192103940
8193000120
8194000040
8194231510
8352002120

Plots of an SSC's trace are shown for 8 March 73 at five stations (Figures 8.15-8.19). The data plotted here are from the search coils. Since the search coils measure changes in the field every fifth of a second, it will be possible to study these events with high time resolution.

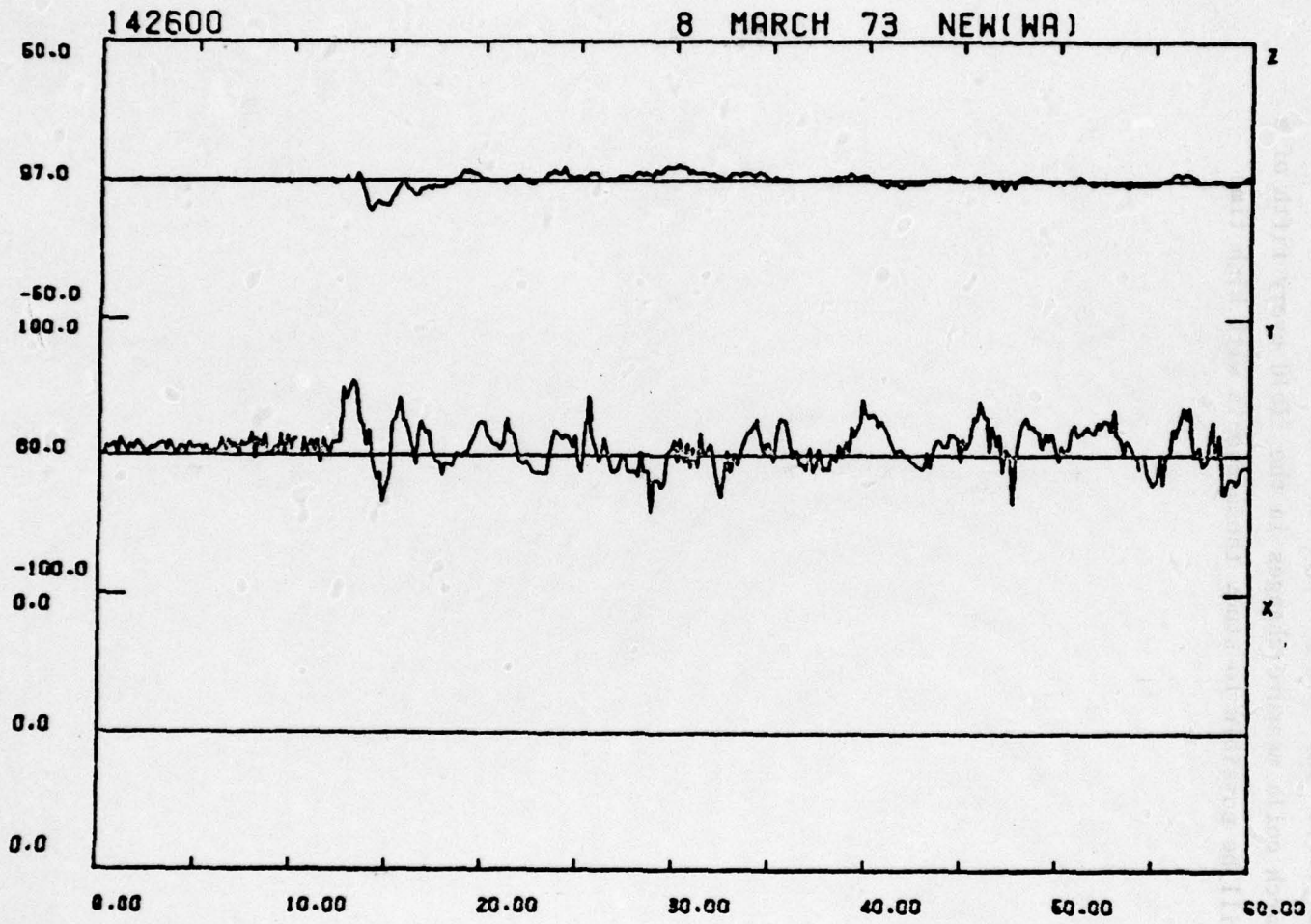
142600
8 MARCH 73 NEW(WA)
50.0
97.0
-50.0
100.0
Z
Y
60.0
-100.0
0.0
X
0.0
0.0
0.00
10.00
20.00
30.00
40.00
50.00
60.00

Fig. 8.15

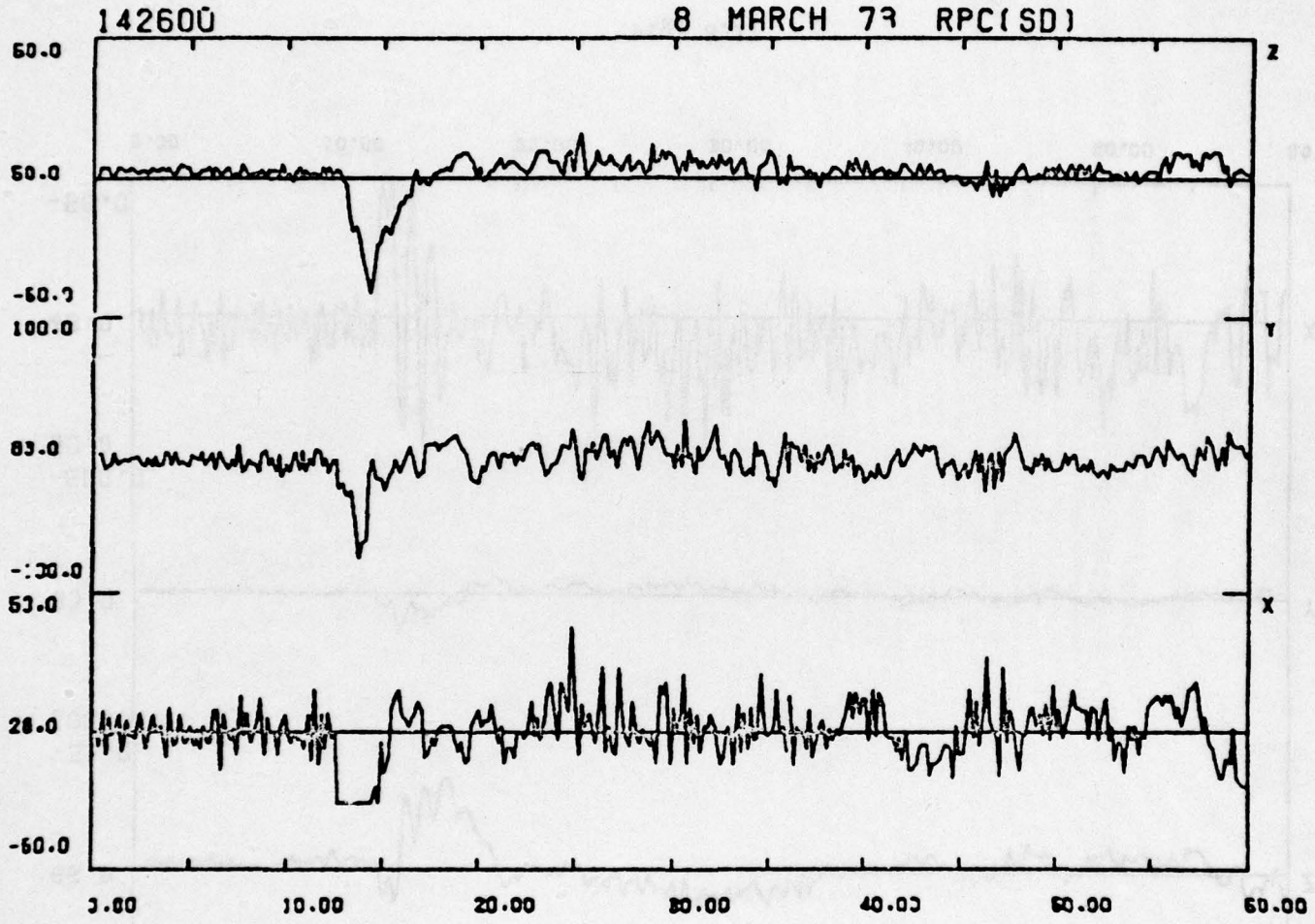
142600
8 MARCH 73 RPC(SD)
60.0
60.0
-60.0
Z
100.0
80.0
Y
50.0
28.0
-60.0
X
0.00
10.00
20.00
30.00
40.00
50.00
60.00

Fig. 8.16

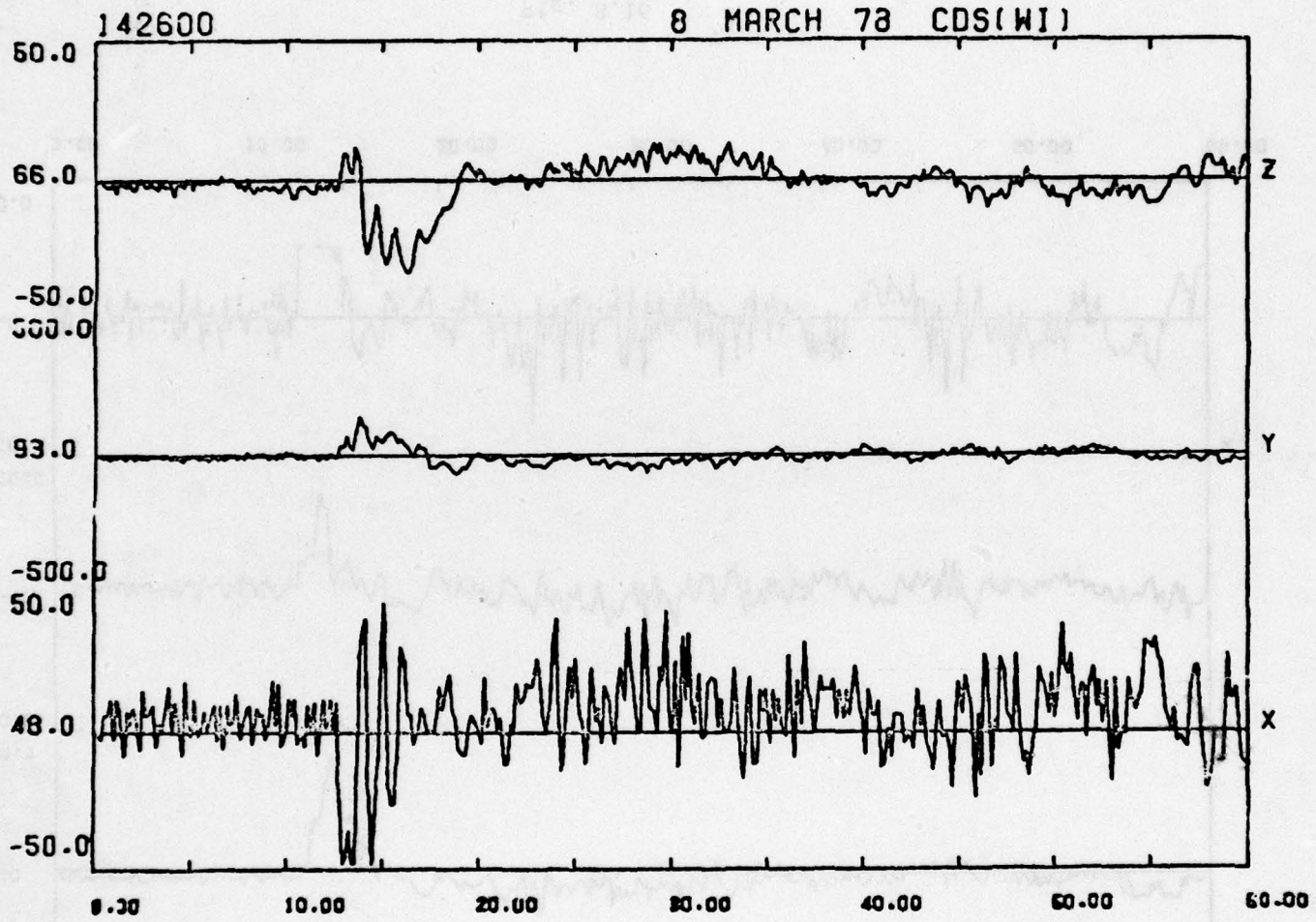
142600
8 MARCH 78 CDS(WI)
50.0
66.0
-50.0
300.0
93.0
-500.0
50.0
48.0
-50.0
Z
Y
X
0.00
10.00
20.00
30.00
40.00
50.00
60.00

Fig. 8.17

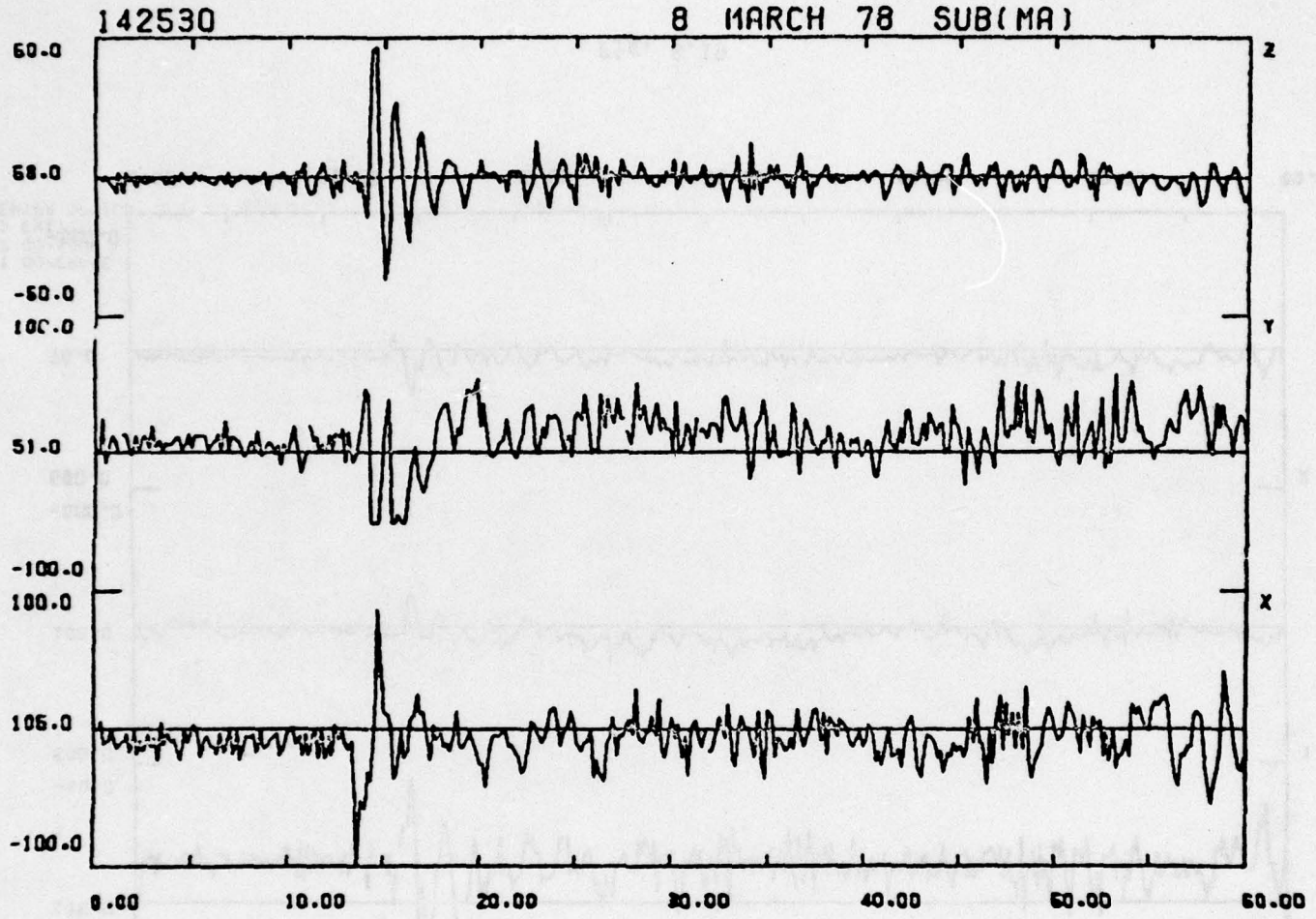
142530
8 MARCH 78 SUB(MA)
60.0
68.0
-60.0
100.0
51.0
-100.0
100.0
105.0
-100.0
Z
Y
X
0.00
10.00
20.00
30.00
40.00
50.00
60.00

Fig. 8.18

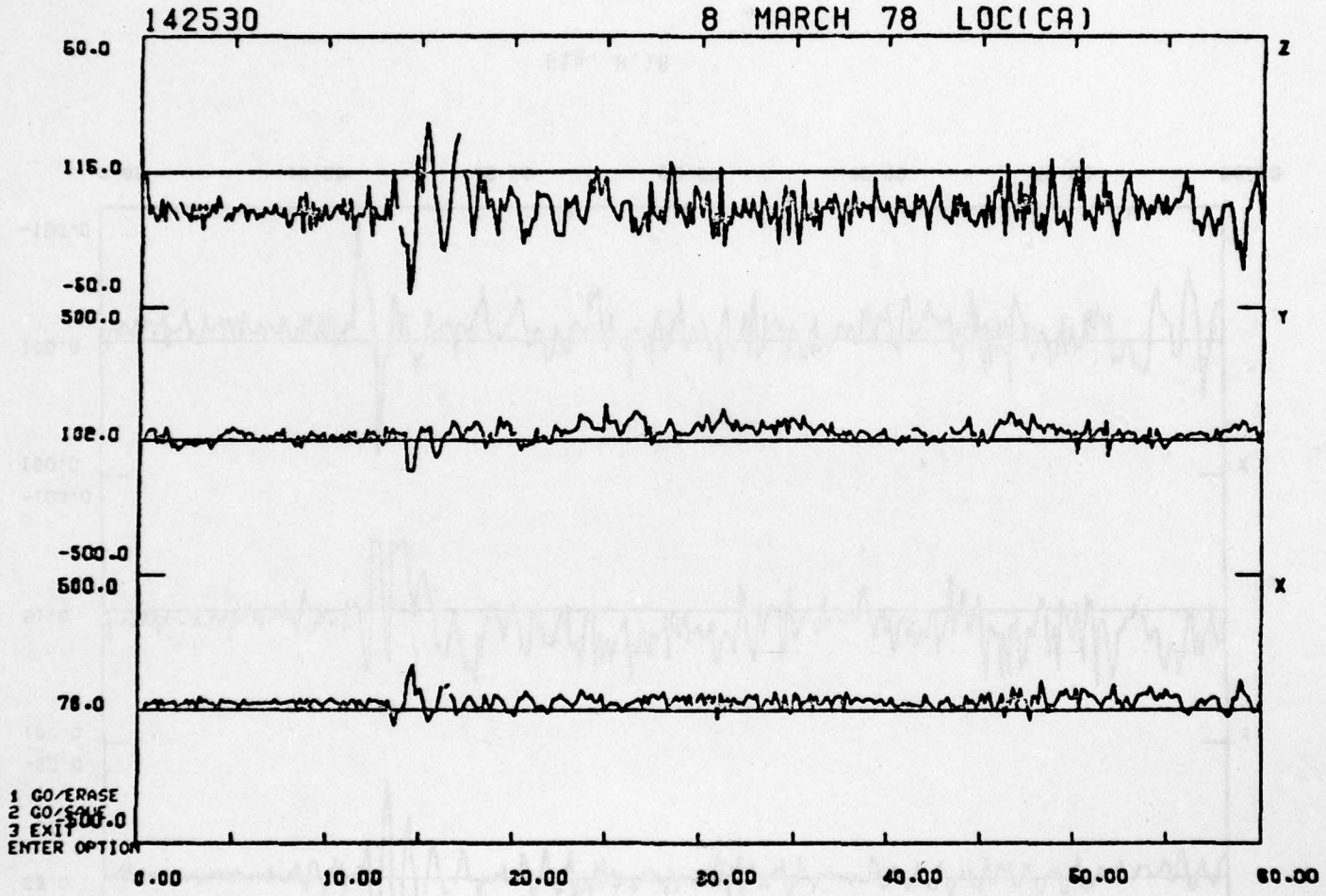
142530
8 MARCH 78 LOC(CA)
60.0
Z
116.0
-60.0
500.0
Y
100.0
-500.0
500.0
X
70.0
-500.0
1 GO/ERASE
2 GO/SAVE
3 EXIT
ENTER OPTION
0.00
10.00
20.00
30.00
40.00
50.00
60.00

Fig. 8.19